รายงานวิจัยฉบับสมบูรณ์

โครงการ

การศึกษาคุณลักษณะเชิงของแข็งและการเปลี่ยนรูปของ นอร์ฟลอกซาซิน ไฮเดรต

โดย

อาจารย์ เภสัชกรหญิง ดร. นฤพร สุตัณฑวิบูลย์ และคณะ

ตุลาคม 2553

สัญญาเลขที่ **DBG4880003**

รายงานวิจัยฉบับสมบูรณ์

โครงการ

การศึกษาคุณลักษณะเชิงของแข็งและการเปลี่ยนรูปของ

นอร์ฟลอกซาซิน ไฮเดรต

คณะผู้วิจัย	สังกัด
1. อาจารย์ ภญ. ดร. นฤพร สุตัณฑวิบูลย์	ภาควิชาเภสัชอุตสาหกรรม คณะเภสัชศาสตร์ จุฬาลงกรณ์มหาวิทยาลัย
2. Professor Stephen R. Byrn	**Purdue University, USA**
3. เภสัชกร วันชัย จงเจริญ	ภาควิชาเภสัชอุตสาหกรรม คณะเภสัชศาสตร์ จุฬาลงกรณ์มหาวิทยาลัย

สนับสนุนโดยสำนักงานกองทุนสนับสนุนการวิจัย

(ความเห็นในรายงานนี้เป็นของผู้วิจัย สกว. ไม่จำเป็นต้องเห็นด้วยเสมอไป)

กิตติกรรมประกาศ

คณะผู้วิจัยขอขอบคุณสำนักงานกองทุนสนับสนุนการวิจัย (สกว.) ที่ได้ให้การสนับสนุนเงินทุนวิจัยพื้นฐานแบบมุ่งเป้าหมาย “เคมีทางยา” ประจำปี 2548 สำหรับดำเนินการวิจัยในโครงการ “การศึกษาคุณลักษณะเชิงของแข็งและการเปลี่ยนรูปของนอร์ฟลอกซาซินไฮเดรต” ตามสัญญาเลขที่ DBG4880003 ทำให้งานวิจัยสำเร็จลุล่วงตามวัตถุประสงค์ทุกประการ

คณะผู้วิจัยใคร่ขอขอบคุณ ภาควิชาเภสัชอุตสาหกรรม (ปัจจุบันคือภาควิชาวิทยาการเภสัชกรรมและเภสัชอุตสาหกรรม) คณะเภสัชศาสตร์ จุฬาลงกรณ์มหาวิทยาลัย และ Purdue University ที่ได้ให้การสนับสนุนด้านบุคลากร เครื่องมือ และสถานที่การทำวิจัย

ที่สำคัญที่สุด คณะผู้วิจัยขอขอบคุณคณะกรรมการพิจารณาทุน รวมทั้งคณะกรรมการติดตามและประเมินผลงานวิจัย ที่ได้ให้ข้อเสนอแนะที่มีคุณค่าและเป็นประโยชน์อย่างยิ่งต่อการพัฒนาและดำเนินการวิจัยในครั้งนี้ ให้ลุล่วงตามวัตถุประสงค์อย่างสมบูรณ์

คณะผู้วิจัย

บทคัดย่อ

รหัสโครงการ: DBG4880003

ชื่อโครงการ: การศึกษาคุณลักษณะเชิงของแข็งและการเปลี่ยนรูปของนอร์ฟลอกซาซินไฮเดรต

ชื่อนักวิจัย: อาจารย์ ภญ. ดร. นฤพร สุตัณฑวิบูลย์
ภาควิชาเภสัชอุตสาหกรรม คณะเภสัชศาสตร์ จุฬาลงกรณ์มหาวิทยาลัย
Professor Stephen R. Byrn
Department of Industrial and Physical Pharmacy, Purdue University
ภก. วันชัย จงเจริญ
ภาควิชาเภสัชอุตสาหกรรม คณะเภสัชศาสตร์ จุฬาลงกรณ์มหาวิทยาลัย

E-mail Address: narueporn.s@chula.ac.th

ระยะเวลาโครงการ: 2 ปี

นอร์ฟลอกซาซินเกิดการจัดเรียงตัวในรูปไฮเดรต 4 แบบ (ไดไฮเดรต เฮมิเพนทะไฮเดร่ต ไตรไฮเดรต เพนทะไฮเดรต) และของแข็งอีกหนึ่งชนิดที่มีการจัดเรียงตัวอย่างไม่เป็นระเบียบ ไฮเดรตทั้งหมดแสดงความเป็นผลึกเมื่อตรวจสอบด้วยการกระเจิงรังสีเอ็กซ์ นอร์ฟลอกซาซินไฮเดรทสามารถเกิดการเปลี่ยนรูปเป็นนอร์ฟลอกซาซินชนิดปราศจากน้ำรูปเอได้ภายใต้อุณหภูมิ 60 องศาเซลเซียสเป็นเวลา 48 ชั่วโมง ยกเว้นนอร์ฟลอกซาซินไดไฮเดรตและนอร์ฟลอกซาซินไตรไฮเดรตที่พบโครงสร้างแบบผสม การลดความชื้นสัมพัทธ์เป็นศูนย์ไม่ทำให้เกิดการเปลี่ยนรูปของนอร์ฟลอกซาซินชนิดปราศจากน้ำรูปเอได้อย่างสมบรูณ์ ผลของความร้อนทำให้นอร์ฟลอกซาซินไฮเดรตเปลี่ยนรูปแบบไม่สมบูรณ์ไปสู่ทรานสิชันนอลไฮเดรต ในขณะที่การลดความชื้นสัมพัทธ์ของนอร์ฟลอกซาซินเพนทะไฮเดรตทำให้เกิดการเปลี่ยนรูปไปสู่ของแข็งที่มีการจัดเรียงตัวอย่างไม่เป็นระเบียบ ในสภาวะความชื้นสูงนอร์ฟลอกซาซินชนิดปราศจากน้ำรูปเอและชนิดไฮเดรต (ยกเว้นไดไฮเดร่ต) เกิดการเปลี่ยนรูปเป็นนอร์ฟลอกซาซินเพนทะไฮเดรต โดยสรุปปัจจัยของความร้อน ความชื้นและเวลาที่สัมผัสต่างมีผลต่อการเปลี่ยนรูปของนอร์ฟลอกซาซินชนิดปราศจากน้ำรูปเอและนอร์ฟลอกซาซินไฮเดรต

พลังงานดีไฮเดรชันของนอร์ฟลอกซาซินเฮมิเพนทะไฮเดรตมีค่าต่ำกว่าพลังงานดีไฮเดรชันของนอร์ฟลอกซาซินไตรไฮเดรตและนอร์ฟลอกซาซินเพนทะไฮเดรต ซึ่งเป็นผลอันเนื่องมาจากจำนวน ตำแหน่ง และความแข็งแรงของพันธะไฮโดรเจนที่เกิดขึ้นระหว่างโมเลกุล ของนอร์ฟลอกซาซินกับโมเลกุลของน้ำในโครงสร้างผลึก ปริมาณพลังงานทั้งหมดในการดีไฮเดรชันของนอร์ฟลอกซาซิน ไฮเดรตทั้งสามชนิด (เฮมิเพนทะไฮเดรต ไตรไฮเดรต และเพนทะไฮเดรต) ไม่ขึ้นกับอุณหภูมิไม่ว่าใช้วิธีการใดในการคำนวน สัมประสิทธิ์การจัดเรียงตัวของน้ำในโครงสร้างผลึกนอร์ฟลอกซาซินไดไฮเดรตมีค่ามาก แสดงว่าโมเลกุลของน้ำมีความพอดีกับช่องว่างในโครงสร้างผลึกนอร์ฟลอกซาซินไดไฮเดรตส่งผลให้มีช่องว่างอิสระในโครงสร้างผลึกน้อย ทำให้โครงสร้างผลึกนอร์ฟลอกซาซินยังคงความสมบูรณ์ได้ภายหลังจากการกำจัดโมเลกุลน้ำออก

คำหลัก: นอร์ฟลอกซาซินไฮเดรต, โครงสร้างผลึก, คุณลักษณะเชิงของแข็ง, การเปลี่ยนรูป, พลังงานดีไฮเดรชัน

Abstract

Project Code: DBG4880003

Project Title: Solid State Characterization and Interconversion of Norfloxacin Hydrates

Investigator: Narueporn Sutanthavibul, Ph.D.
Faculty of Pharmaceutical Sciences, Chulalongkorn University
Professor Stephen R. Byrn, Ph.D.
Department of Industrial and Physical Pharmacy, Purdue University
Wanchai Chongcharoen
Faculty of Pharmaceutical Sciences, Chulalongkorn University

E-mail Address: narueporn.s@chula.ac.th

Project Period: 2 years

Four stoichiometric norfloxacin (NF) hydrates (dihydrate, hemipentahydrate, trihydrate, pentahydrate) and one disordered NF state, were generated by various methods and characterized. X-ray powder diffraction (XRPD) patterns of all NF hydrates exhibited crystalline structures. NF hydrates transformed to anhydrous NF Form A after gentle heating at 60 °C for 48 hours except dihydrate and trihydrate where mixture in XRPD patterns between anhydrous NF Form A and former structures existed. Desiccation of NF hydrates at 0% RH for 7 days resulted in only partial removal of water molecules from the hydrated structures. The hydrated transitional phase and the disordered NF state were obtained from the incomplete dehydration of NF hydrates after thermal treatment and desiccation of pentahydrate NF, respectively. Anhydrous NF Form A and NF hydrates transformed to pentahydrate NF when exposed to high moisture environment except dihydrate. In conclusion, moisture levels, temperatures and duration of exposure influenced the interconversion pathways and stoichiometry of anhydrous NF and its hydrates.

NF hydrates did not show significant particle size reduction after dehydration due to the very compact structures and by high K_{chan} value obtained for dihydrate NF. Thus, NF hydrates were physically very stable and less likely to collapse after dehydration. Dehydration energy of lower stoichiometric hydrate (hemipentahydrate NF) was lower than higher hydrates (trihydrate NF and pentahydrate NF) due to the number, position and strength of hydrogen bonding between crystalline water and NF moiety in crystal lattice structure. The total dehydration energy for every NF hydrates were very high and found to be independent of temperature used.

Keywords: norfloxacin hydrate, crystal structure, interconversion, dehydration energy

สารบัญ

	หน้า
กิตติกรรมประกาศ	ii
บทคัดย่อภาษาไทย	iii
บทคัดย่อภาษาอังกฤษ	iv
สารบัญ	v
สารบัญรูป	vi
สารบัญตาราง	x
คำอธิบายสัญลักษณ์และคำย่อที่ใช้ในการวิจัย	xi
บทที่ 1 Introduction	1
บทที่ 2 Experimental	3
บทที่ 3 Results and Discussion	10
บทที่ 4 Conclusions	69
References	71
Appendices	77
บทที่ 5 ข้อเสนอแนะสำหรับงานวิจัยในอนาคต	83
Output จากโครงการวิจัย	84
ภาคผนวก	87

สารบัญรูป

Figure **หน้า**

1 Model of IDSC thermogram of NF hydrate during isothermal dehydration 8

2 DSC and TGA thermograms of anhydrous NF Form A (A), disordered NF state (B), dihydrate NF (C), hemipentahydrate NF (D), trihydrate NF (E) and pentahydrate NF (F) 11

3 Comparative HPLC chromatograms of various hydrates NF with standard NF in conjunction with the use of methyl paraben (MP) as internal standard 13

4 XRPD patterns of anhydrous NF Form A (A), disordered NF state (B), dihydrate NF (C), hemipentahydrate NF (D), trihydrate NF (E) and pentahydrate NF (F) 14

5 HSM photomicrographs of NF hydrates immerse in mineral oil upon heating (hemipentahydrate NF at ambient temperature (A), hemipentahydrate NF at temperarature over 120°C (B), pentahydrate NF at ambient temperature (C), pentahydrate NF at temperarature over 120°C (D), dihydrate NF at ambient temperature (E), dihydrate NF at temperarature over 100°C (F)) 15

6 Scanning electron photomicrographs of anhydrous NF Form A (A), pentahydrate NF obtained from 100%RH vapor exposure (B) and pentahydrate NF from directly dispersed in water (C) 17

7 Photomicrographs of anhydrous NF Form A after dispersed in water at various contact time at the magnification of 400. (A. initial, B. 15 minutes, C. 60 minutes and D.180 minutes) 18

8 DSC thermograms of disordered NF with respect to different heating temperature programs 20

9 XRPD patterns of disordered NF state (A), after D-I (B), after D-II (C) and anhydrous NF Form A (D) 20

10 XRPD patterns of disordered NF states exposed to different relative humidity for 7 days 21

11 FT-IR spectra of anhydrous NF Form A, disordered NF state and other stoichiometric hydrates of NF 22

12 Dynamic water vapor moisture sorption and desorption isotherms of anhydrous NF Form A at 25°C 23

13 XRPD patterns of anhydrous NF Form A under different relative humidity for 7 days 25

14 XRPD patterns of dihydrate NF under 100% RH for 7 days 25

15 XRPD patterns of hemipentahydrate NF under desiccant (0% RH) as a function of exposure time 26

16 XRPD patterns of trihydrate NF under desiccant (0% RH) as a function of exposure time 27

17 XRPD patterns of anhydrous NF Form A (A), disordered state NF (B), hemipentahydrate NF (C) and pentahydrate NF (D) after heated at 60°C for 48 hours 28

18 XRPD patterns of dihydrate NF after heated at 60°C for various time period 29

19 XRPD patterns of trihydrate NF after heated at 60°C for various time period 29

20 Summary of the solid state interconversion of anhydrous NF Form A and its hydrates 30

21 IDSC thermograms of hemipentahydrate NF during isothermal dehydration at various T_{iso} 31

22 XRPD diffractograms of dehydrated hemipentahydrate NF after isothermal dehydration with respect to T_{iso} 32

23 α-t curves of dehydration of hemipentahydrate NF at different T_{iso} 34

24 SEM photomicrographs of hemipentahydrate NF after complete dehydration at various T_{iso} 35

25 Comparative activation energy of dehydration derived from model independent solid state kinetic of different stoichiometric NF hydrates 36

26 IDSC thermograms of trihydrate NF during isothermal dehydration at various T_{iso} 37

27 IDSC thermograms of pentahydrate NF during isothermal dehydration at various T_{iso} 38

28 XRPD diffractograms of dehydrated trihydrate NF after first step of isothermal dehydration with respect to T_{iso} 41

29 XRPD diffractograms of dehydrated pentahydrate NF after first step of isothermal dehydration with respect to T_{iso} 42

30 XRPD diffractograms of dehydrated trihydrate NF after complete dehydration with respect to T_{iso} 43

31 XRPD diffractograms of dehydrated trihydrate NF after complete dehydration with respect to T_{iso} 44

32 SEM photomicrographs of dehydrated trihydrate NF during isothermal dehydration after the first dehydration step with respect to T_{iso} 47

33 SEM photomicrographs of dehydrated pentahydrate NF during isothermal dehydration after the first dehydration step with respect to T_{iso} 48

34 SEM photomicrographs of dehydrated trihydrate NF during isothermal dehydration after the complete dehydration with respect to T_{iso} 49

35 SEM photomicrographs of dehydrated pentahydrate NF during isothermal dehydration after the complete dehydration with respect to T_{iso} 50

36 α-t curves during dehydration of trihydrate NF at different T_{iso} 51

37 α-t curves during dehydration of pentahydrate NF at different T_{iso} 51

38 The regular non isothermal DSC (NIDSC) thermograms of some NF hydrates at the heating rate of 10 °C /min 54

39 Model of NIDSC thermogram (X to A) before IDSC thermorgram (A to C) of NF hydrate during isothermal dehydration 54

40 The relationship between stoichiometry and dehydration energy of NF hydrates obtained by different calculation methods (◆ IDSC method alone, ○ regular NIDSC) 56

41 Photomicrographs of dihydrate NF during isothermal dehydration at various T_{iso} as a function of heating time 58

42 SEM photomicrographs of dihydrate NF after 360 mins of isothermal dehydration with respect to different T_{iso}. 59

43	The atomic positions of NF moiety and water of crystallization molecules of dihydrate NF	62
44	The hydrogen bonding in crystal lattice of dihydrate NF structure	62
45	The crystallographic arrangement of water channel in dihydrate NF structure along different unit cell axis (free red dots are crystalline water)	64

สารบัญตาราง

TABLE Page

1 Water content (KF), percent weight loss (TGA) and stoichiometry between NF and water molecules……..... 12

2 Dehydration energy, residual water content and particle size of dehydrated hemipentahydrate NF after complete dehydration at different T_{iso}…… 32

3 The activation energy of isothermal dehydration of hemipentahydrate NF with various solid state kinetic models……..... 36

4 Dehydration energy, residual water content and particle size of dehydrated trihydrate NF after dehydration at different T_{iso} …….. 39

5 Dehydration energy, residual water content and particle size of dehydrated pentahydrate NF after dehydration at different T_{iso}…… 40

6 The activation energy of isothermal dehydration of trihydrate NF with various solid state kinetic models……..... 52

7 The activation energy of isothermal dehydration of pentahydrate NF with various solid state kinetic models……..... 52

8 The hydrogen bonds position and molecular property in dihydrate NF crystal structure from crystallographic data…….. 63

9 Crystal data of dihydrate NF……... 66

10 Crystallographic data of anhydrous NF Form A obtained from Powder Indexing program of MATERIAL STUDIO® software simulated with XRPD data……..... 68

คำอธิบายสัญลักษณ์และคำย่อที่ใช้

A	pre exponential or frequency factor
AUC	area under the curve
cm^{-1}	the reciprocal of cemtrimetre
et al.	et alli, and others
E_a	activation energy
g	gram
HPLC	high performance liquid chromatography
J	joule
k	rate constant
K_{chan}	the coefficient of packing
kJ	kilo joule
kV	kilo voltage
ln	natural logarithm
α	reacted fraction
mA	milliampere
mg	milligram
ml	milliliter
min	minute
mol	mole
r^2	correlation of determination
s	second
T	absolute temperature
UV	ultra violet
W	watt
°C	degree centigrade
$°2\theta$	degree of two theta
μl	microlitre
%RH	percentage relative humidity
w/v	weight by volume
w/w	weight by weight
%T	percentage transmission

บทที่ 1

INTRODUCTION

Pharmaceutical manufacturing process plays an important role for new drug formulation development. One of the most significant processes in the pharmaceutical manufacturing procedure is drying operation. Drying can generally be achieved by employing either elevated temperature or reduced pressure. However, thermal drying is commonly used more than vacuum drying in industrial scale due to ease of operation. Regarding thermal drying, the solid phase conversion of materials may occur during dehydration (Byrn et al., 1999).

Proteins and peptides are well known for their thermal-labile property. Therefore, chemical properties of proteins often changed upon drying. Thermal dehydration of proteins eventually lead to stability problems and a failure in dosage form development (Abdul-Fattah, Kalonia and Pikal, 2007). Physical properties will also markedly be affected during dehydration such as cracks on the outer surface of particles can take place after thermal drying for some materials (Sakata, Shiraishi and Otsuka, 2004). Molecular adduct is an example which showed the solid state transformation during thermal dehydration. Ansolvate, a solvate without solvent molecules in the crystal structure, will be generated after the solvate is subjected to high temperature. The solvent molecule in the solvate is impeded as a result of the input energy from high temperature. Consequently, packing integrity of dehydrated materials will be altered and lead to structural weakness and finally structural collapse (Byrn et al., 1999). For example, drying of beclomethasone dipropionate monohydrate (BDM), antiasthmatic drug, resulted in the particle size reduction up to several folds after drying (Amolwan Chinapak, 2000). In addition, several groups of pharmaceutical solvates showed the same behavior as BDM where the particle sizes were reduced by desolvation. The removed solvent molecule from a solvate is a key factor to determine the extent of particle size reduction. This phenomenon has a complex behavior because the dehydration and size reduction occurred synchronously. The dehydration energy and the energy required to reduce the particle size of BDM are of great concern. Furthermore, different in stoichiometry of solvate/hydrate might determine the possibility of the particle size reduction by dehydration. Thus, it is important to study the relationship between molecular structures of solvate/hydrate and the dehydration energy required. In this study, norfloxacin (NF) is selected as model compound due to the versatility of stoichiometric

hydrates. It is necessary to determine the interconversion pathways amidst NF hydrates prior to evaluate the dehydration energy by thermal dehydration of the different stoichiometric NF hydrates.

Objectives of This Study

1. To crystallize and characterize solid state properties of various stoichiometry of NF hydrates
2. To determine the interconversion pathways between various stoichiometric NF hydrates and anhydrous NF
3. To evaluate energy required to induce the solid state interconversion between each stoichiometric NF hydrate and anhydrous NF

บทที่ 2

EXPERIMENTAL

CHEMICALS

- Norfloxacin (anhydrous) Form A (Sigma Aldrich, USA)
- Isopropanol (IPA) (Mallinkrodt Chemicals, USA)
- Acetone (Mallinkrodt Chemicals, USA)
- Dichloromethane (Mallinkrodt Chemicals, USA)
- Ammonium hydroxide (J.T. Baker, USA)
- Hydrogen peroxide, 30% w/v (PanReac, Spain)
- Ortho-phosphoric acid (Univar, Australia)
- Lithium chloride, magnesium chloride, potassium carbonate, sodium bromide, sodium chloride, potassium bromide, potassium chloride, dextrose monohydrate, and potassium nitrate (Unilab, Australia)
- Anhydrous calcium sulfate (Drierite®, USA)
- Double distilled water

INSTRUMENTS

- Differential Scanning Calorimeter (822^{e}, Mettler Toledo, Switzerland)
- Thermogravimetric Analyzer (TGA/SDTA851^{e}, Mettler Toledo)
- Hot Stage (FP90, Mettler Toledo, Switzerland) equipped with optical microscope (Eclipse E2000, Nikon, Japan)
- Karl Fischer (720 KFS Titrino and 703 Ti Stand, Metrohm, Switzerland) with heating oven (KF 707, Metrohm, Switzerland)
- High Performance Liquid Chromatography (LC 10-ADvP, Shimadzu, Japan)
- X-ray Powder Diffractometer (D5000, Siemens, Germany)
- Scanning Electron Microscope (JSM-5410 LV, Jeol, Japan)
- Diffused ATR-Fourier Transformed Infrared Spectophotometer (Spectrum One® , Perkin Elmer, USA)
- Symmetrical Gravimetric Analyzer (SGA-100, VTI Corporation, Hialeah FL., USA).

METHODS

Preparation of NF hydrates

Dihydrate NF

Anhydrous NF Form A was dissolved in a mixture of IPA and water (0.915 mole fraction of IPA) at 60 ^{o}C in a light resistant container. The final NF concentration was equal to 1.5 mg/ml. The clear solution was allowed to cool down and left undisturbed at ambient condition to facilitate recrystallization. The resultant crystalline powder was harvested and kept in a tight and light-resistant container.

Trihydrate NF

Preparation of trihydrate NF was modified from the method reported by Puechagut et al. (1998). Anhydrous NF Form A was dissolved in 20% w/v aqueous ammonia solution to give a final clear solution at a concentration of 17.5 mg/ml. Antisolvent was obtained by mixing 564 ml of acetone and 156 ml of dichloromethane. The aqueous ammonia NF solution of 68.5 ml was gradually poured into antisolvent with continuous agitation. White and fluffy precipitates were developed and harvested. Dichloromethane was used to wash the resultant precipitates. The product was then placed in the drying oven at 50 ^{o}C for approximately 1 hour to remove residual solvents.

Hemipentahydrate and Pentahydrate NF

Hemipentahydrate NF and pentahydrate NF were prepared by hydration of anhydrous NF Form A at specified % RH level. Anhydrous NF Form A was placed under 75% RH and 100% RH at ambient temperature for 1 week to yield hemipentahydrate NF and pentahydrate NF, respectively (Katdare et al., 1986; Yuasa et al., 1982). Additionally, pentahydrate NF was also prepared by suspending anhydrous NF Form A in excess amount of double distilled water with continuous stirring. Dispersed solid was filtered and dried at ambient condition.

Solid state characterization of NF hydrates

Thermal analysis

The thermal properties of NF crystalline hydrates were evaluated using DSC with STAR^{e} software. Samples (5 mg) in aluminum pan with one pinhole were evaluated from 30-230 ^{o}C at a scanning rate of 10 ^{o}C/min under nitrogen purge at 60 ml/min.

TGA/SDTA was employed to investigate the liberation of volatile substance. The TGA operating conditions were the same as those used in the DSC study.

Hot stage microscopy (HSM)

HSM equipped with optical microscope was employed to evaluate solvates or hydrates (Vitez et al., 1998). Heating rate and temperature range were 10 $^{\circ}$C/min and 30-240 $^{\circ}$C, respectively. A small amount of sample was initially suspended in mineral oil and placed on a glass slide before being fixed on to the heating station. The liberation of gas bubbles at specified temperature was observed and recorded.

Karl Fischer titrimetry (KF)

The water contents of NF hydrates were monitored. Due to low solubility of NF hydrates in methanol, heating oven was selected as an additional attachment. Approximately 50 mg of the sample was inserted into the heating oven. The oven temperature of 160 $^{\circ}$C was gradually increased to initiate the evaporation of water molecules. Water vapor was carried by dried nitrogen gas to react with KF reagents in the titration vessel where water contents were finally quantified.

X-ray Powder Diffraction (XRPD)

X-ray diffractometry was done with CuKα radiation at 40 kV and 20 mA. Samples were measured at a step size of 0.04 °2θ with a scan speed 5 °2θ/min from 5° to 35 °2θ.

Fourier Transformed Infrared Spectroscopy (FT-IR)

ATR FT-IR was employed to observe the changes in peak position between anhydrous NF and NF hydrates. The samples were triturated and gently ground with dried potassium bromide in an agate mortar. The spectra were recorded as percent transmittance (%T) with respect to wave number (ν) in the range of 450 to 4000 cm^{-1}.

Stability Indicating High Performance Liquid Chromatography (SI-HPLC)

SI-HPLC method was modified from the method used by Cordoba-Borrego et al.(1999). HPLC equipped with Hypersil BDS-C18 column in conjunction with C18-guard column was used. The mobile phase comprised of 0.1% v/v aqueous o-phosphoric acid:

acetonitrile at volume ratio of 70:30. The flow rate was equal to 1 ml/min. UV detection was carried out at 278 nm. Degradation product of NF was prepared by dispersing anhydrous NF in 30%w/v hydrogen peroxide in clear glass vial and was exposed to light and heat (80 °C) in an oven up to 8 hours. In addition, forced degradation in basic environment condition was evaluated according to the method used to prepare trihydrate NF. Small amount of anhydrous NF was added to 20% w/v aqueous ammonia solution and heated at 80 ^{O}C to initiate degradation.

Scanning Electron Microscopy (SEM)

The morphology of sample was recorded with a SEM at 15kV. The sample was carefully attached on the metal stub. It was then coated with gold by Sputter coater for 3 minutes at 0.05 mbar, 15mA with a working distance of 5 cm.

Solid State Interconversion of NF Hydrate

In an attempt to explore the interconversion pathways among NF hydrates and the anhydrous form, specific conditions were identified. Temperature and surrounding % RH were of main interest.

Effect of Relative Humidity on the Conversion of Anhydrous NF and NF Hydrates

The effect of relative humidity on the conversion of anhydrous NF Form A was evaluated. Preliminary study on sorption and desorption behaviors of anhydrous phase was investigated by dynamic vapor sorption (DVS) using symmetrical gravimetric analyzer. Fifteen milligrams of anhydrous NF Form A was dried in a vacuum at 25 ^{O}C for 6 hours to minimize traces of surface associated water. Isothermic equilibrium condition of the cycle was 0.01% w/w within 15 min with a maximum step time of 75 min. The step change of % RH in both sorption and desorption phase were 5% RH/step. The change in sample weight against % RH was recorded.

Due to limited amounts of the samples obtained by DVS experiments, the sample at each equilibrium % RH was not sufficient to be collected in order to monitor for their solid state characteristics by XRPD. Thus, larger amounts of anhydrous NF Form A were exposed to specific moisture levels. The generation of various % RH in an air tight and light resistant container was made by using saturated solutions of lithium chloride (11.3% RH), magnesium chloride (32.8% RH), potassium carbonate (43% RH), sodium bromide

(57.5% RH), sodium chloride (75% RH), potassium bromide (81% RH), potassium chloride (84% RH), dextrose monohydrate (87% RH), potassium nitrate (93.7% RH) and purified water (100% RH) at 25 $^{\circ}$C (Nyquist, 1983; Kotny and Conners, 2002). The sample powders were exposed to each relative humidity for 7 days before being characterized.

The preliminary results obtained by DVS and relative humidity exposures, indicated that phase transformation of anhydrous NF Form A to various stoichiometric hydrates occurred. Thus, every stoichiometric NF hydrate produced was subjected to an extreme moisture level of 100% RH and an extremely dry environment of 0% RH (Drierite®) and monitored for further transformation. The samples were stored for 7 days and then characterized by XRPD compared to the corresponding references. Additional storage time was needed in some cases where 7 days was insufficient to induce any changes in solid state transformation of NF hydrates.

Effect of Temperature on the Conversion of NF Hydrates

The temperature effect, particularly heating, was aimed to investigate dehydration of NF hydrates. A moderate temperature of 60 °C was selected in an attempt to avoid chemical degradation. NF hydrates were placed in the drying oven at 60 °C for 48 hours before being characterized by XRPD. However, additional exposure time up to one month was needed for some NF hydrates to confirm the solid state transformation.

Isothermal Dehydration of NF Hydrates

In order to control the effect of particle size on thermal dehydration, particle sizing was carried out with sieve analysis. The particle sizes of sample were in the range of 150 to 250 microns by using sieve No. 100 and No. 60, respectively.

Isothermal dehydration of NF hydrates was performed by isothermal DSC (IDSC). Four levels of isothermal dehydration temperatures (T_{iso}) were 80 ºC, 85 ºC, 90 ºC and 95 ºC. Each sample was weighed approximately 20 mg and placed in aluminum pan (100 μl) with manually pierced lid and sealed. It was then positioned onto DSC and the power level of DSC was monitored as a function of dehydration time (t_{iso}). Nitrogen gas, with a flow rate of 60 ml/min, was purged into the system as a protective gas to prevent any possible oxidative reaction at high temperature.

From the preliminary test, the T_{iso} for different NF hydrates were varied depending on the nature of the hydrate structures. The results showed that trihydrate NF and pentahydrate NF consisted of two steps of dehydration. Thus, the solid samples for the

above NF hydrates were investigated at the end of each dehydration step. Unfortunately, hemipentahydrate NF did not show distinct steps of dehydration like trihydrate NF and pentahydrate NF. Therefore, the solid sample of hemipentahydrate was only obtained at the end of complete dehydration test.

The water content, particle size and crystal structure of dehydrated NF hydrates were measured by TGA, laser diffraction particle size analyzer and XRPD, respectively. The physical appearance of dehydrated sample was also observed with scanning electron microscope (SEM).

Determination of Dehydration Energy of NF Hydrates

Quantitative determination of energy used during dehydration was calculated based on the concept of the area under the curve (AUC) of IDSC thermogram. Total AUC obtained by trapezoidal rule from energy consumption-dehydration time profile was defined as the dehydration energy (Kishore, 1978). In addition, the determination of AUC of the dehydration of NF hydrate was specifically defined due to an uncommon IDSC thermogram seen from preliminary studies (Figure 1). During the early period of experiment, the power of IDSC was increase due to the equilibration of system (from point A to B). The later step from point B to C was an endothermic dehydration reaction. Thus, the extrapolation from point B to A' was additionally done and calculated as a part of the total AUC. Therefore, the total AUC was equivalent to the summation of the AUC of early stage of dehydration (from A' to B) and the AUC of the later stage of dehydration (from B to C).

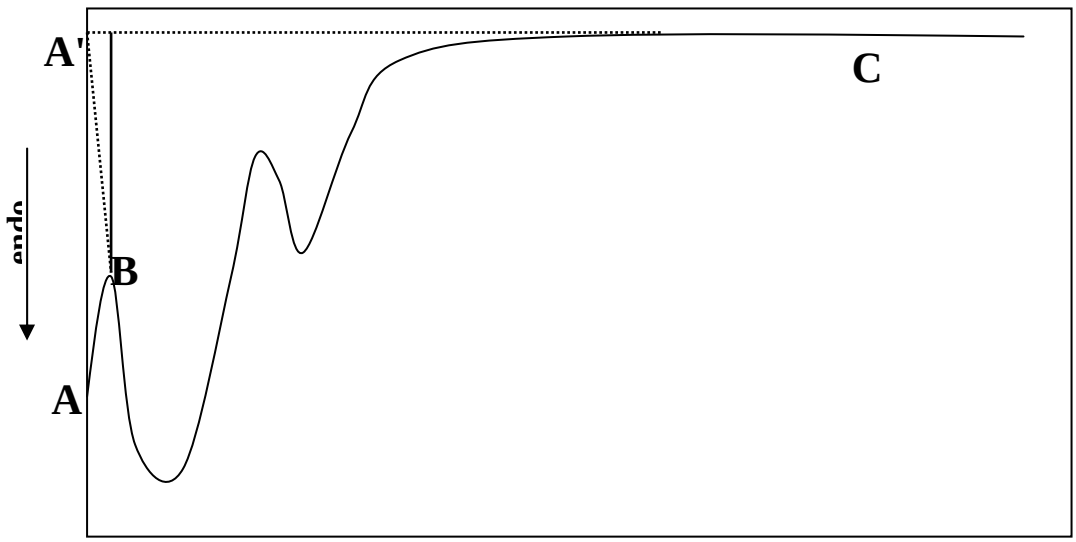

Figure 1 Model of IDSC thermogram of NF hydrate during isothermal dehydration

On the other hand, the calculation of activation energy (E_a) for dehydration was determined by both model dependent and model independent solid state kinetic. Model dependent kinetic was determined from a plot of ln k from the solid state kinetic model versus reciprocal absolute temperature (1/T) provides E_a of dehydration from the slope ($-E_a/R$) (Byrn et al., 1999). Model independent kinetic, the slope from linear relationship of ln t and 1/T was calculated and resolved as E_a of dehydration (Dong et al., 2002 and Zhou et al., 2003).

บทที่ 3

RESULTS AND DISCUSSION

Solid State Characterization of NF Hydrates

Anhydrous NF starting material was characterized by XRPD, DSC and TGA. TGA revealed negligible mass loss of less than 1% w/w which was in accordance with USP and BP specifications of anhydrous NF (USP 27; BP 2002). DSC and TGA thermograms of various NF forms are shown in Figure 2. DSC confirmed a single sharp endotherm at a temperature range of approximately 220 to 225 °C for anhydrous NF (Figure 2A). XRPD of anhydrous NF (Figure 4A) showed characteristic peak positions identical to those reported for NF Form A (Barbas et al., 2006; Katdare et al., 1986; Yuasa et al., 1982). It was hence concluded that the anhydrous NF in our experiment was polymorphic anhydrous NF Form A.

Slow recrystallization of NF solution in IPA:water mixture resulted in dihydrate NF. Thermal properties and water content of this hydrate are shown in Figure 2C. DSC and TGA thermograms showed endothermic peaks along with weight loss at the same temperature range of 80 to 140 °C. HSM also showed water vapor bubbles within the same temperature range (Figure 5F). Water content obtained by KF titration agreed well with the weight change obtained by TGA (Table 1) which indicated a stoichiometric dihydrate formation. XRPD pattern of the dihydrate NF was not reported in any previous publications for reference. Thus, a single crystal X-ray diffraction (SC-XRD) data from crystals obtained by the above recrystallization method was compared to NF dihydrate single crystal X-ray diffraction data reported by Florence et al. (2000) and were found to be identical. Therefore, the experimental XRPD pattern of NF dihydrate (Figure 4C) was confirmed by the calculated powder diffraction pattern generated from SC-XRD data by MERCURY® software and served as reference XRPD pattern for dihydrate NF in future experiments. However, this recrystallization process was time-consuming and chemical degradation of NF is of great concern. The results obtained from SI-HPLC of the recrystallized NF dihydrate did not show degradation (Figure 3). Thus, the quality of NF dihydrate produced was essentially free from degraded compounds and was acceptable to be used as the reference for future studies.

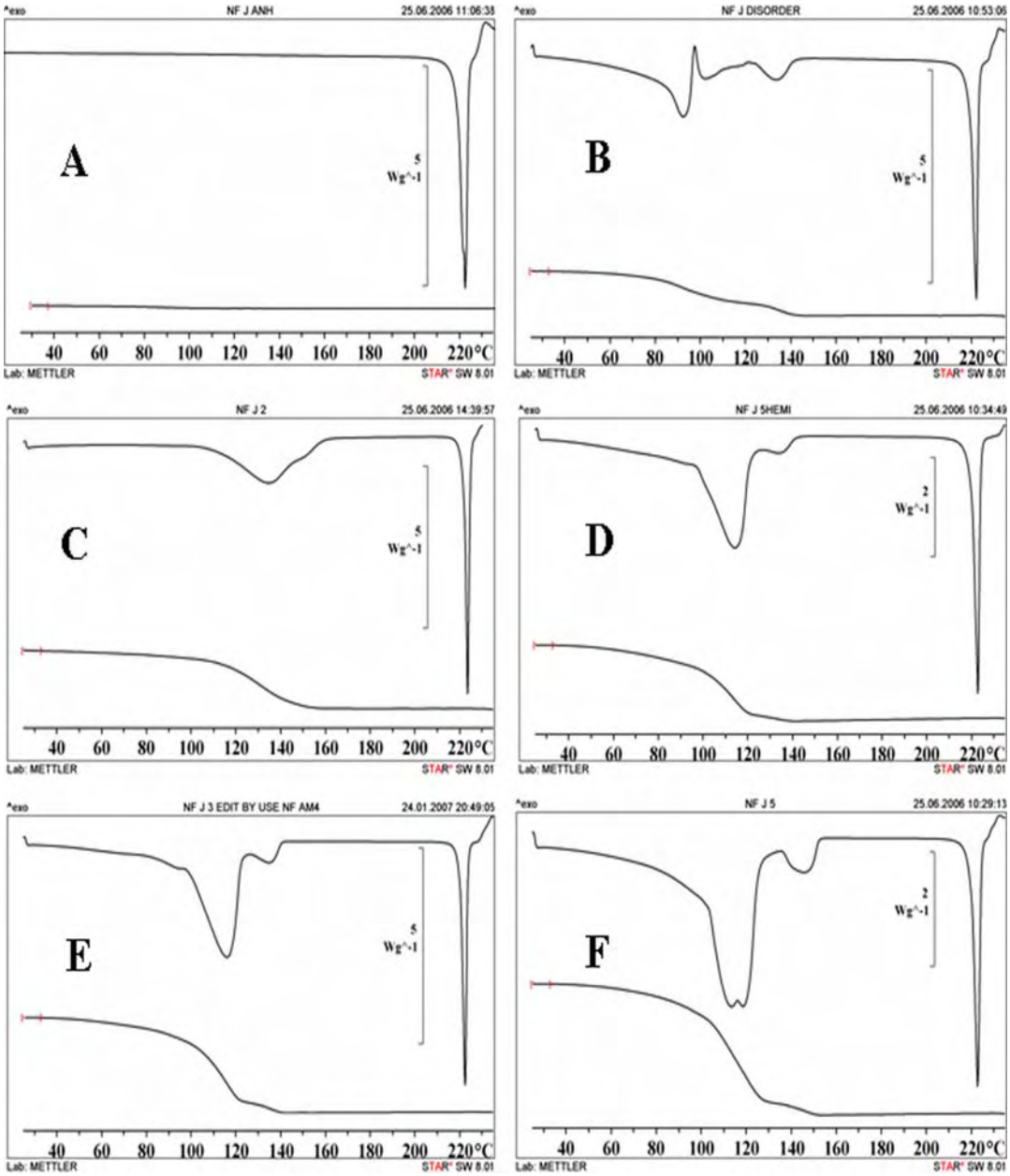

Figure 2 DSC and TGA thermograms of anhydrous NF Form A (A), disordered NF state (B), dihydrate NF (C), hemipentahydrate NF (D), trihydrate NF (E) and pentahydrate NF (F)

Table 1 Water content (KF), percent weight loss (TGA) and stoichiometry between NF and water molecules

Method of preparation	**KF water content (%)**	**TGA % weight loss**	**Stoichiometry (NF:water molecule)**
Desiccation NF pentahydrate	5.55(0.561)	6.24(0.372)	---
Recrystallization from IPA:water mixture	10.10 (0.080)	9.34 (0.136)	1:2
Exposure to 75% RH	11.55 (0.611)	12.12 (0.039)	1:2.5
Precipitate from aqueous ammonia solution	14.49 (0.342)	14.81 (0.046)	1:3.0
Exposure to 100%RH	20.55 (0.367)	20.87 (0.153)	1:5.0

SD shown in parentheses.

Trihydrate NF generated from antisolvent precipitation was characterized. The results from HSM confirmed the existence of solvate or hydrate as seen from the evolution of vapor bubbles during heating. DSC yielded a large endotherm immediately followed by another minor endotherm at the temperature range of 80 to 130 °C (Figure 2E). Total weight loss obtained by TGA was 14.81% w/w and occurred at the same temperature range as that of the DSC endotherm (Figure 2E). Meanwhile, KF confirmed the trihydrate stoichiometry of the crystalline precipitate (Table 1). XRPD pattern shown in Figure 4E was used as reference XRPD pattern of trihydrate due to the fact that no reference XRPD pattern was available in any previous works. In addition, SI-HPLC did not detect any NF degradation after trihydrate NF was generated (Figure 3).

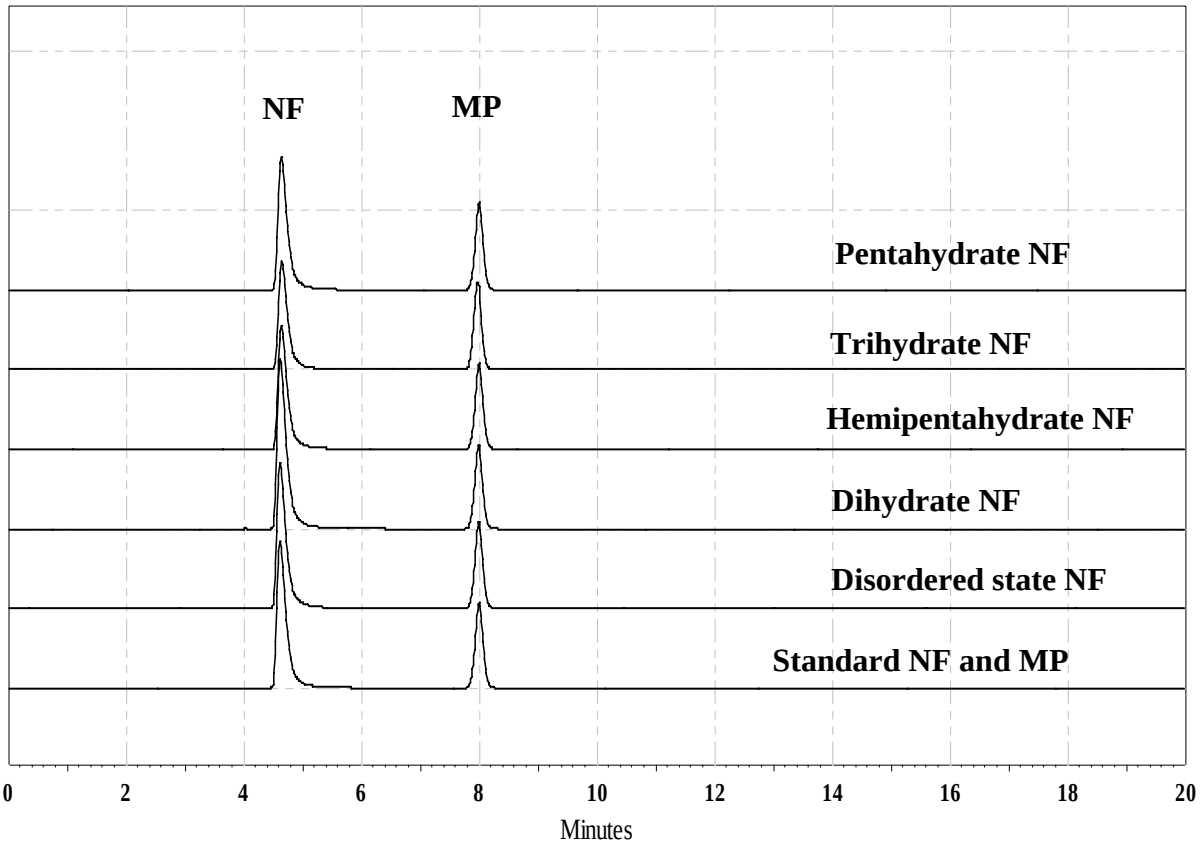

Figure 3 Comparative HPLC chromatograms of various hydrates NF with standard NF in conjunction with the use of methyl paraben (MP) as internal standard

DSC analysis of the hemipentahydrate NF (Figure 2D) and the pentahydrate NF (Figure 2F) which were produced from direct exposure to moisture, showed large endotherm followed by a smaller endotherm at approximately 120 °C and 140 °C, respectively. TGA showed a two step weight loss at the same temperature as achieved by DSC. The total weight loss from TGA and the water content obtained from KF were in good agreement confirming the stoichiometry of the hemipentahydrate NF and the pentahydrate NF (Table 1). HSM showed continuous liberation of vapor bubbles during the temperature ranges corresponding to their DSC and TGA dehydration endotherms (Figure 5A to 5D). XRPD of both hydrates are illustrated in Figure 4D and 4F and the XRPD patterns were essentially the same as XRPD of the hemipentahydrate NF and the pentahydrate NF reported by Yuasa et al (1982).

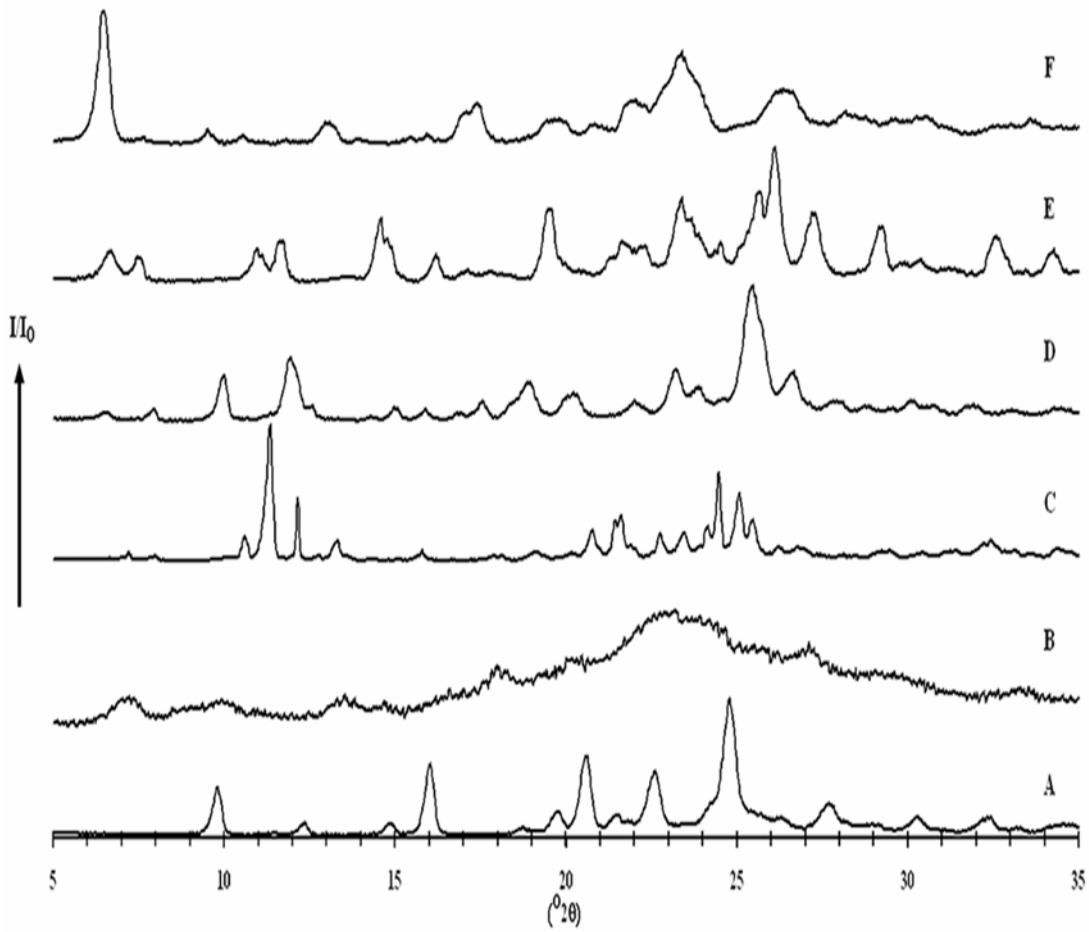

Figure 4 XRPD patterns of anhydrous NF Form A (A), disordered NF state (B), dihydrate NF (C), hemipentahydrate NF (D), trihydrate NF (E) and pentahydrate NF (F)

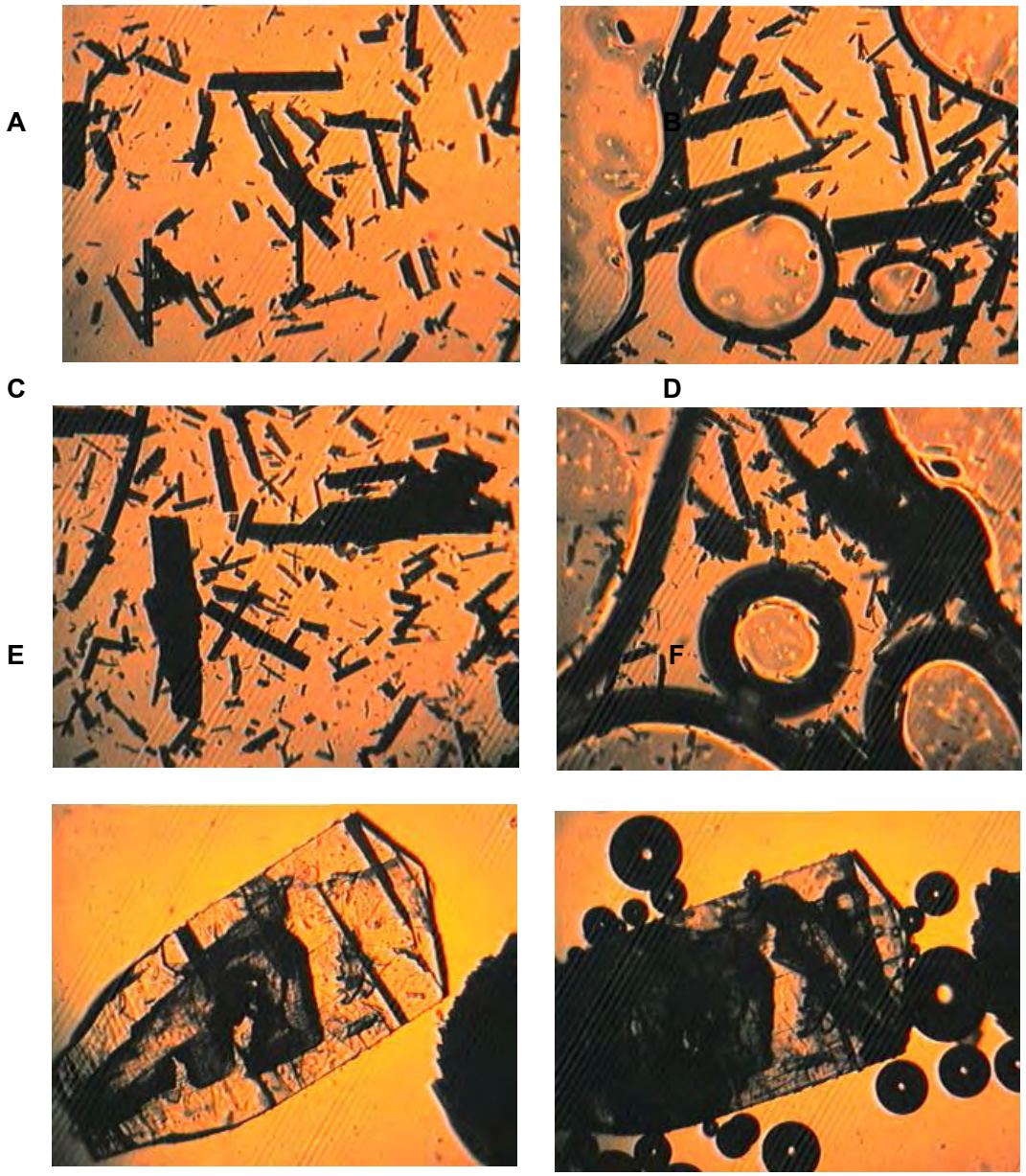

Figure 5 HSM photomicrographs of NF hydrates immerse in mineral oil upon heating (hemipentahydrate NF at ambient temperature (A), hemipentahydrate NF at temperarature over 120°C (B), pentahydrate NF at ambient temperature (C), pentahydrate NF at temperarature over 120°C (D), dihydrate NF at ambient temperature (E), dihydrate NF at temperarature over 100°C (F))

Pentahydrate NF, which was obtained from an alternative method of suspending anhydrous NF Form A in water also provided the same thermal behavior and XRPD pattern as the one hydrated NF at 100% RH. However, the crystal habits of the two pentahydrate NF were different. SEM micrographs of each solid were generated. Light yellow and coarse powder of anhydrous NF Form A (Figure 6A) was converted to opaque white, needle-like fluffy pentahydrate NF after having directly came into contact with water (Figure 6C). In contrast, exposure of anhydrous NF Form A to 100% RH did not change the appearance of the original powder (Figure 6A) even when the structure was found to be converted to the pentahydrate NF.

A different method of preparation and level of moisture in an environment greatly impacted on the formation of hydrate NF. The direct contact between anhydrous NF Form A with water was an issue. The precipitation of dispersed anhydrous NF Form A in excess amount of water was filtered and dried at ambient condition. An intact physical appearance of anhydrous NF Form A (light yellow fine powder) was rapidly converted to fluffy and waxy solid with opaque white color. SEM photomicrograph of solid obtained was fine needle-like particles fused together forming a network (Figure 6). It might be due to water partially dissolved the surface of anhydrous NF crystal and recrystallized and bridged together as NF hydrates. Light microscopy was used to investigate such phenomena. Anhydrous NF Form A with a drop of water was prepared on glass slide. The result suggested that the transformation of anhydrous NF Form A to the new unknown form immediately happened after contact with water (Figure 7B-D). The longer the contact time the more developed the new unknown NF form. The new unknown form was characterized and found to be pentahydrate NF. Thus, different methods of preparation could provide an identical internal structure of NF hydrate with different observable habit.

The phase transformation of anhydrous NF Form A to pentahydrate after direct contact with water is a valuable data for the pharmaceutical industries. Some made NF tablets by wet granulation with aqueous binder showed the physical transformation of powder blend after binder was added. The new physical character of the powder blend was hard and waxy agglomerates. It directly impact on the mixing efficiency and working capability of mixer. In the case of low efficiency mixer, mixer was usually broken during the mixing/granulating process. High efficiency mixer could overcome the above problem. However, the uniformity of powder blend was argued. It was suggested that a new phase in powder blend was strongly contributed from the transformation of anhydrous NF Form A to the pentahydrate NF with needle-like appearance. Non-aqueous binding solution was

suggested to protect the solid state transformation of anhydrous NF Form A.

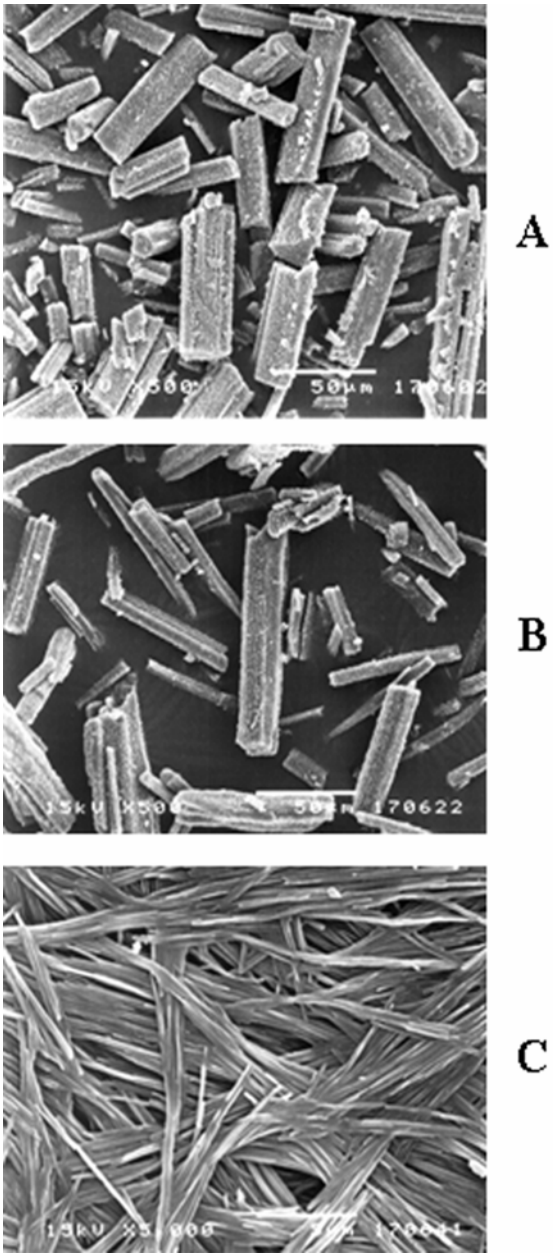

Figure 6 Scanning electron photomicrographs of anhydrous NF Form A (A), pentahydrate NF obtained from 100%RH vapor exposure (B) and pentahydrate NF from directly dispersed in water (C)

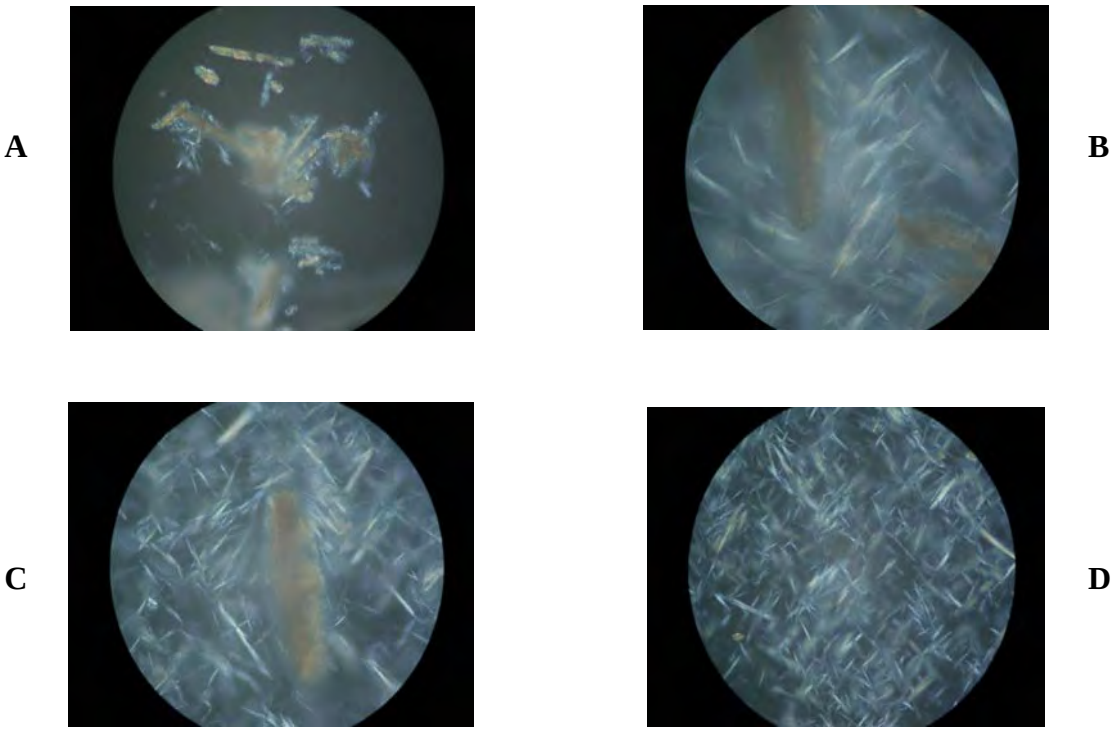

Figure 7 Photomicrographs of anhydrous NF Form A after dispersed in water at various contact time at the magnification of 400. (A. initial, B. 15 minutes, C. 60 minutes and D.180 minutes)

Another NF hydrate form found in this study, the disordered NF state, has not been previously reported elsewhere. Dehydration of pentahydrate NF via desiccation over time produced a so-called disordered NF state. DSC and TGA of the disordered NF state are shown in Figure 2B where a complex dehydration behavior was observed. Dehydration was detected during the first broad endotherm (100 °C) and immediately followed by a sharp exotherm (115 °C) and another broad endotherm. Mass loss of disordered NF state also took place over the same temperature range as found in the DSC. The sharp exotherm was possibly due to the rearrangement of NF molecules after water molecules were partially removed. Disordered NF provided an XRPD pattern similar to the amorphous material (Figure 4B). However, minor peak intensity in certain regions could still be observed. In comparison with amorphous NF (Šuštar et al., 1993), the DSC of disordered NF showed large endotherm with rapidly changing exotherm at the range of approximately 80 ºC to 110 ºC while amorphous NF exhibited an endotherm immediately followed by an exotherm from 80 to 150 ºC. In addition, disordered NF showed two broad endothermic peaks while this thermal behavior was not seen in an amorphous NF upon heating. Thus, the disordered NF was believed not to be a true amorphous but only microcrystalline disorder state. The

mild condition used to remove water molecules from pentahydrate NF might perturbed the crystal structure and led to a new arrangement or disordered state. Thus, short range order of crystal lattice was still preserved. Amorphous or disordered state generally occurred with anhydrous materials. However, some amorphous materials absorbed water molecules in the structure. For example, raffinose pentahydrate could become amorphous with water content equivalent to stoichiometric monohydrate (Hogan and Buckton, 2001).

In order to characterize the complex thermal behavior of the disordered NF, XRPD was utilized to monitor the molecular rearrangement of intact and heated disordered NF at predetermined times by using DSC. One sample was heated from 25 to 120 $^{\circ}$C (D-I) and the other sample was heated from 25 to 160 $^{\circ}$C (D-II). The DSC thermograms of heated sample of D-I and D-II are illustrated in Figure 8. DSC thermogram of D-I showed a complete disappearance of the initial complex thermal behavior comprised of large endotherm with followed by rapid exotherm. Subsequently, D-II exhibited the thermogram consisted of only second endotherm after the initial thermal event was removed. It indicated that two complex thermal events of disordered NF did not have any interaction together. After the first two events were removed, DSC thermogram displayed only one sharp endotherm correlated to the melting endotherm of anhydrous NF Form A. It could be initially concluded that two locations of water molecules of disordered NF were separated in different lattice space. Moreover, the XRPD pattern of D-I is displayed in Figure 9B. It showed increased in crystallinity compared to the initial disordered NF. Initial disordered NF was also heated from and its XRPD pattern is illustrated in Figure 9C. The solid obtained after D-II exhibited higher order than that of initial disordered NF and after D-I treatment. The XRPD pattern was shown to be identical to that of the anhydrous NF Form A. TGA confirmed that the solid obtained after D-II treatment showed no weight loss. It could, hence, be concluded that solid collected after D-II treatment is an anhydrous Form A. The total weight change from D-I to D-II was approximately 1.64% which was higher than the value allowed for anhydrous NF in the official monographs (less than 1%) (USP 27; BP 2002). Thus, the solid resulted from D-I treatment was a hydrated transitional phase which, in turn, would convert to the anhydrous Form A upon further heating. In addition, the water content of hydrated transitional phase obtained from TGA was in the range of 2.5 to 3.5 %w/w that was in the range of hemipentahydrate NF form. It should be indicated the hydrated transitional phase was the one hydrate form of NF.

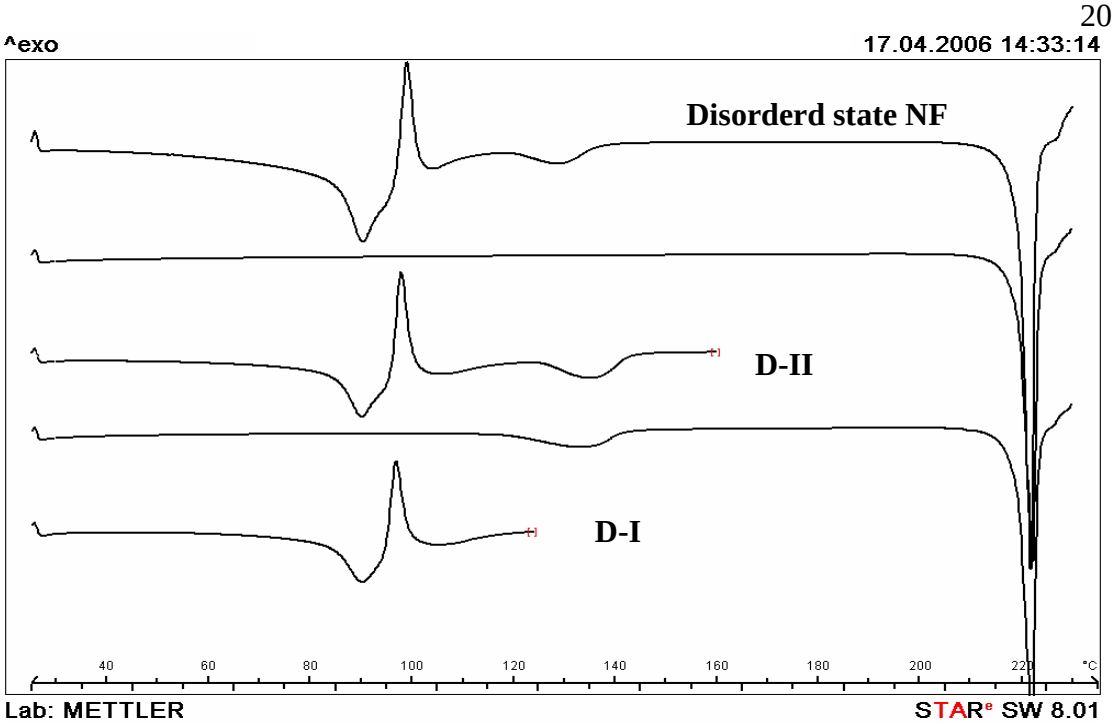

Figure 8 DSC thermograms of disordered NF with respect to different heating temperature programs

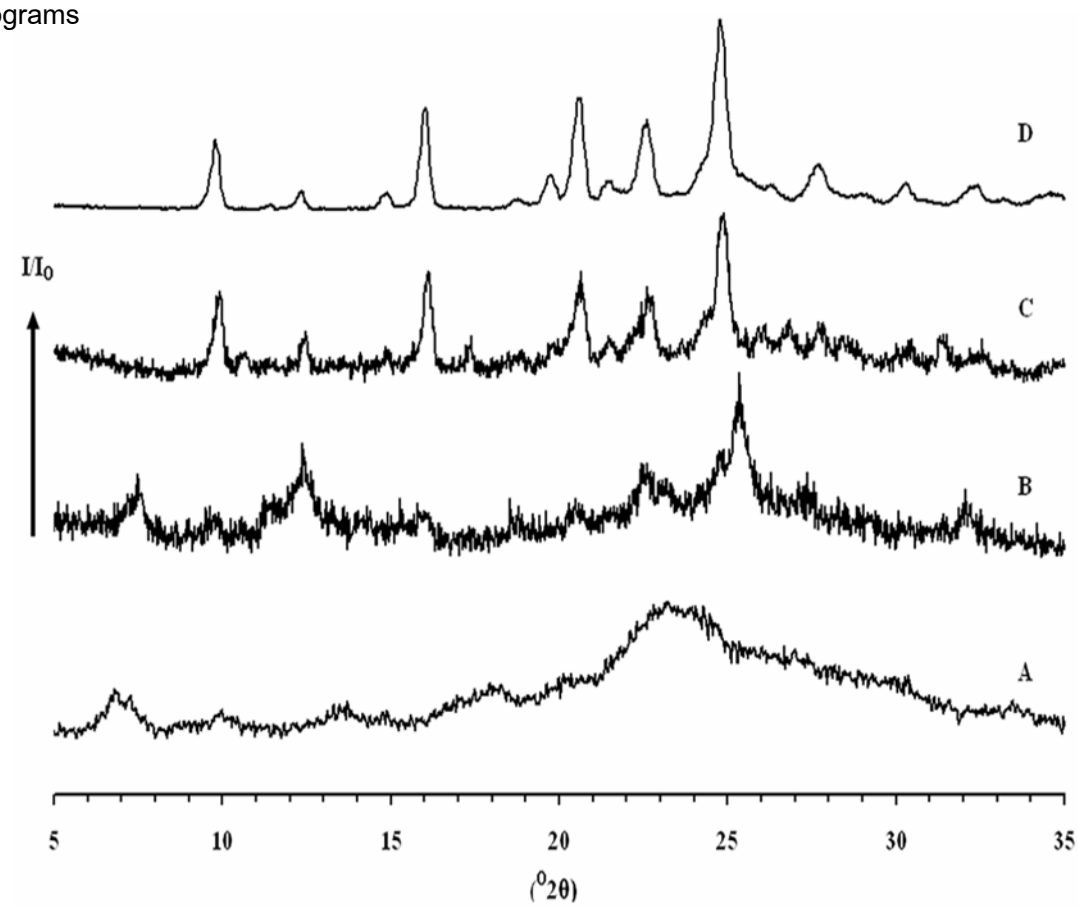

Figure 9 XRPD patterns of disordered NF state (A), after D-I (B), after D-II (C) and anhydrous NF Form A (D)

In general, materials of disordered molecular arrangement are more sensitive to moisture than the ordered crystalline phase. Consequently, the moisture sensitivity of the disordered NF was a critical issue. The disordered NF was thus exposed to various humidity levels for 7 days and the XRPD patterns were recorded (Figure 10). The transformation of the disordered NF to the crystalline pentahydrate NF form was completed when at least 57% RH was used. At 32.8% RH, partial transformation to the pentahydrate was seen according to the presence of peaks at 6.40, 13.00, 17.28, 23.36 and 26.20 °2θ. On the other hand, the disordered NF state was stable under 11.3% RH for at least 2 months similar to the XRPD pattern after 7 days exposure to 11.3% RH. Thus, exposing the disordered NF to more than 32.8% RH would eventually generate the crystalline pentahydrate NF. However, at humidity of 11.3% RH or below, the disordered NF structure was retained.

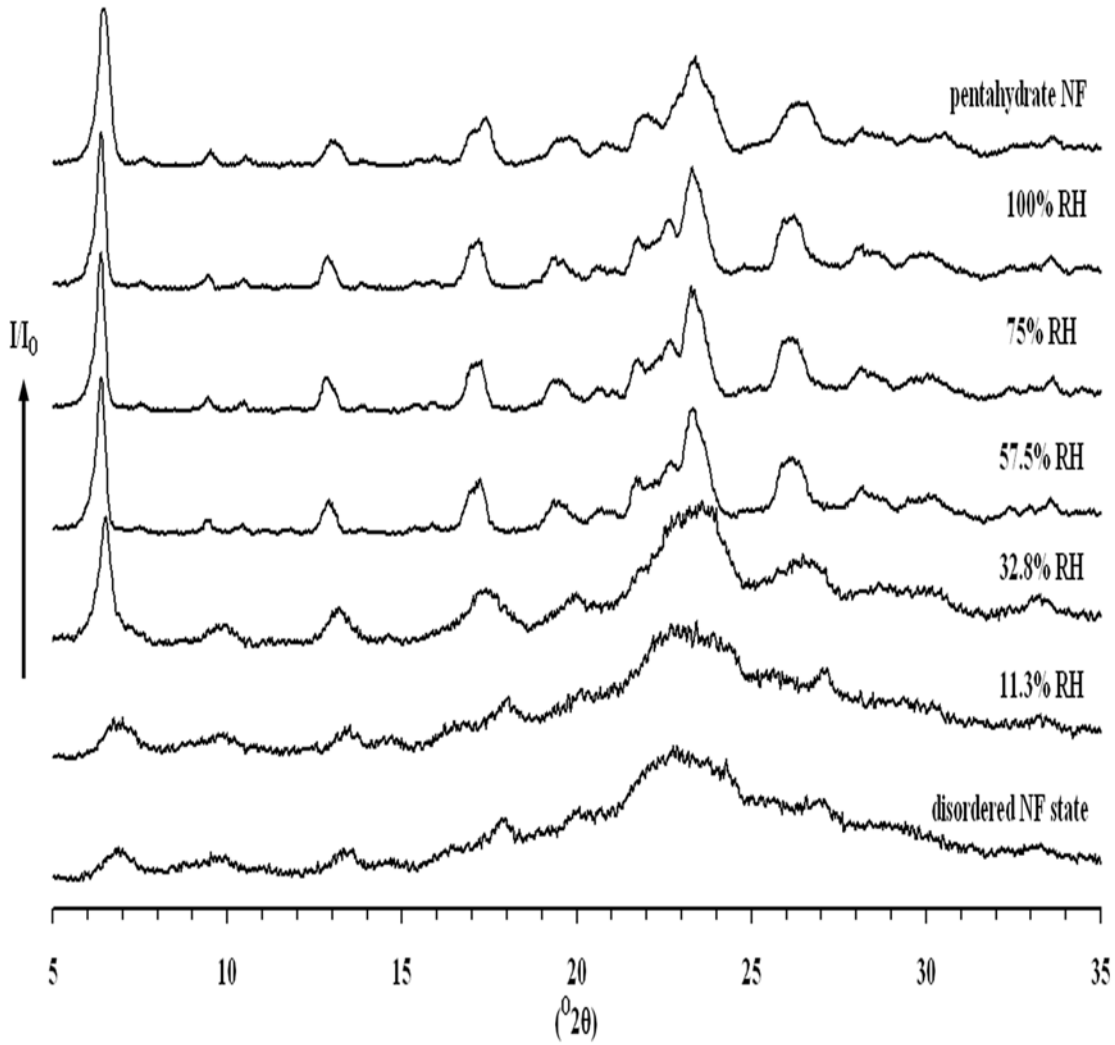

Figure 10 XRPD patterns of disordered NF states exposed to different relative humidity for 7 days

Chemical interaction between water of crystallization and active moiety of every NF hydrate was investigated by spectroscopic FT-IR. The spectra of every NF hydrate form were recorded and compared (Figure 11). The signal at specific wavenumber can be interpreted in terms of the functional group of the material. The IR spectrum of anhydrous NF Form A exhibited main absorption peaks at 1732 and 1253 cm^{-1} indicating C=O and C-O bond stretching of carboxylic group, respectively. When water molecules are incorporated into the crystal structure, the response of C=O and C-O are found to gradually decrease as a function of increased number of water of crystallization (Mazuel, 1991). Meanwhile, the responses at 1584 and 1340 cm^{-1} of carboxylate anion are markedly increased. The above results suggested that structures of the carboxylic group in these hydrates are the carboxylate anion (Hu et al., 2002). In addition, the responses in the regions of 3700 to 3250 cm^{-1} owing to OH stretching were clearly present in all NF hydrates, signifying hydrogen bonding between carboxylic group and water molecules in the crystal structure (Byrn et al., 1999). The FT-IR spectrum of the disordered NF was also investigated. The presence of peaks at 1581 and 1334 cm^{-1} confirmed the occurrence of carboxylate anion identical to other hydrates and the lack of responses at 1732 and 1253 cm^{-1} confirmed that C=O and C-O stretching of carboxylic group was disturbed by water molecule as well. It can be concluded that water molecules in disordered NF formed structural hydrogen bonds with NF molecules similar to those of other stoichiometric hydrates. Thus, it is believed that the disordered NF form was not a true amorphous state but a metastable phase with short range ordered structure.

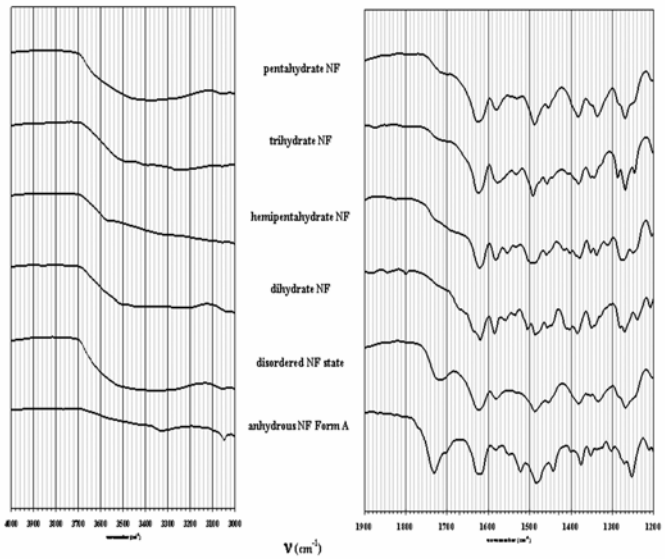

Figure 11 FT-IR spectra of anhydrous NF Form A, disordered NF state and other stoichiometric hydrates of NF

Solid State Interconversion of NF Hydrates

XRPD patterns of NF hydrates (Figure 4) were used as reference patterns to show specific characteristics of each form and were used to identify the solid state transformation. The following studies gathered evidences on the solid state transformation of NF hydrates under different environmental i.e. relative humidity and temperature. It should be noted that the observed trends are based on visual inspection of the diffraction patterns and are not intended to be quantitative.

Effect of Relative Humidity on Solid State Transformation of NF Hydrates

Moisture content in the environment usually plays the most pivotal part in hydrate formation of many organic compounds (Zhu et al., 1996a; Zhu and Grant, 1996b). The anhydrous NF Form A placed under different %RH were found to form varying stoichiometric NF hydrates (Katdare et al., 1986; Yuasa et al., 1982). The moisture sorption study was used as a rough evaluation on the hydrate formation behavior due to moisture. Moisture vapor sorption data of the anhydrous NF Form A obtained by DVS showed that under 60% RH, the anhydrous structure was retained (Figure 12). On the other hand, at moisture levels higher than 60% RH, anhydrous NF Form A showed a marked mass increase. The higher the relative humidity of the environment above 60% RH the higher the weight gain. The final solid structure formed at the end of the sorption phase was later found to be the pentahydrate NF by XRPD.

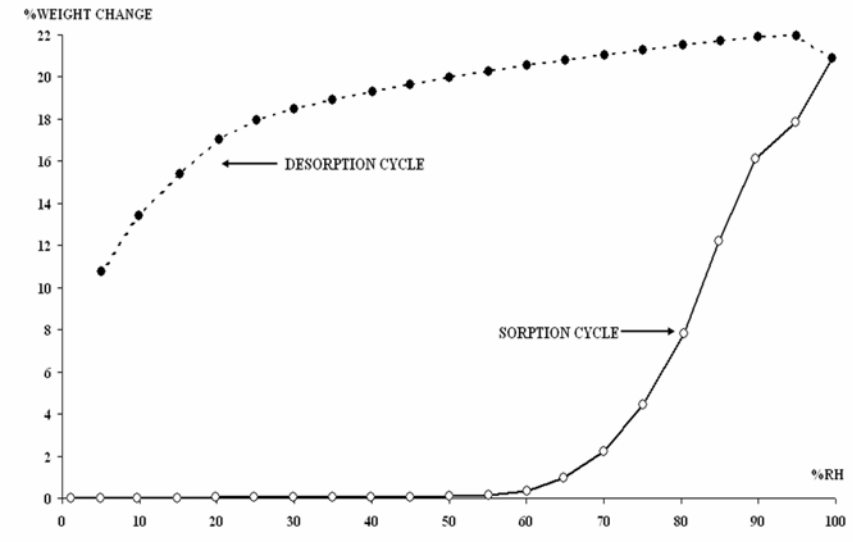

Figure 12 Dynamic water vapor moisture sorption and desorption isotherms of anhydrous NF Form A at 25°C

Desorption phase of the induced the pentahydrate NF showed that the pentahydrate NF was very stable even at below 30% RH. However, when the environment reached very low humidity of below 20% RH, significant weight loss occurred. The result suggested that for dehydration of the pentahydrate NF to occur the environment must reach very low relative humidity. These data could be used to determine a suitable storage condition of NF raw material. The suggested storage condition for the anhydrous NF Form A should be in an environment where moisture level is not more than 60% RH at room temperature. The pentahydrate NF form should not be stored in areas where relative humidity is below 20% RH to prevent dehydration.

The degree of hydration of anhydrous NF Form A with respect to relative humidity was investigated and characterized by XRPD (Figure 13). The hemipentahydrate NF was achieved when anhydrous NF Form A was exposed to 75%RH as mentioned in the previous section. XRPD patterns of the anhydrous NF Form A which were stored between 81%RH to 87%RH, however, showed mixed characteristics at 6.48 °2θ and 25.48 °2θ of the pentahydrate NF and the hemipentahydrate NF, respectively. Increasing the moisture level was found to accentuate the intensity of the peak at 6.48 °2θ. Meanwhile the intensity at 25.48 °2θ was reduced. When anhydrous NF Form A was exposed to humidity higher than 93.7%RH, pure pentahydrate NF was found. In addition, exposure of the anhydrous NF Form A at very high humidity did not generate any degradation products as confirmed by SI-HPLC.

NF hydrates were placed under 100%RH for 7 days after which XRPD patterns were recorded. The XRPD results revealed that every sample converted to the pentahydrate NF, except the dihydrate NF. The dihydrate NF exposed to 100% RH showed mixed characteristics of both dihydrate NF and pentahydrate NF (Figure 14). It could be inferred that the pentahydrate NF was the most stable form in extremely high moisture environments.

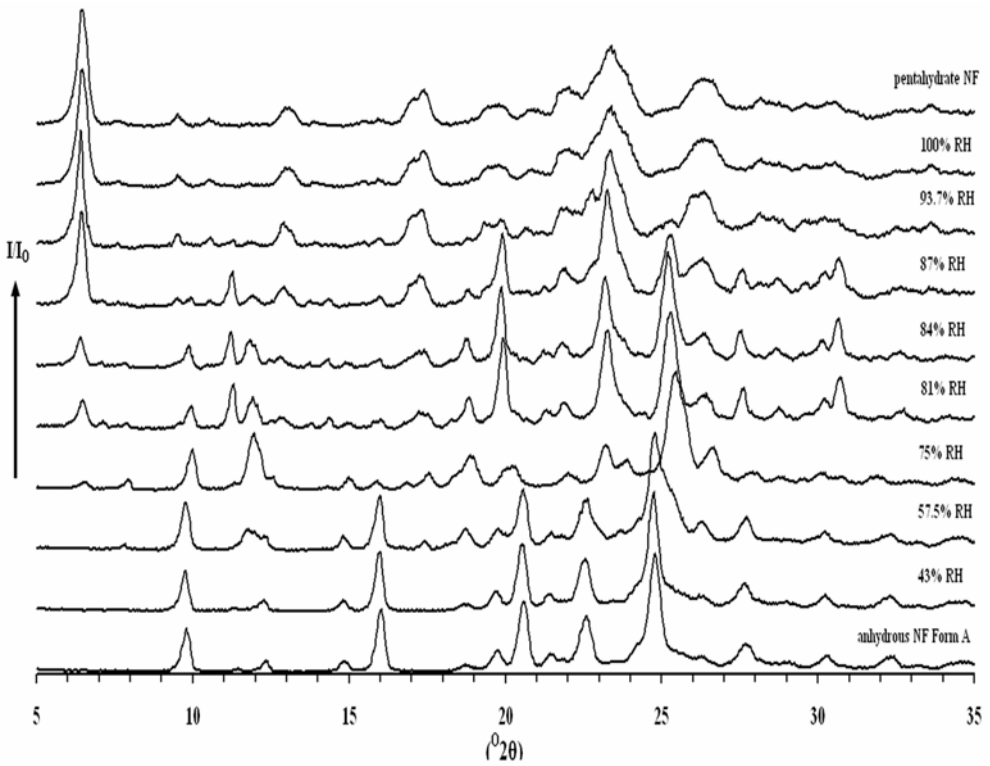

Figure 13 XRPD patterns of anhydrous NF Form A under different relative humidity for 7 days

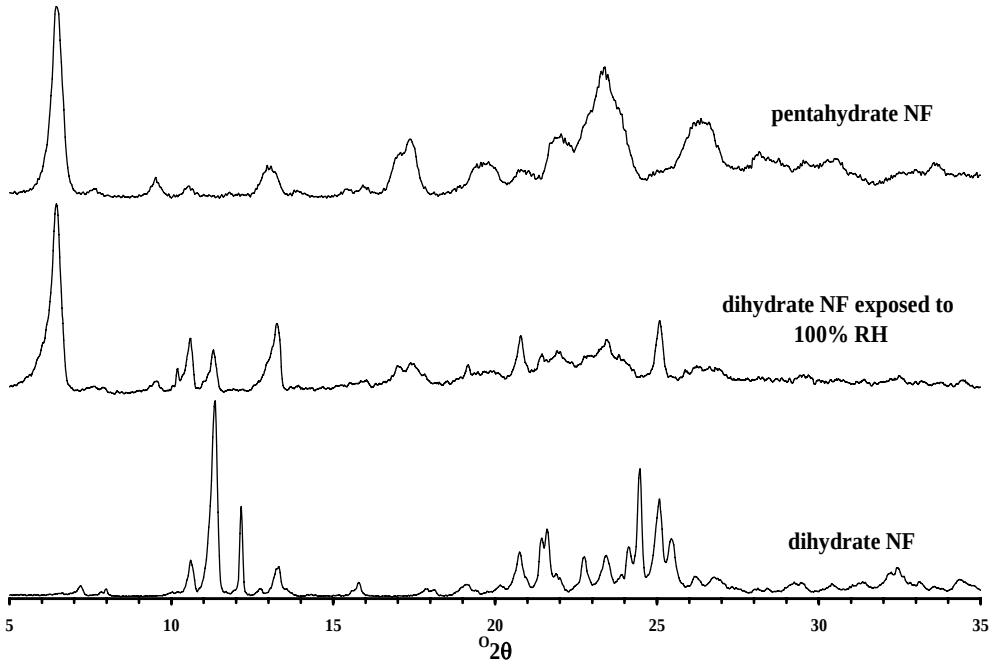

Figure 14 XRPD patterns of dihydrate NF under 100% RH for 7 days

On the other hand, the reduction to near 0%RH was also investigated. The pentahydrate NF was transformed to the disordered NF state as discussed earlier. The XRPD pattern of the hemipentahydrate NF at 0% RH is illustrated in Figure 15. The characteristic peak at 25.48 °2θ was slightly shifted to lower angle of 24.84 °2θ which corresponded to the anhydrous NF Form A. Meanwhile, the intensity at 26.68 °2θ gradually decreased as a function of exposure time. The longer contact time to dry environment led to the formation of a mixture of the two forms. The trihydrate NF showed the same phenomenon on the conversion to the anhydrous NF Form A during exposure to 0% RH condition. The XRPD patterns of the trihydrate NF during dehydration are shown in Figure 16. After 7 days of dehydration, peak responses at 9.84, 20.52 and 24.84 °2θ of the sample were found to be of the anhydrous NF Form A. Peak positions at 7.52 and 25.40 °2θ were also apparent and related to the hydrated transitional phase similar to the heat treated (D-I) of the disordered NF state (Figure 9B). Meanwhile, other strong and characteristic trihydrate peaks still existed. In summary, dehydration by reduction of environmental moisture was not an effective method to convert neither the hemipentahydrate NF nor the trihydrate NF to the pure anhydrous NF Form A even after 90 days exposure. Therefore, the dihydrate NF was not further evaluated due to lack of dehydration efficiency by this approach.

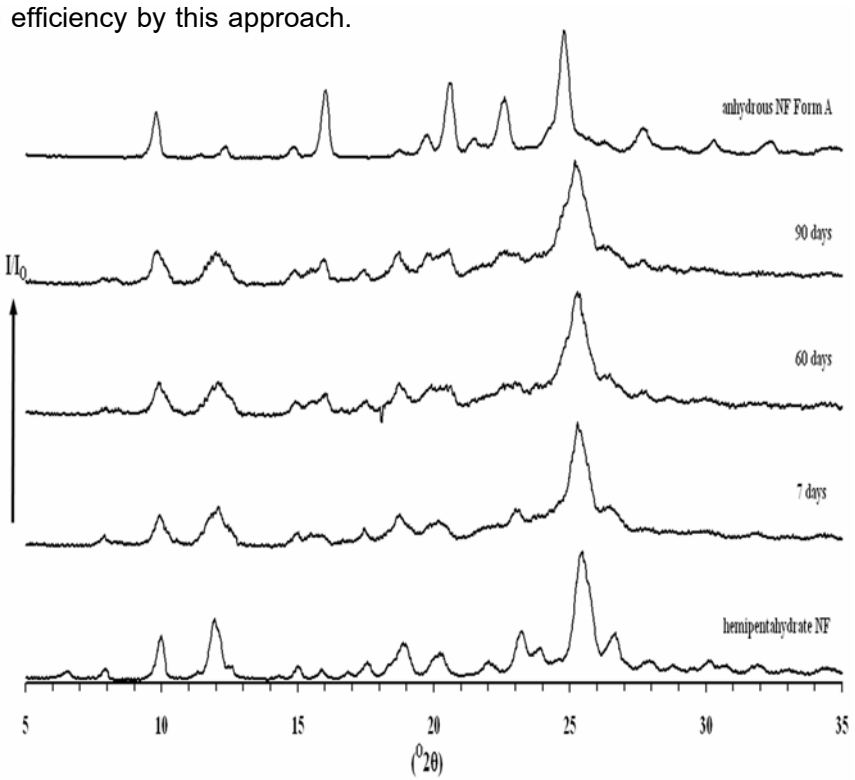

Figure 15 XRPD patterns of hemipentahydrate NF under desiccant (0% RH) as a function of exposure time

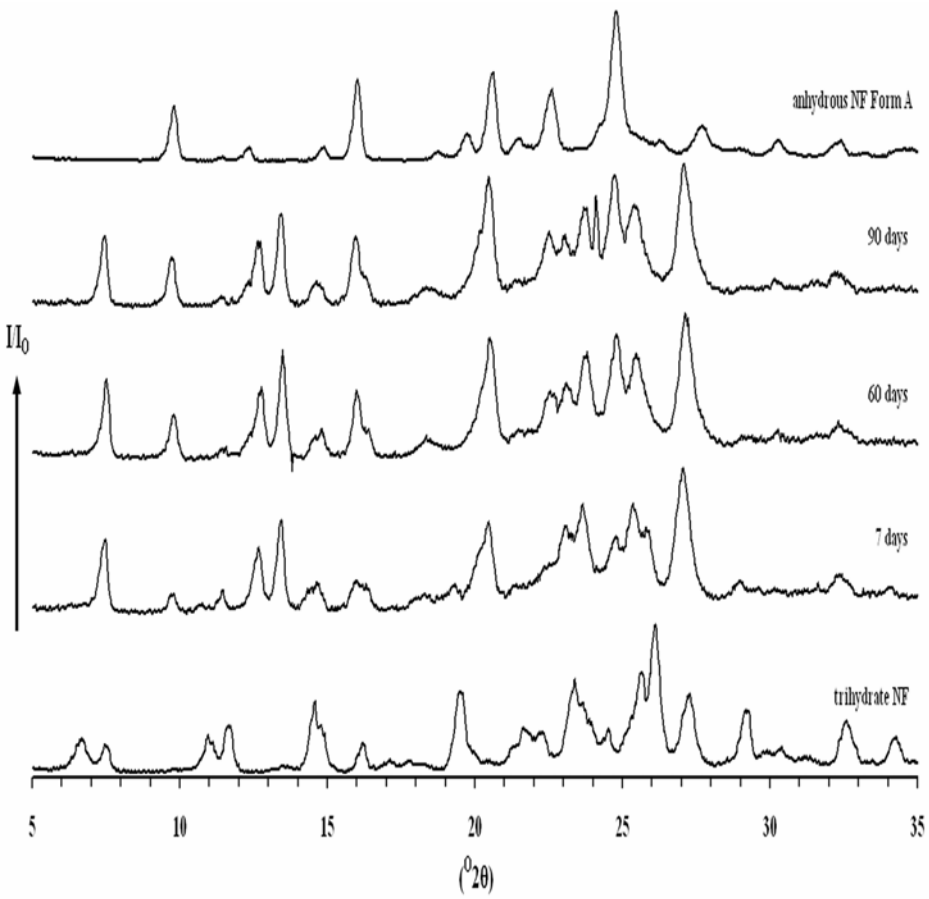

Figure 16 XRPD patterns of trihydrate NF under desiccant (0% RH) as a function of exposure time

Effect of Elevated Temperature on Solid State Transformation of NF Hydrates

Thermal dehydration is the most common way to prepare anhydrous materials in the pharmaceutical industry. There are many publications reported the polymorphic transformation or occurrence of desolvation upon thermal treatment (Lin and Chien, 2003; Willart et al., 2002; Landgraf et al., 1998; Hakanen and Laine, 1995). Hence, the conversion of NF hydrates using selected elevated temperature was performed. In this study, a moderate temperature of 60 °C was selected to minimize potential chemical degradation associated with higher temperatures.

The disordered NF was heated at 60 °C for 48 hours. XRPD showed that the anhydrous NF Form A was transformed from the disordered NF after heating (Figure 17B). The residual water content of the heated samples was investigated using KF. The water contents were 1.02, 0.60 and 0.46 for heated samples of the disordered NF, the hemipentahydrate NF and the pentahydrate NF, respectively. The results revealed that all heated samples were essentially anhydrous because the water content was approximately

at or below the maximum limit (1%) for NF anhydrous specified in the monograph (USP 27; BP 2002). In the case of the heated hemipentahydrate NF, the XRPD pattern was similar to that of the disordered NF (Figure 17C). Note that the heated pentahydrate NF resulted in a similar XRPD pattern to that of the anhydrous Form A but with two additional peaks at 7.52 and 25.40 °2θ (Figure 17D). These two peaks were assumed to be the residual of the hydrated transitional phase (Figure 9B) found during D-I treatment of the disordered NF state.

The results from the heated dihydrate NF and the heated trihydrate NF are shown in Figures 18 and 19, respectively. The XRPD of the dehydrated dihydrate NF revealed that a partial anhydrous phase was generated after thermal dehydration for 48 hours. However, peaks at 10.60, 11.32 and 13.16 and 25.00 °2θ corresponding to the dihydrate NF were still present. Extended heating time of up to 1 month gave material with an identical pattern to that of the 48-hour treated sample. Thus, the longer heating time did not fully convert the dihydrate NF to the anhydrous NF Form A. The trihydrate NF also behaved in the same way upon thermal dehydration. XRPD of the treated trihydrate NF showed the anhydrous Form A peaks at 9.80, 16.04, 22.68 and 24.84 °2θ. Additional peak position at 7.52 and 25.40 °2θ were also noticeable and related to the hydrated transitional phase while the trihydrate NF peak at 23.36 °2θ remained pronounced indicating a mixture of the three forms. Extended thermal dehydration of the trihydrate NF at 60°C of up to 1 month did not generate the pure anhydrous NF Form A.

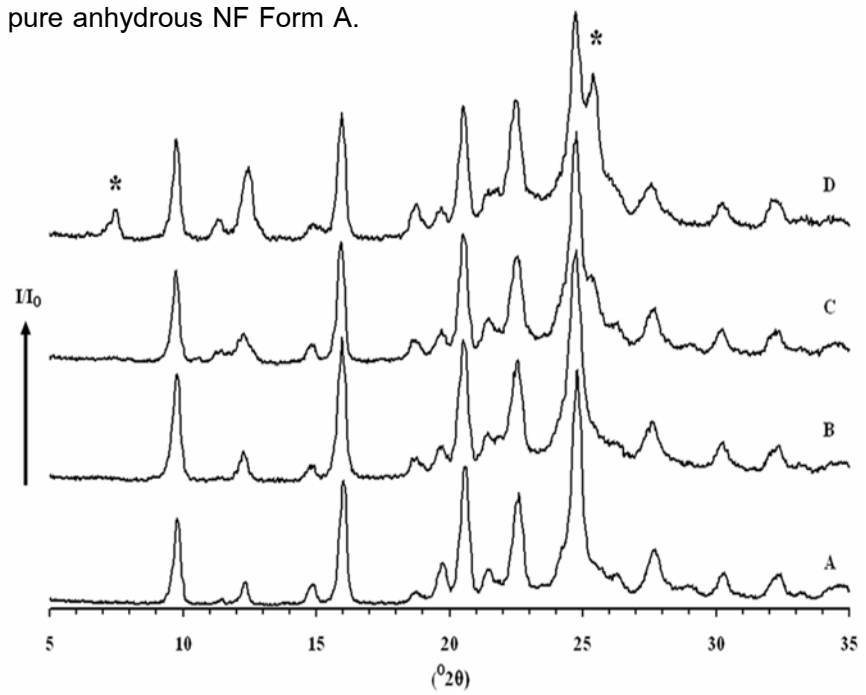

Figure 17 XRPD patterns of anhydrous NF Form A (A), disordered state NF (B), hemipentahydrate NF (C) and pentahydrate NF (D) after heated at 60°C for 48 hours

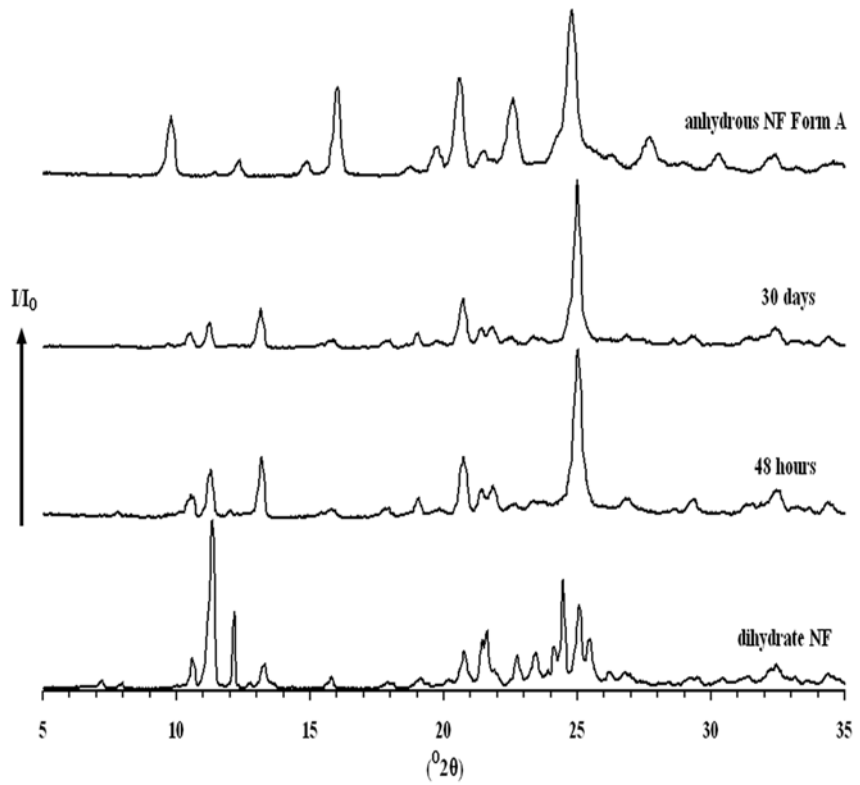

Figure 18 XRPD patterns of dihydrate NF after heated at 60°C for various time period

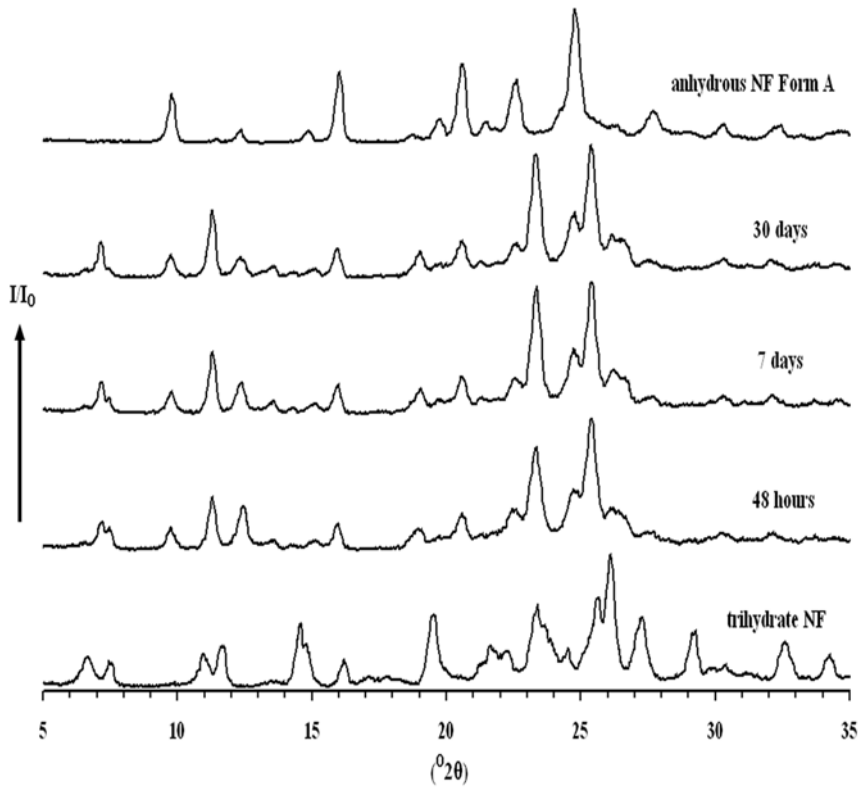

Figure 19 XRPD patterns of trihydrate NF after heated at 60°C for various time period

The solid state interconversion of NF hydrates is summarized in Figure 20. The anhydrous NF Form A and the other hydrate forms transformed to the pentahydrate NF when exposed to saturated water vapor. Meanwhile, the anhydrous NF Form A could be produced from thermal dehydration of the disordered NF state and hemipentahydrate NF. On the contrary, dihydrate NF, trihydrate NF and pentahydrate NF were not fully converted to the anhydrous NF Form A upon heating. Dehydration of NF hydrates with the aid of desiccant did not provide pure anhydrous NF Form A. Instead, it generated the disordered NF state from the pentahydrate NF. The disordered NF state had specific rehydration behavior and instability against humidity such that it could easily be transformed to the pentahydrate NF starting at very low moisture of 32.8% RH compared to the anhydrous NF Form A where it needs 93.7% RH to convert to the pentahydrate NF.

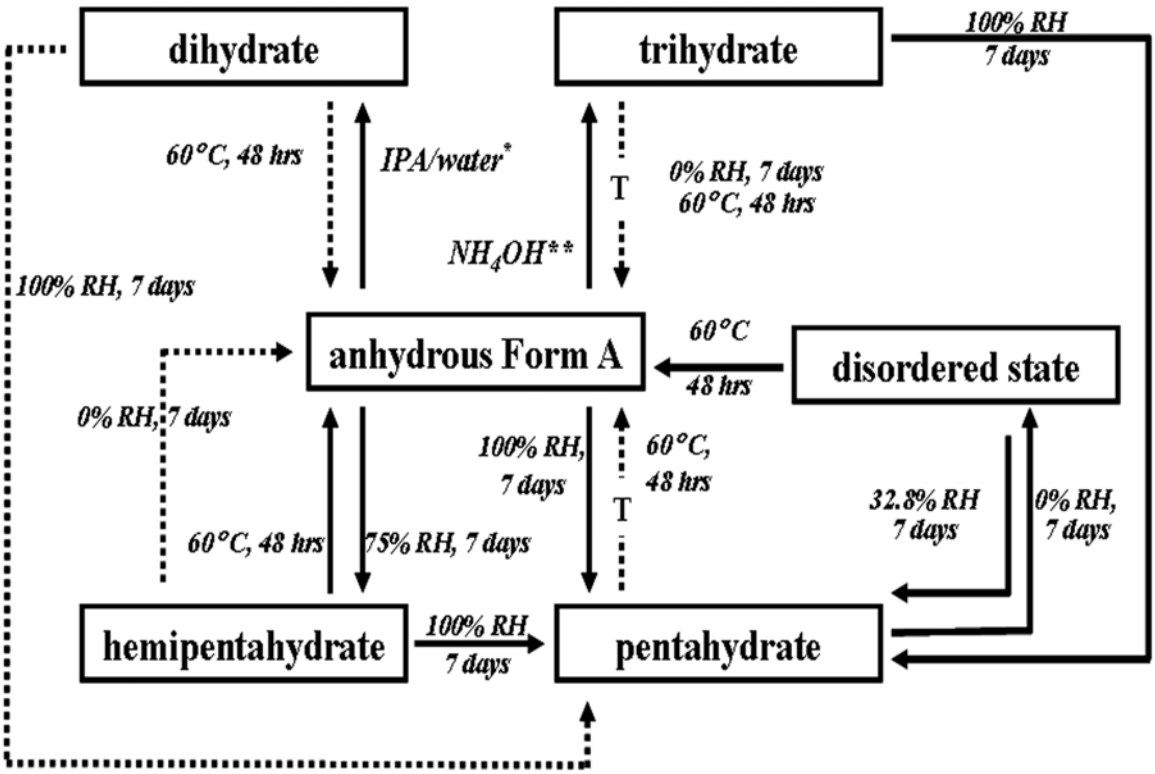

Figure 20 Summary of the solid state interconversion of anhydrous NF Form A and its hydrates (▬ = complete transformation, --- = incomplete transformation, T = hydrated transitional phase or hemipentahydrate NF, * = the dihydrate NF derived from recrystallization in the mixture of IPA and water, ** = the trihydrate NF generated by antisolvent precipitation from aqueous ammonia NF solution)

Isothermal Dehydration of Hemipentahydrate NF

IDSC patterns during dehydration of hemipentahydrate NF are illustrated in Figure 21. The T_{iso} of hemipentahydrate NF at various T_{iso} were different and depend on the nature of dehydration. The T_{iso} was determined by observing an unchanged power in IDSC thermograms. The T_{iso} of the dehydration of hemipentahydrate NF was determined to be at 180 mins at 95 °C and 300 mins at 80 °C, 85 °C and 90 °C. IDSC patterns of all hemipentahydrate NF showed two steps consecutive dehydration. However, the dehydration steps were not clearly separated. Energy calculation of the dehydration process was possible only when dehydration was completed. The AUC of IDSC patterns at various T_{iso} were calculated and are tabulated in Table 2. The result revealed that dehydration energies at every T_{iso} were insignificantly different. It could be concluded that the total energy needed for dehydration of hemipentahydrate NF was temperature independent within the investigated range of 80 °C to 95 °C.

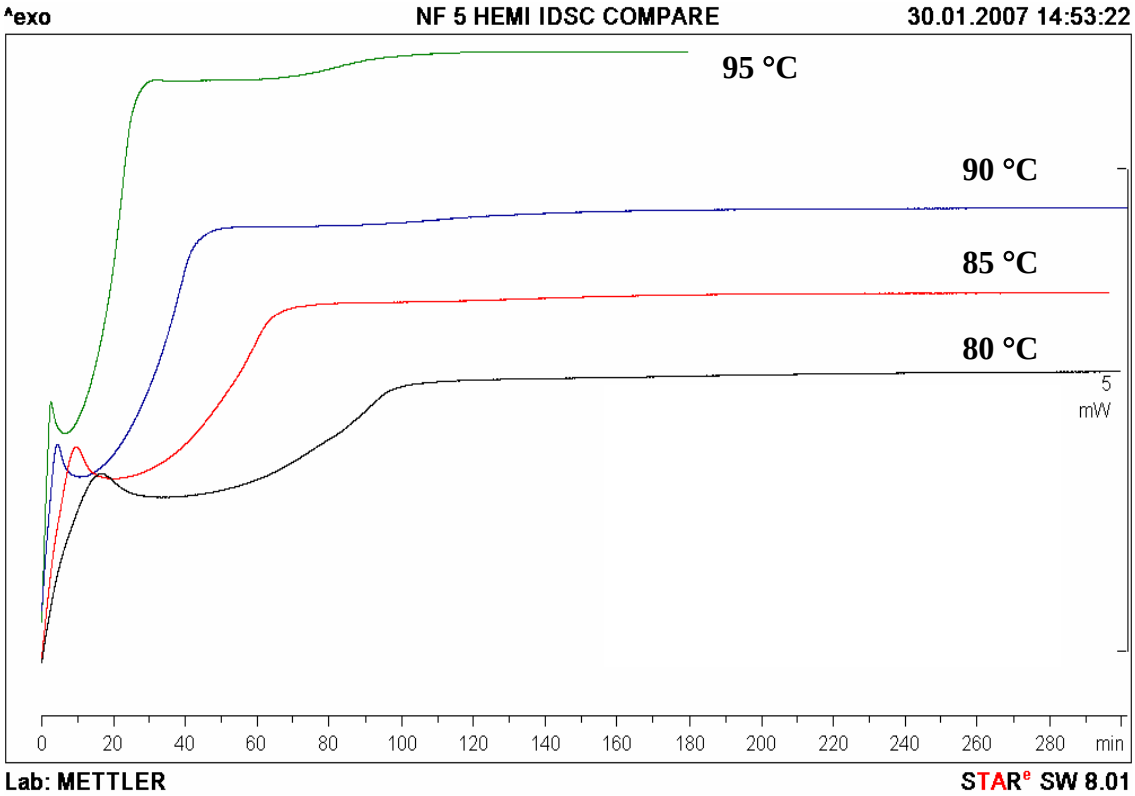

Figure 21 IDSC thermograms of hemipentahydrate NF during isothermal dehydration at various T_{iso}

Table 2 Dehydration energy, residual water content and particle size of dehydrated hemipentahydrate NF after complete dehydration at different T_{iso}

T_{iso} (^{o}C)	Dehydration energy (J/g)	Residual water content by TGA (%w/w)	d [v,0.5] (micron)
Intact form	-	12.12 ± 0.04	248.88 ± 2.91
80	285.12 ± 5.34	0.38 ± 0.06	240.68 ± 5.53
85	290.33 ± 6.57	0.43 ± 0.36	225.03 ± 8.16
90	292.38 ± 5.75	0.37 ± 0.27	212.17 ± 5.89
95	277.57 ± 12.56	0.24 ± 0.13	237.13 ± 1.50

The residual water contents of all dehydrated hemipentahydrate NF were lower than 1% w/w (Table 2) indicating the generation of the anhydrous phase of NF. XRPD of every dehydrated hemipentahydrate NF after exposure to different T_{iso} showed the specific character of anhydrous NF Form A (Figure 22).

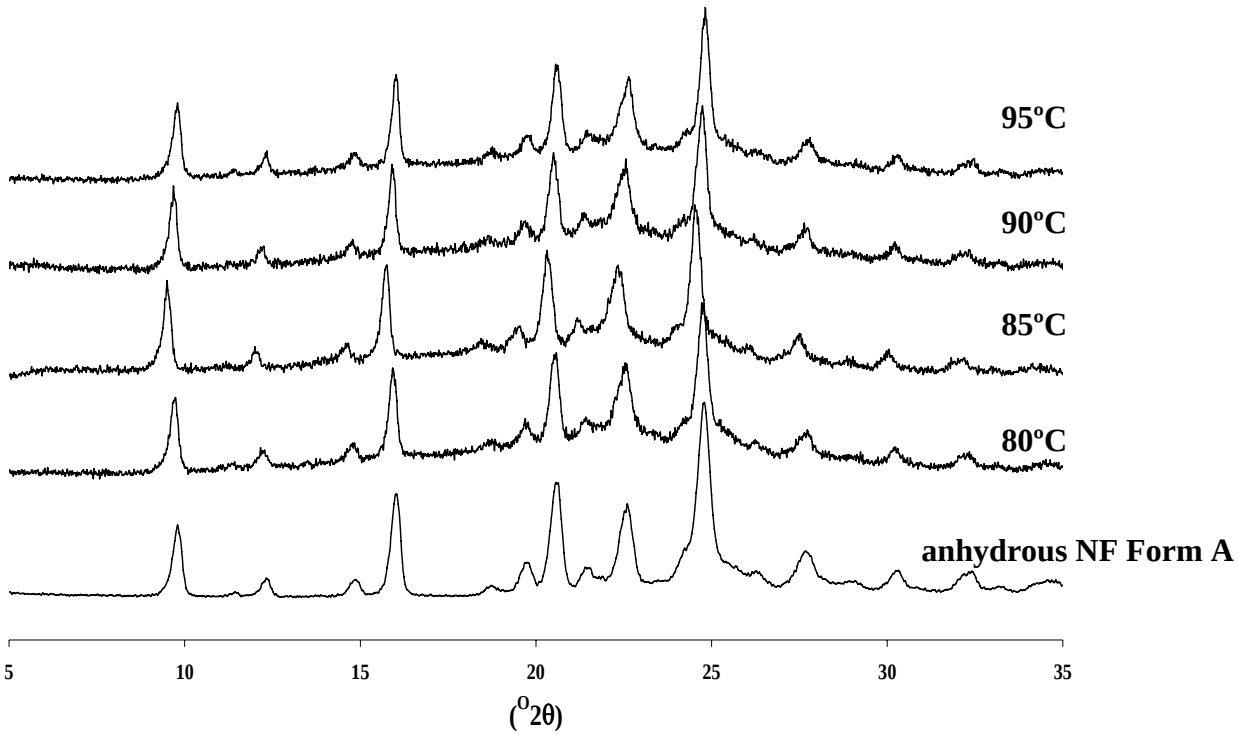

Figure 22 XRPD diffractograms of dehydrated hemipentahydrate NF after isothermal dehydration with respect to T_{iso}

Investigation of particle size changes during dehydration are also demonstrated in Table 2. According to statistical comparison, the difference of particle size between intact hemipentahydrate NF and all dehydrated hemipentahydrate NF were found to be significantly different ($p<0.05$). The particle sizes of intact hemipentahydrate NF and dehydrated samples at 85 $^{\circ}$C and 90 $^{\circ}$C were significantly different ($p<0.05$), while there was no difference between the particle size of intact hemipentahydrate NF and the dehydrated samples at 80 $^{\circ}$C and 95 $^{\circ}$C. It might be due to the fact that the particle size reduction of hemipentahydrate NF depends on the heating rate at different T_{iso} while dehydration energies of all dehydrated samples were similar. At the lowest T_{iso} of 80 $^{\circ}$C, SEM photomicrographs did not show particle size disruption (Figure 24). SEM photomicrographs of dehydrated hemipentahydrate NF at higher T_{iso} of 85 $^{\circ}$C and 90 $^{\circ}$C showed surface defects and resulted in the smaller particles of anhydrous NF Form A. However, at the highest T_{iso} of 95 $^{\circ}$C, anhydrous barrier was rapidly generated and retard the escape of water molecules and led to the retained hydrated structure. The statistically significant difference in particle size between intact and dehydrated hemipentahydrate NF was determined but it could not be concluded that the particle size reduction was evident because the maximum difference was within the range of 25 micron. Thus, the apparent energy used for particle size reduction of hemipentahydrate NF by isothermal dehydration was not determined in this study.

The relationship between fraction reacted (α) and time (t) of dehydration of hemipentahydrate NF by model dependent solid state kinetic are presented in Figure 23. It was directly derived from IDSC data at each T_{iso} and showed two steps of dehydration from observable two phases of the slopes. The calculated E_a with different solid state kinetic equations were in the range of approximately 76 kJ/mol and 120 kJ/mol for the early and the later stage of dehydration, respectively. The Avrami Eroféev equations with one and two dimensional gave a good fit of the dehydration of hemipentahydrate NF. The random nuclei generated along one or two dimensions and progressively ingested other nuclei was defined as main mechanism of dehydration. Beside, the phase boundaries model also showed good agreement. It indicated the advancement of dehydrated phase from the outside of particle concerned to the inside. Therefore, the main mechanism of dehydration was not able to be explained by either single Avrami Eroféev model or Phase Boundaries model. Model independent approach resulted in E_a in between of 80 to 120 kJ/mol which was similar to the E_a obtained from model dependent (Figure 25). These results indicated that the “rate” of dehydration of hemipentahydrate NF for both steps depended on the

dehydration temperature. The higher E_a of the initial step of dehydration strongly indicated the temperature dependency of the dehydration rate. On the other hand, the gradual and continuous decrease in E_a during dehydration indicated less energy barrier for dehydration which resulted from the disruption of the structural integrity of hydrate particles without particle size reduction.

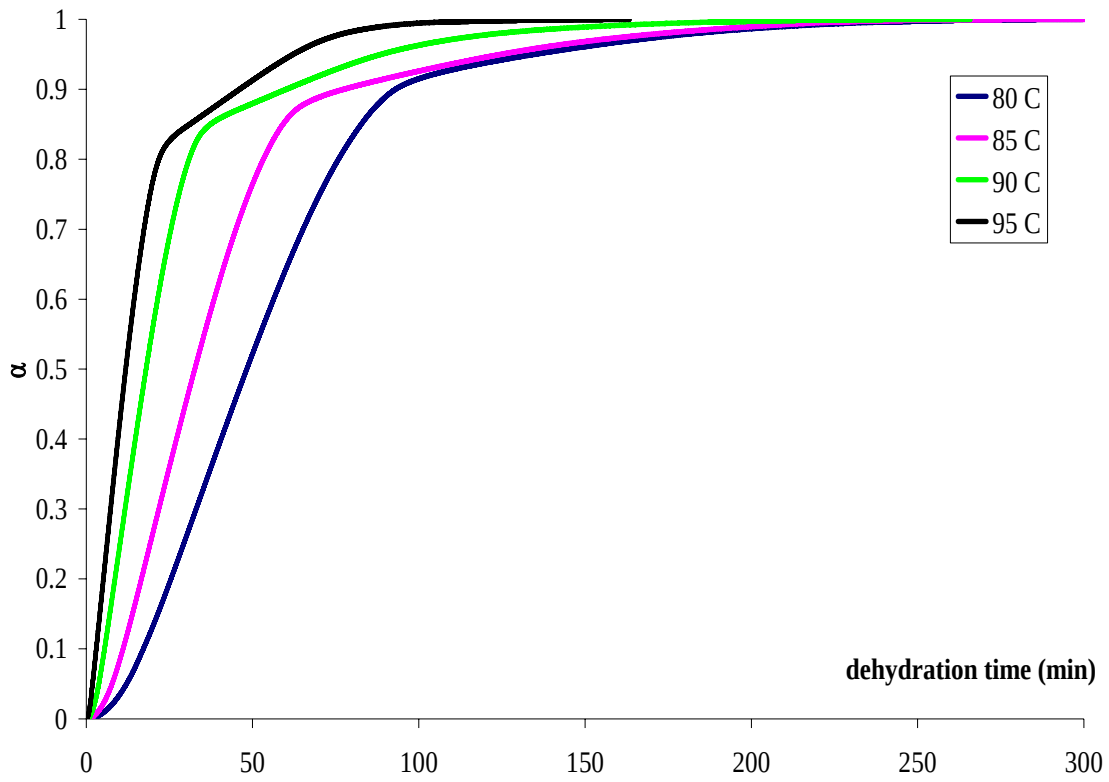

Figure 23 α-t curves of dehydration of hemipentahydrate NF at different T_{iso}

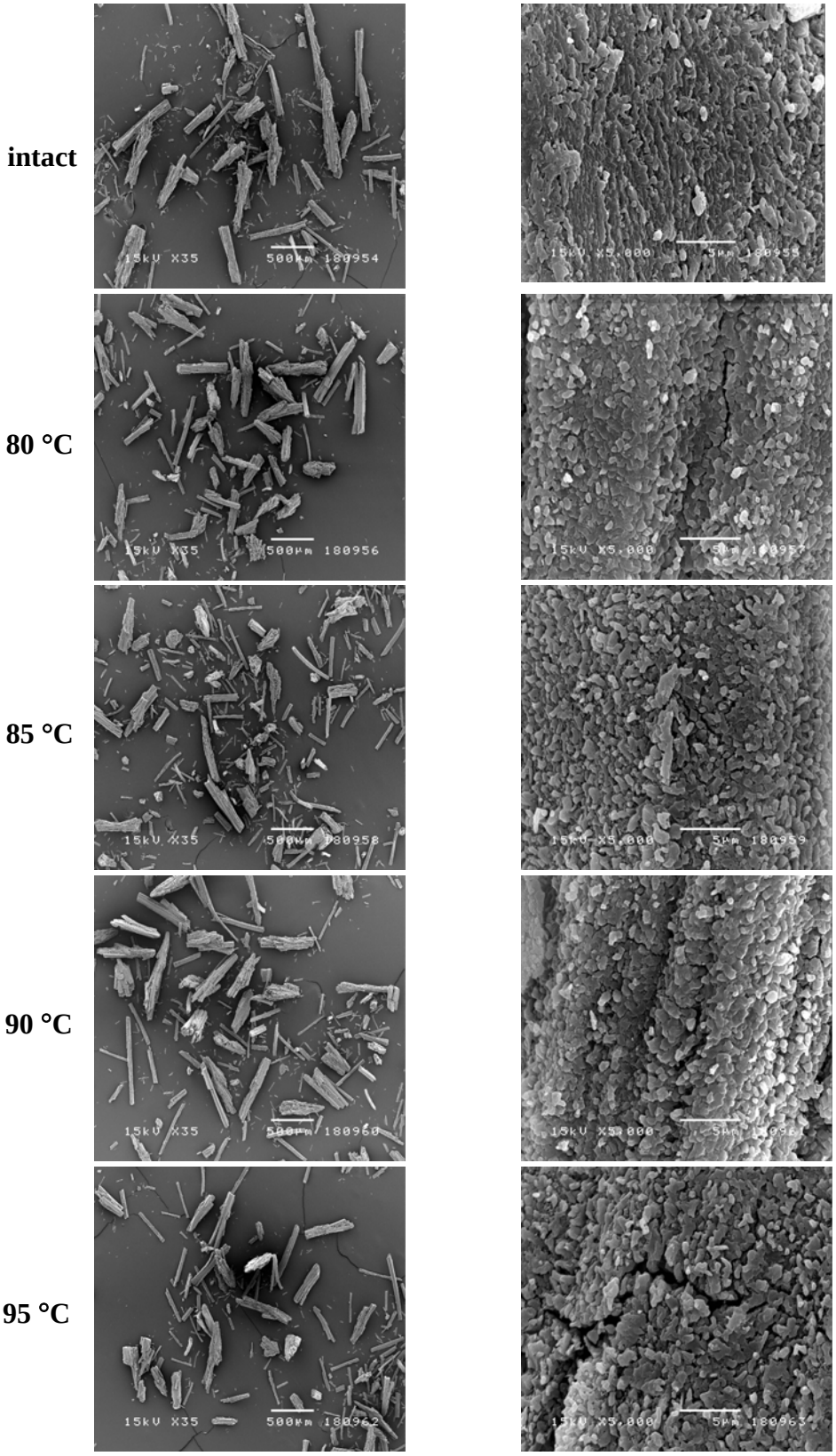

Figure 24 SEM photomicrographs of hemipentahydrate NF after complete dehydration at various T_{iso} (left column at the magnification of 35, right column at the magnification of 5000)

Table 3 The activation energy of isothermal dehydration of hemipentahydrate NF with various solid state kinetic models

Model equation	E_a (kJ/mol)	
	First step of dehydration (0.20 to 0.80 of α)	Second step of dehydration (0.93 to 0.97 of α)
Avrami Eroféev		
1 dimensional	76.56	119.23
2 dimensional	75.84	119.19
Phase Boundary		
2 dimensional	76.95	120.45
3 dimensional	77.22	121.10

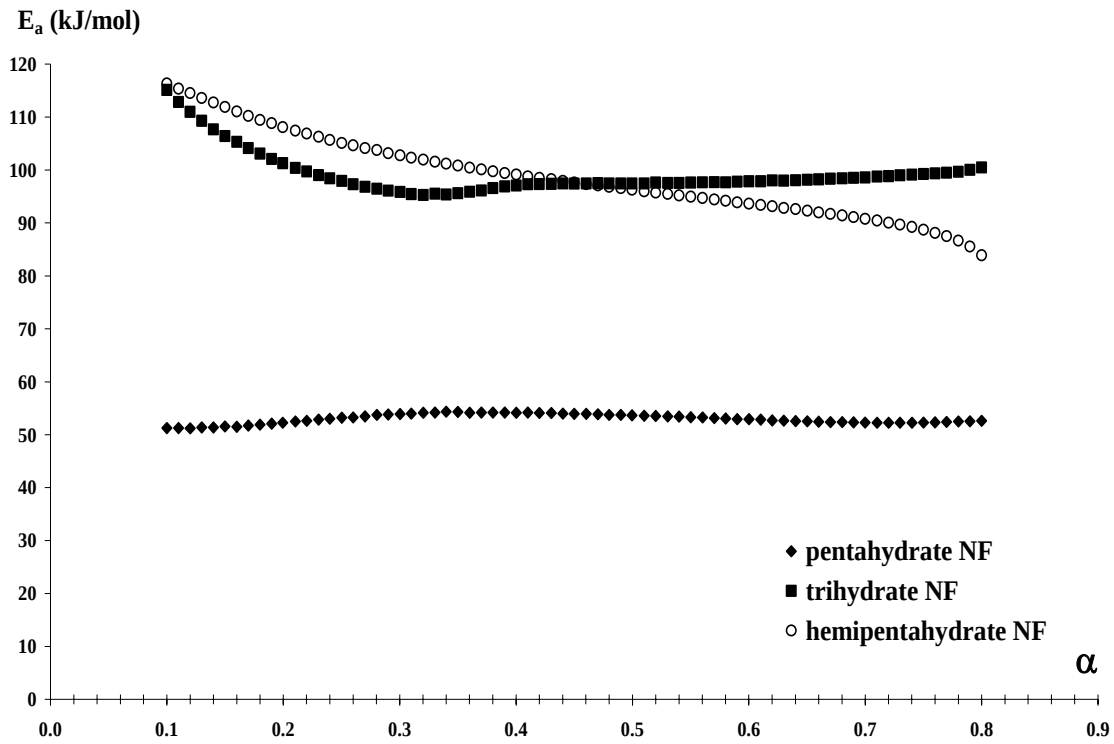

Figure 25 Comparative activation energy of dehydration derived from model independent solid state kinetic of different stoichiometric NF hydrates

Isothermal Dehydration of Trihydrate NF and Pentahydrate NF

Due to a complex dehydration behavior of trihydrate NF and pentahydrate NF, IDSC of both hydrate NF (Figure 26 and Figure 27) showed consecutive dehydration similar to hemipentahydrate NF. However, these behaviors showed clearer separation between two phases of dehydration than that of hemipantahydrate NF. The T_{iso} of trihydrate NF and pentahydrate NF at different T_{iso} were able to be elucidated as two points. The first T_{iso} was selected between the first and second dehydration endotherm while the second T_{iso} was the time of unchanged power of later dehydration phase in IDSC thermogram. In this study, the T_{iso} of first step dehydration for trihydrate NF were 310, 180, 110 and 80 mins while the T_{iso} of second step or complete dehydration were 750, 510, 330 and 210 mins at 80 ^{o}C, 85 ^{o}C, 90 ^{o}C and 95 ^{o}C, respectively. On the other hand, the first T_{iso} of pentahydrate NF were 240, 140, 90, 70 mins and the second T_{iso} for complete dehydration were 600, 390, 330, 240 mins at 80 ^{o}C, 85 ^{o}C, 90 ^{o}C and 95 ^{o}C, respectively. The direct energy measurement of the first and the second steps (complete dehydration) were determined and tabulated in Tables 4 and 5. Additional data of residual water content and particle size of each dehydrated sample were also included in these tables.

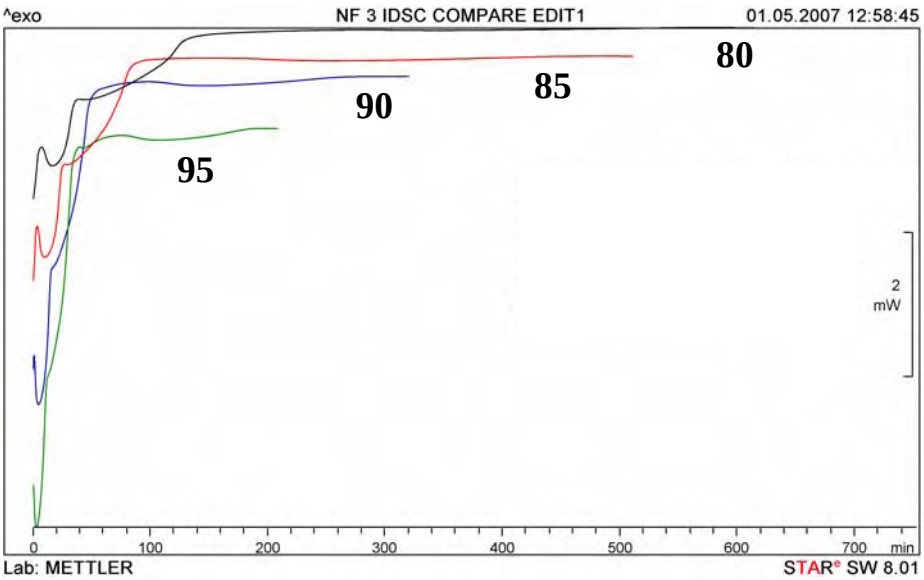

Figure 26 IDSC thermograms of trihydrate NF during isothermal dehydration at various T_{iso}

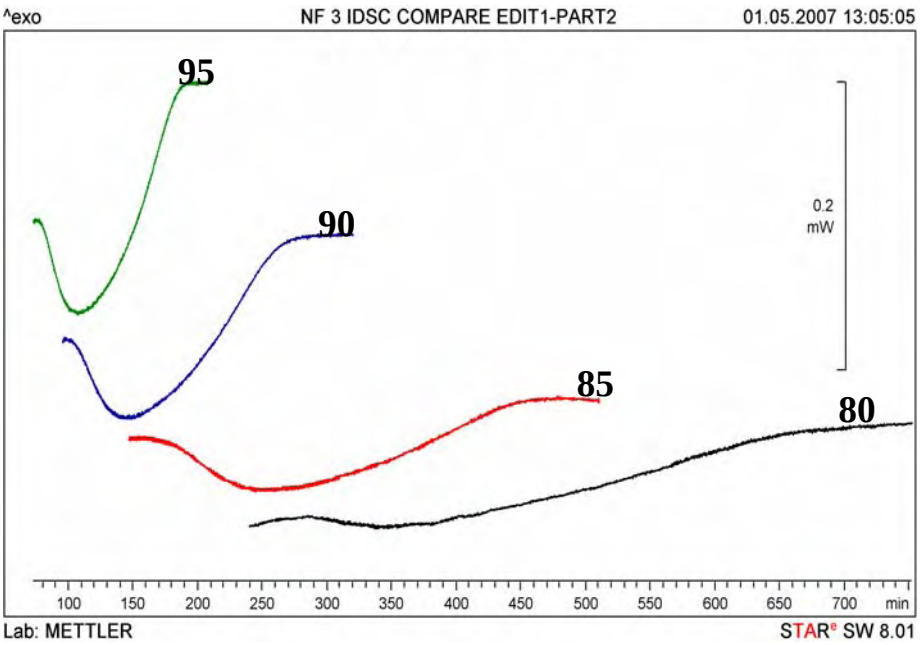

Figure 26 (cont.) IDSC of the second step of the thermograms obtained from trihydrate NF during isothermal dehydration at various T_{iso}

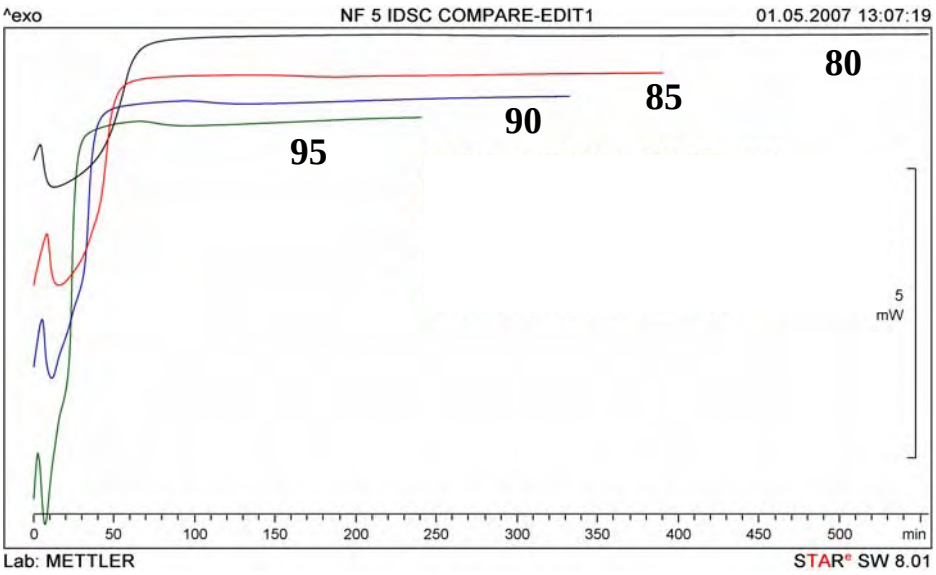

Figure 27 IDSC thermograms of pentahydrate NF during isothermal dehydration at various T_{iso}

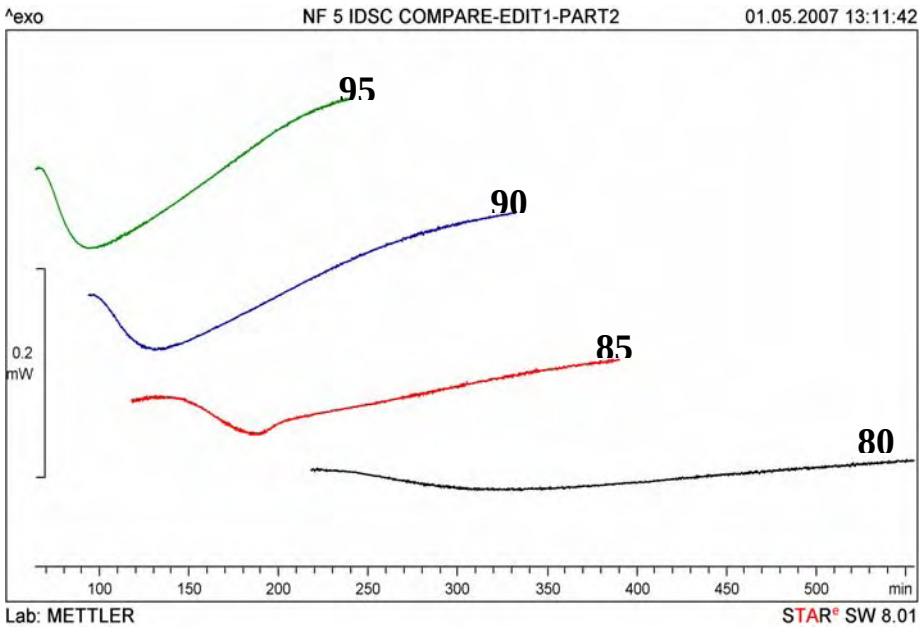

Figure 27 (cont.) IDSC of the second step of the thermograms obtained from pentahydrate NF during isothermal dehydration at various T_{iso}

Table 4 Dehydration energy, residual water content and particle size of dehydrated trihydrate NF after dehydration at different T_{iso}

Step of dehydration	T_{iso} (^{o}C)	Dehydration energy (J/g)	Residual water content by TGA (% w/w)	d [v,0.5] (micron)
Intact form	-	-	14.88 ± 0.08	241.71 ± 1.95
First step	80	375.46 ± 17.78	3.03 ± 0.42	227.58 ± 4.66
	85	379.73 ± 10.21	2.64 ± 0.21	235.53 ± 2.97
	90	374.73 ± 2.34	2.91 ± 0.40	231.67 ± 2.27
	95	360.74 ± 4.16	3.43 ± 0.09	236.13 ± 1.39
Complete dehydration step	80	455.38 ± 7.56	0.56 ± 0.35	234.86 ± 2.17
	85	436.29 ± 42.09	0.36 ± 0.16	215.09 ± 3.89
	90	435.82 ± 18.74	0.11 ± 0.01	229.81 ± 0.35
	95	436.57 ± 3.87	0.15 ± 0.07	228.65 ± 2.13

Table 5 Dehydration energy, residual water content and particle size of dehydrated pentahydrate NF after dehydration at different T_{iso}

Step of dehydration	T_{iso} (^{o}C)	Dehydration energy (J/g)	Residual water content by TGA (%w/w)	d [v,0.5] (micron)
Intact form	-	-	20.87 ± 0.15	211.04 ± 1.46
First step	80	409.32 ± 3.18	3.09 ± 0.08	199.52 ± 0.99
	85	392.63 ± 11.20	2.75 ± 0.17	198.91 ± 2.23
	90	387.12 ± 9.86	3.47 ± 0.19	168.52 ± 2.19
	95	400.25 ± 16.29	2.62 ± 0.15	203.14 ± 2.75
Complete dehydration step	80	416.59 ± 21.18	1.09 ± 1.16	205.58 ± 1.84
	85	436.90 ± 12.96	0.72 ± 0.30	187.77 ± 1.64
	90	434.50 ± 13.96	0.73 ± 0.12	197.51 ± 1.75
	95	448.12 ± 11.16	0.75 ± 0.01	192.52 ± 3.76

The direct energy measurement within each group of dehydration step with respect to temperatures used for T_{iso} for trihydrate NF and pentahydrate NF were insignificantly different. However, the differences of the energies between the first step dehydration and the complete step of dehydration for trihydrate NF and pentahydrate NF were statistically found ($p<0.05$). The results revealed that the total required energy for complete dehydration of both hydrates NF were not affected by the temperatures used similar to hemipentahydrate NF. The residual water contents of both trihydrate NF and pentahydrate NF after the first step of dehydration was approximately 2.5-3.5% w/w (Tables 4 and 5), indicating an incomplete dehydration of both hydrates after the first step of dehydration. Furthermore, XRPD patterns of both dehydrated trihydrate NF (Figure 28) and pentahydrate NF (Figure 29) after the first step of dehydration shown to be a mixture of anhydrous NF Form A and the hydrated transitional phase. However, only anhydrous NF Form A was found after allowing the complete dehydration for both NF hydrates (Figures 30 and 31). The low level of residual water contents of trihydrate NF and pentahydrate NF were at or below 1% w/w after the complete dehydration and confirmed the conversion to anhydrous NF Form A.

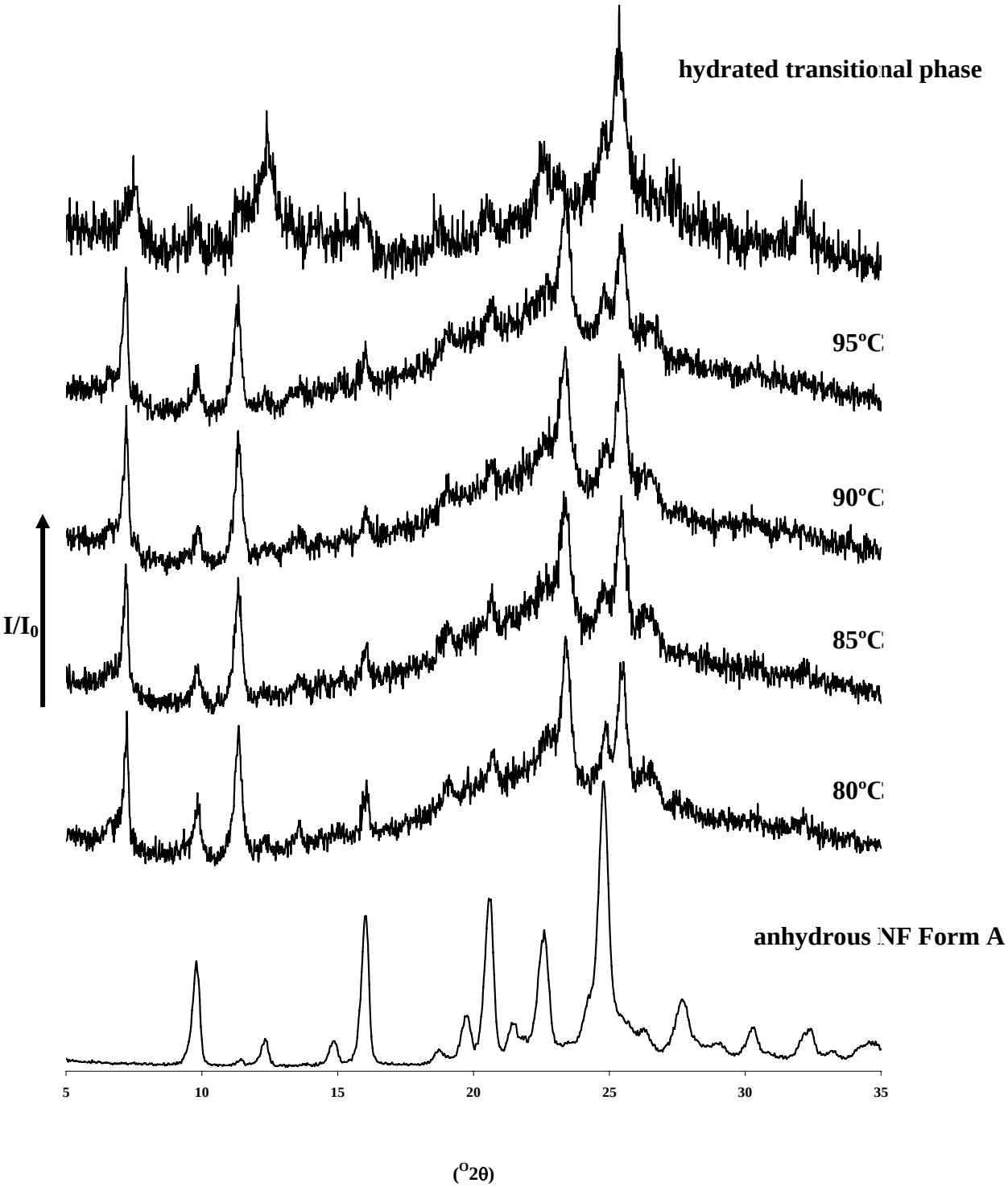

Figure 28 XRPD diffractograms of dehydrated trihydrate NF after first step of isothermal dehydration with respect to T_{iso}

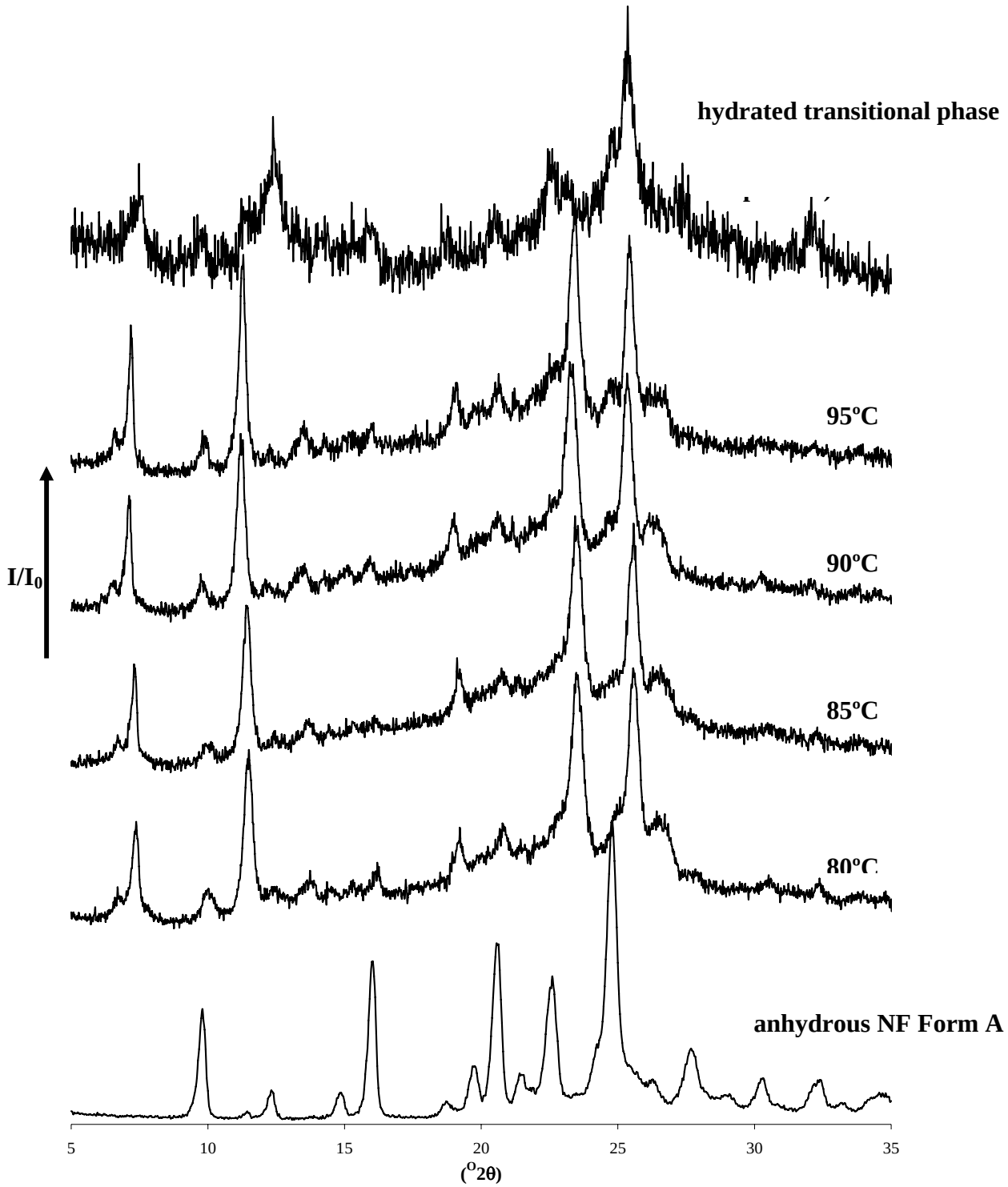

Figure 29 XRPD diffractograms of dehydrated pentahydrate NF after first step of isothermal dehydration with respect to T_{iso}

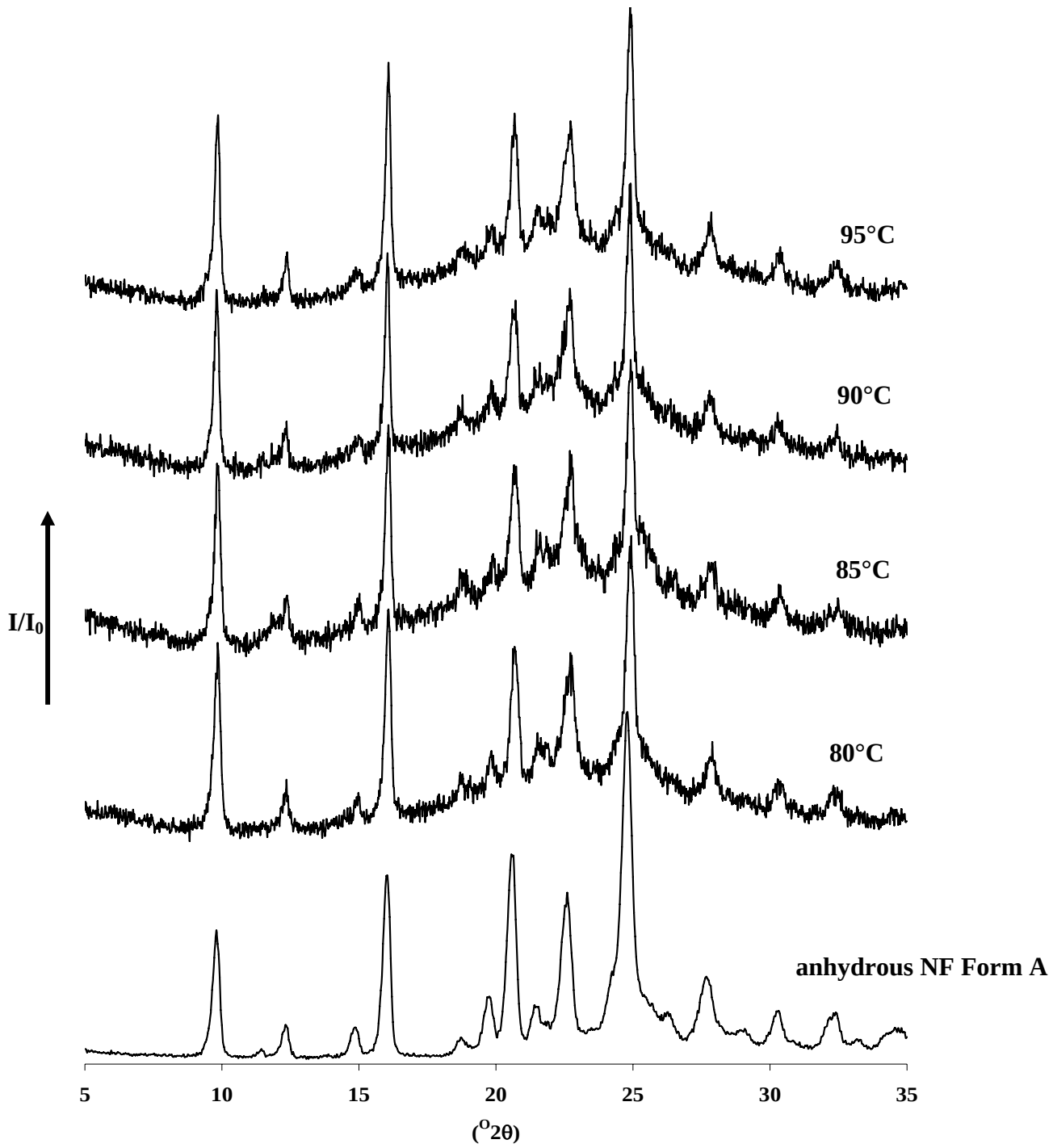

Figure 30 XRPD diffractograms of dehydrated trihydrate NF after complete dehydration with respect to T_{iso}

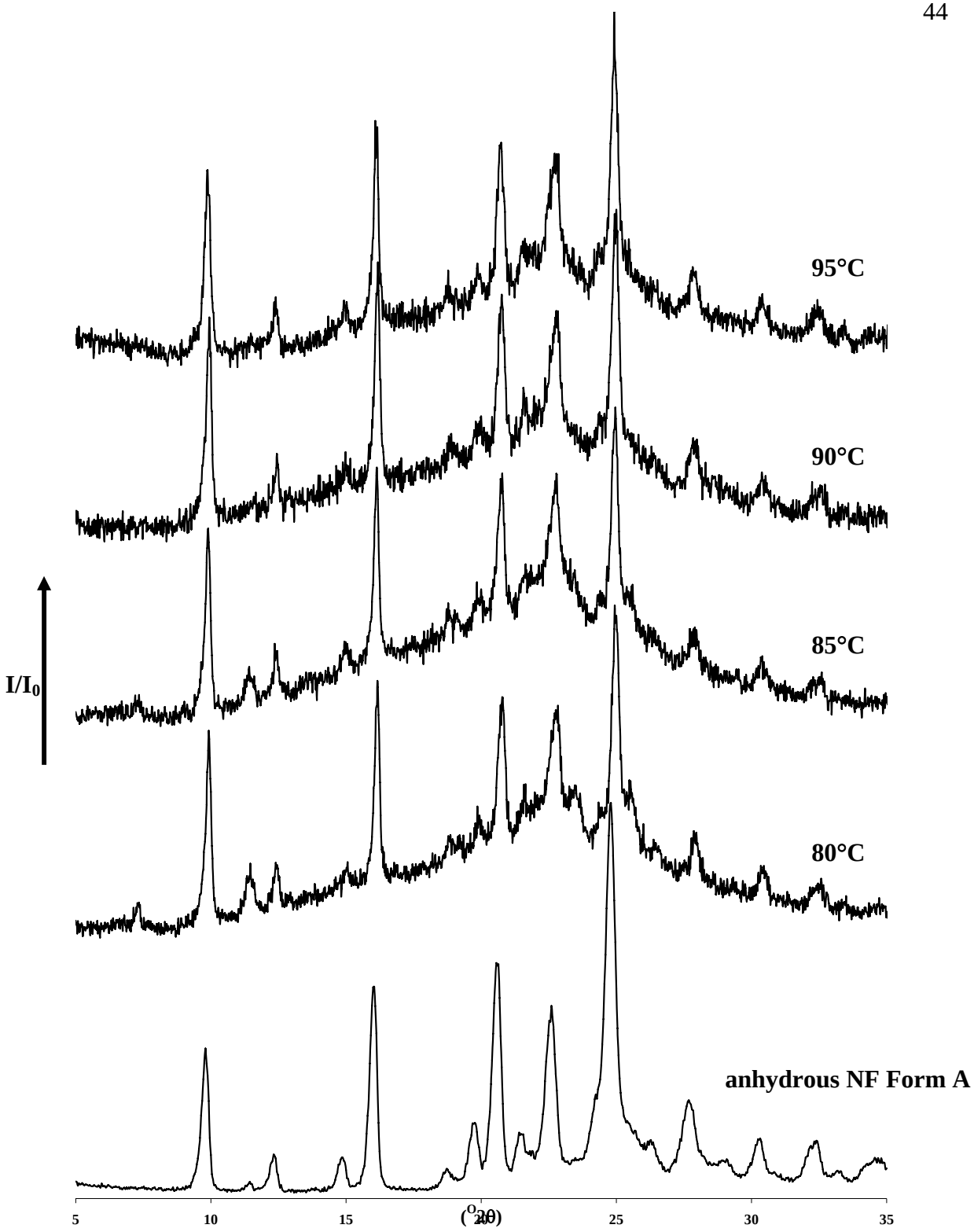

Figure 31 XRPD diffractograms of dehydrated trihydrate NF after complete dehydration with respect to T_{iso}

The particle size of dehydrated trihydrate NF and dehydrated pentahydrate NF were different from the particle size of intact form. However, these findings could not be concluded that particle size reduction of trihydrate NF and pentahydrate NF were clearly seen after dehydration. Because the maximum magnitude of particle size reduction of trihydrate NF and pentahydrate NF were approximately 25 microns and 40 microns, respectively. In summary, thermal dehydration could not reduce the particle size to a significant level for both trihydrate NF and pentahydrate NF.

Although thermal dehydration could not generate small particles of trihydrate NF and pentahydrate NF, the disruption of crystal took place as shown in SEM photomicrographs. Dehydration of trihyhydrates NF and pentahydrate NF with different steps of dehydration showed cracks on the surface of particles (Figures 32 - 35) but it could not promote the individually scattered small particles as seen in BDM. However, the defects seen on large particles may potentially generate small particles with the manipulation of only very mild mechanical force. For example, mild pulverizing of deammoniated methabarbital gave the small particle than intact methabarbital (Sekiguchi et al., 1984).

The relationship between fraction reacted (α) and dehydration time (t) of trihydrate NF and pentahydrate NF are presented in Figures 36 and 37, respectively. In the case of trihydrate NF, the dehydration reaction may be separated in three steps due to unequal slopes whereas two different slopes were determined for the dehydration of pentahydrate NF. In term of model dependent kinetics, the E_a of each defined dehydration steps of trihydrate NF and pentahydrate NF are presented in Tables 6 and 7, respectively. Model dependent approach gave E_a of the dehydration of trihydrate NF of approximately 80 J/g, 98 J/g and 94 J/g for first, second and third step of dehydration, respectively. These results revealed that the “rate” of dehydration of all three steps were considered to be temperature dependent and the magnitude of dehydration rate dependent on temperature were similar. Meanwhile model independent approach showed the value of E_a of 85-115 kJ/mol which are similar to the energy barriers of each step of dehydration (Figure 24). The E_a from model independent of trihydrate NF showed initial decrease and gradually increased at later step of dehydration. It indicated the reduction of energy barrier due to the partially disrupted structure. However, the structure integrity was regenerated at the later stage seen from an increase of E_a. Thus, destroyed structure of trihydrate NF during partial dehydration supported the particle size reduction even the stable structure later exists. For pentahydrate NF, model dependent showed E_a of dehydration at approximately 50 J/g, 70-90 J/g for early and later step of dehydration, respectively. These data were different from the data

obtained with trihydrate NF. It indicated that the magnitude of temperature dependency in early step was lower than that of the later step of dehydration. Thus, the rate of dehydration of pentahydrate NF at early phase changed did not depend wholly on the dehydration temperature was raised equally. On the other hand, the E_a of pentahydrate NF from model independent, 50 kJ/mol, was equal to the E_a obtained from the early step of dehydration by model dependent. Moreover, the pattern of the change of E_a over the α of 0.1 to 0.8 was negligible changed. It should provide the stable structure and unchanged particle size of pentahydrate NF after dehydration. However, the particle size reduction of pentahydrate NF experimentally occurred. Hence, it should have other controlled factors of the particle size reduction of pentahydrate NF upon heating.

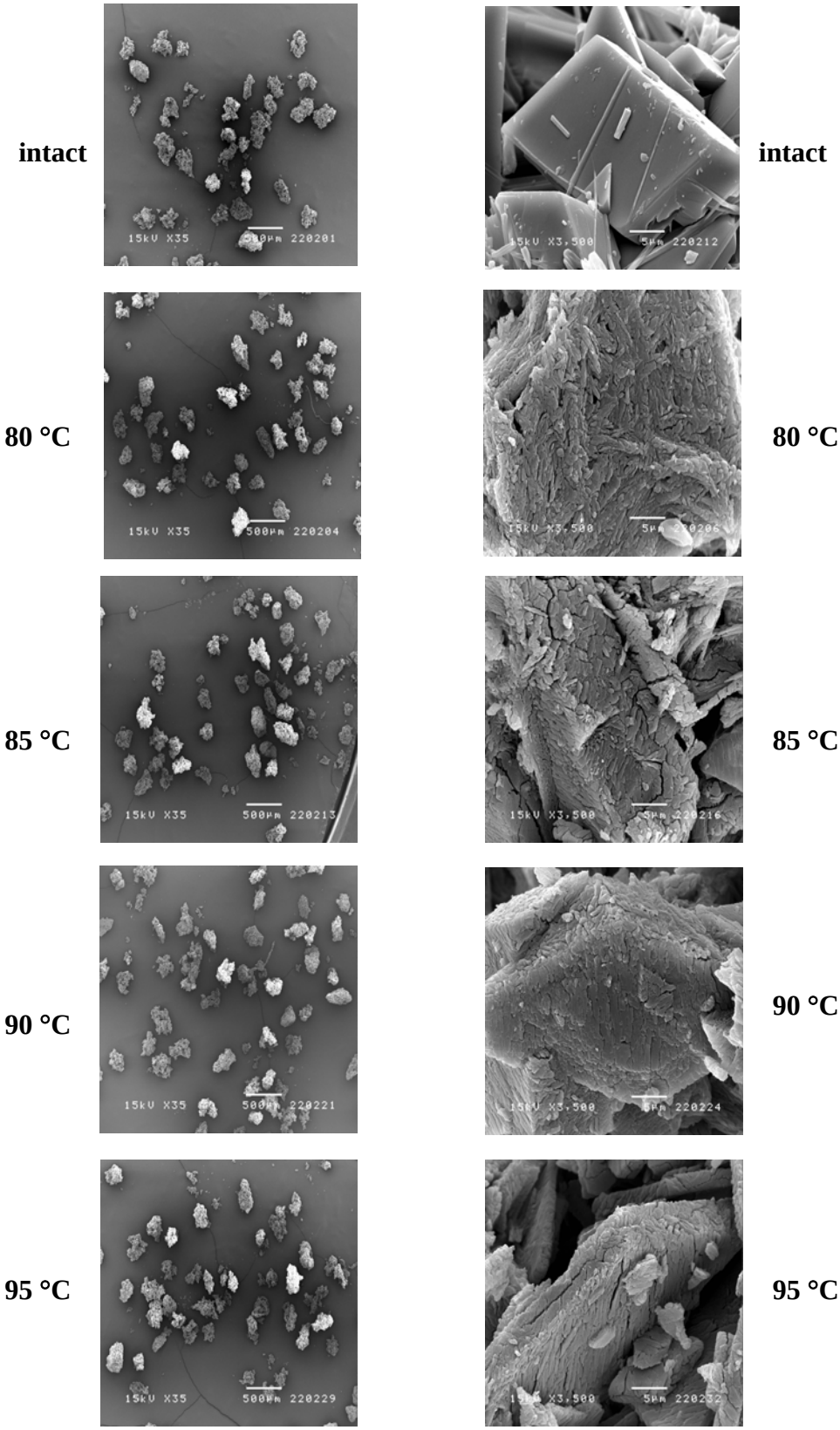

Figure 32 SEM photomicrographs of dehydrated trihydrate NF during isothermal dehydration after the first dehydration step with respect to T_{iso} (left column at the magnification of 35, right column at the magnification of 3500)

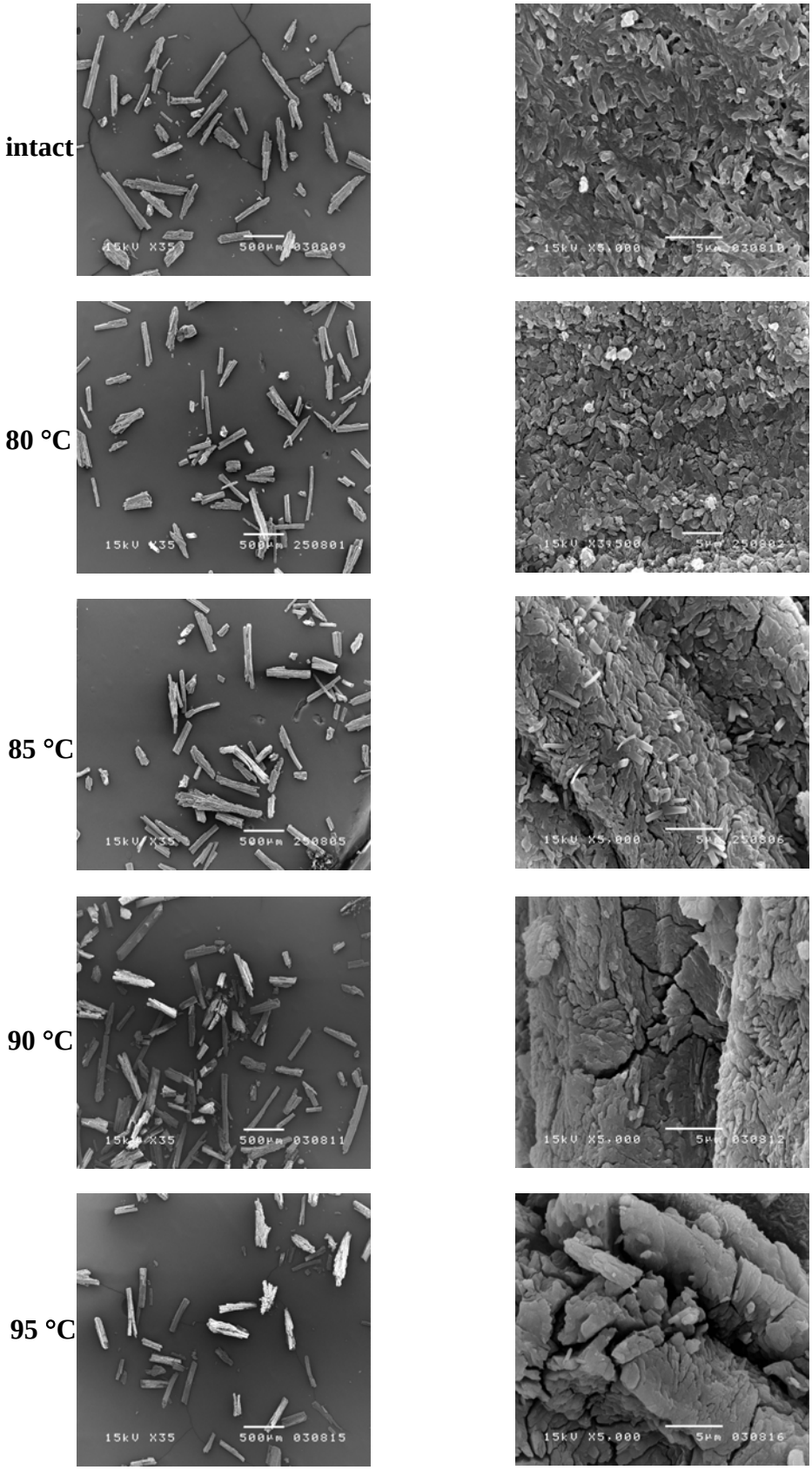

Figure 33 SEM photomicrographs of dehydrated pentahydrate NF during isothermal dehydration after the first dehydration step with respect to T_{iso}(left column at the magnification of 35, right column at the magnification of 5000 except of 80°C at 3500)

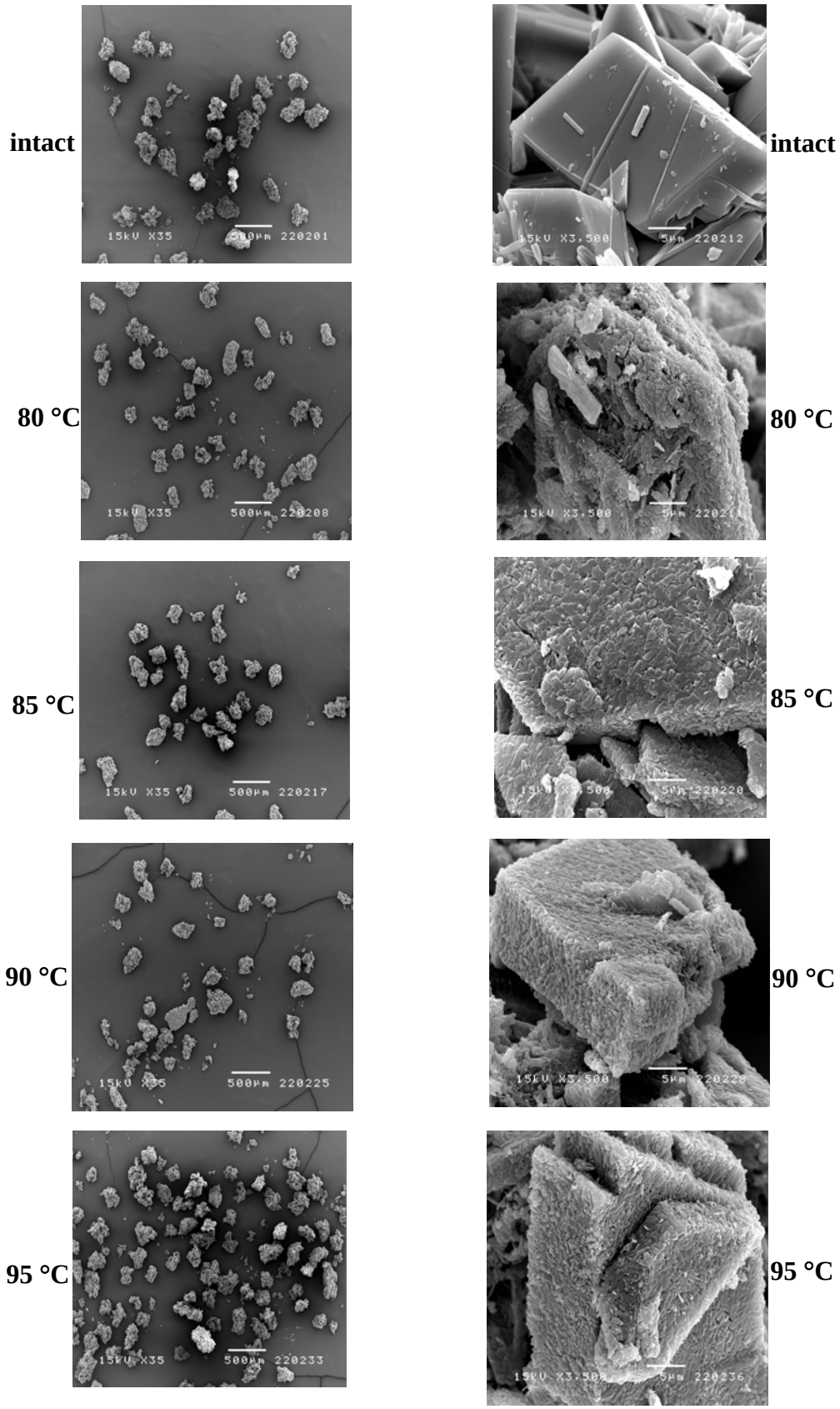

Figure 34 SEM photomicrographs of dehydrated trihydrate NF during isothermal dehydration after the complete dehydration with respect to T_{iso}(left column at the magnification of 35, right column at the magnification of 3500)

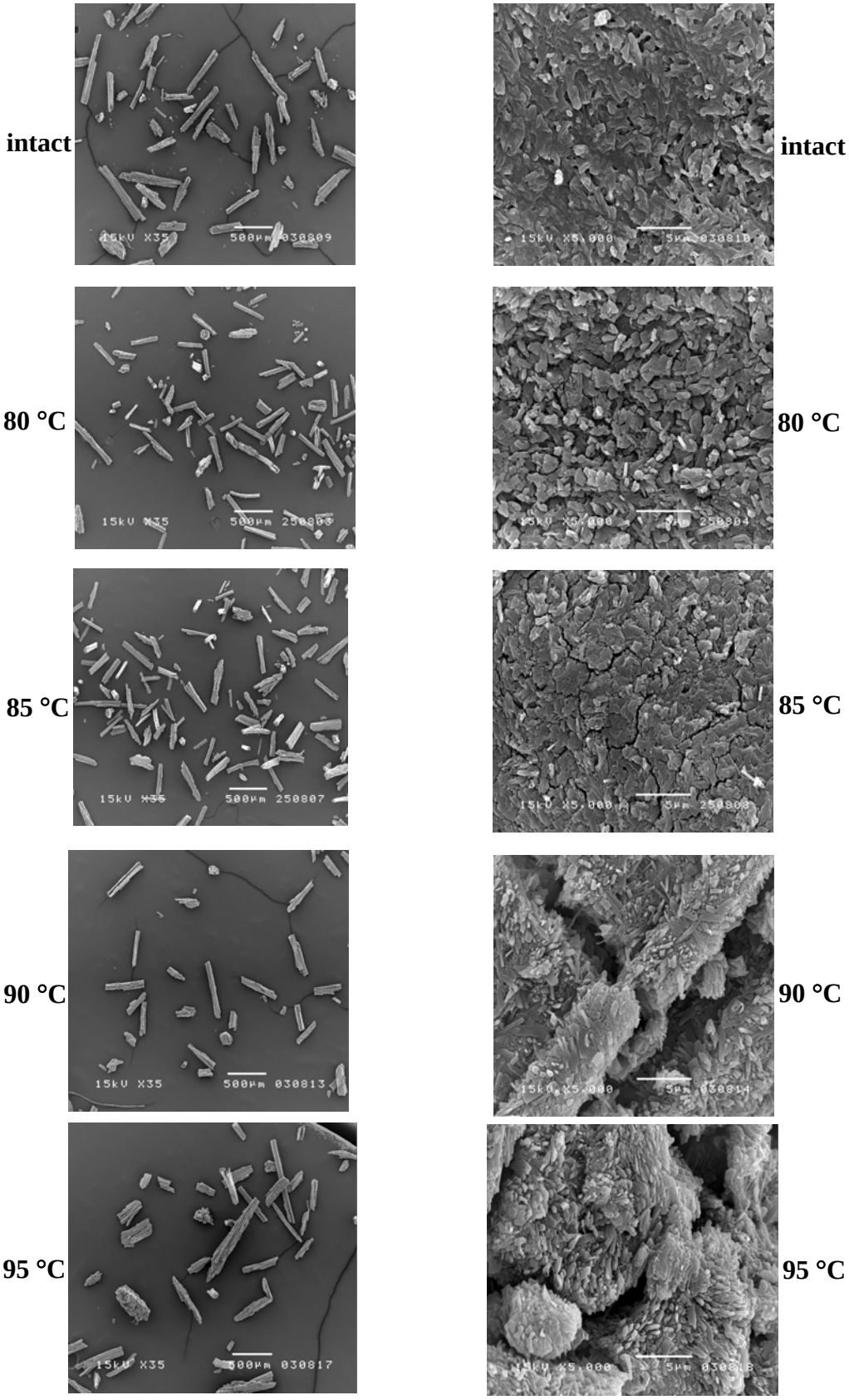

Figure 35 SEM photomicrographs of dehydrated pentahydrate NF during isothermal dehydration after the complete dehydration with respect to T_{iso} (left column at the magnification of 35, right column at the magnification of 5000)

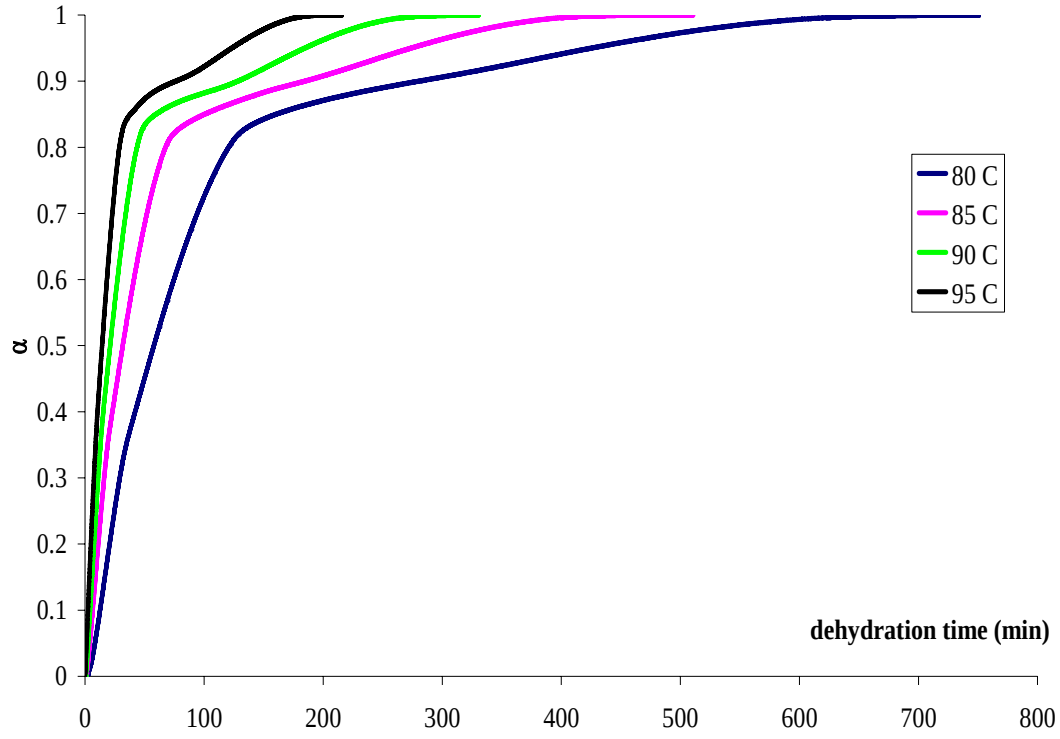

Figure 36 α-t curves during dehydration of trihydrate NF at different T_{iso}

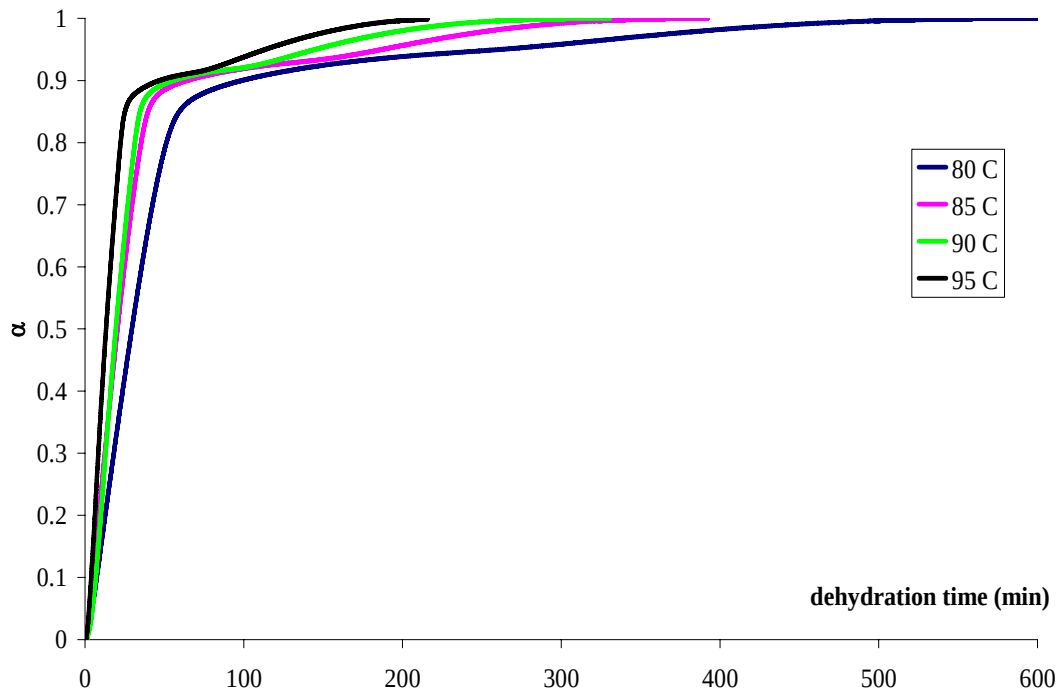

Figure 37 α-t curves during dehydration of pentahydrate NF at different T_{iso}

Table 6 The activation energy of isothermal dehydration of trihydrate NF with various solid state kinetic models

Model equation	E_a (kJ/mol)		
	First step of dehydration (0.10 to 0.30 of α)	Second step of dehydration (0.40 to 0.70 of α)	Third step of dehydration (0.93 to 0.97 of α)
Avrami Eroféev			
1 dimensional	80.52	97.02	93.69
2 dimensional	79.74	97.66	93.75
Order reaction			
1st order	82.79	101.28	93.45
Phase Boundary			
1 dimensional	81.77	97.71	94.80

Table 7 The activation energy of isothermal dehydration of pentahydrate NF with various solid state kinetic models

Model equation	E_a (kJ/mol)	
	First step of dehydration (0.20 to 0.80 of α)	Second step of dehydration (0.93 to 0.97 of α)*
Diffusion Controlled		
1 dimensional	51.21	87.52
Phase Boundary		
1 dimensional	51.18	88.66
2 dimensional	51.38	71.68

* The values are calculated from the IDSC data of T_{iso} 85, 90 and 95 ºC

The crystallographic data of materials are generally solved by SC-XRD and used as platform to evaluate and confirm the possibility of size reduction during thermal dehydration. In this study, hemipentahydrate NF, trihydrate NF and pentahydrate NF were generated with an inappropriate property to be tested by SC-XRD even several attempts were performed. To alternatively gain crystallographic data, XRPD was employed with the aid of specific software, PowderSolve®. Unfortunately, XRPD of all NF hydrates could not be indexed and did not provide valid lattice parameter. Therefore, it was not possible to

determine the NF hydrate structures. The lattice structures which will lead to the explanation of the possibility of particle size reduction via thermal dehydration of hemipentahydrate NF, trihydrate NF and pentahydrate NF was not achievable.

According to an ineffective process of particle size reduction by thermal dehydration of the stoichiometric NF hydrates, the relationship between the apparent particle size reduction energy and stoichiometry could not be established. However, dehydration energy of different stochiometric NF hydrates would be considered instead of the apparent energy for particle size reduction. The calculated total dehydration energy from IDSC of various NF hydrates (Tables 2, 4 and 5) were found to be lower than the enthalpy of dehydration obtained by regular non-isothermal DSC (NIDSC) in Figure 38. It may be due to the condition of IDSC that generated temperature shift (from ambient temperature to the desired dehydration temperature) before the signal of IDSC was recorded. The energy loss during the initial temperature adjustment of NF hydrate samples by IDSC were determined as a function of dehydration temperature in conjunction with NIDSC at a heating rate of 10 ºC/min prior to IDSC measurements (Figure 39). The initial energy calculation during initial NIDSC portion was obtained from the AUC starting at point X to point A as seen in Figure 39. The initial energy loss during heating of hemipentahydrate NF was 96.75, 101.70, 120.11 and 137.56 J/g at 80, 85, 90 and 95 °C, respectively. When the initial energy loss were added to the dehydration energy calculated from IDSC at each dehydration temperature, the total energy were in the range of 380-415 J/g and found to be close to the enthalpy of dehydration of hemipentahydrate NF obtained by regular NIDSC which was 408.79 J/g (Figure 38). For trihydrate NF, the initial energy loss were 87.01, 107.11, 120.16 and 133.25 at 80, 85, 90 and 95 °C, respectively while they were 101.66, 118.53, 137.93 and 151.60 at 80, 85, 90 and 95 °C, respectively for pentahydrate NF. The sum between the initial energy loss and calculated total dehydration energy from IDSC were 540-570 and 520-600 J/g for trihydrate NF and pentahydrate NF. These results were similar to the total enthalpy of dehydration from regular NIDSC of trihydrate NF (557.95 J/g) and pentahydrate NF (614.65 J/g). Thus, it should be reminded that IDSC method for the determination of dehydration energy of NF hydrates would lack the initial portion of the total dehydration energy. However, the dehydration energy from IDSC could preliminary be used to roughly evaluate the relationship between the stoichiometry of hydrates and required energy for dehydration.

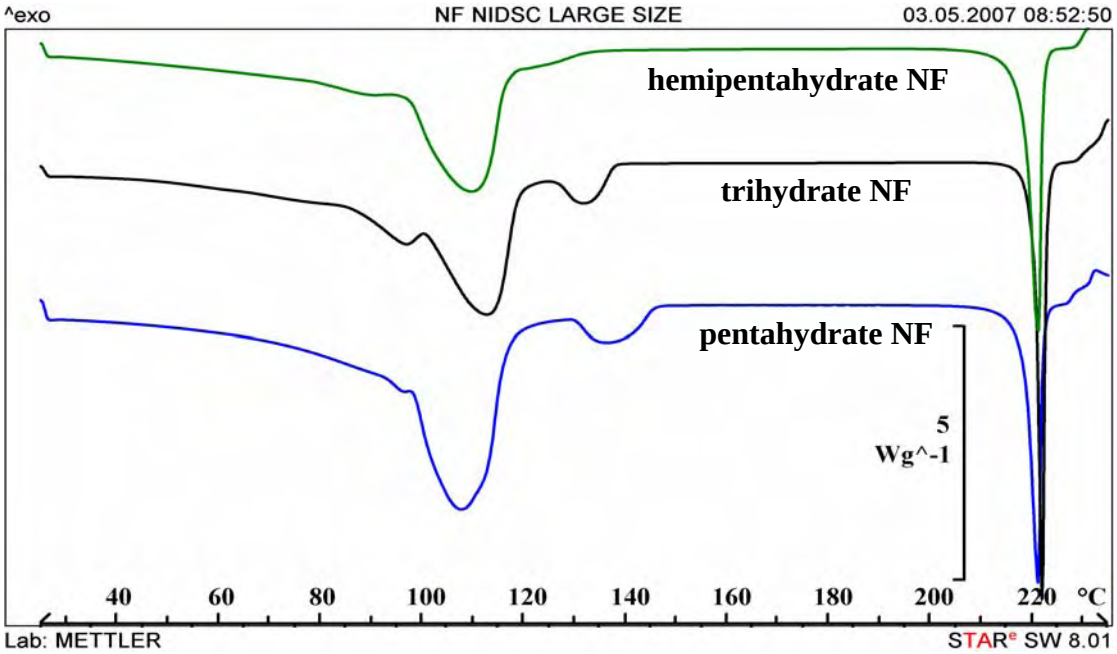

Figure 38 The regular non isothermal DSC (NIDSC) thermograms of some NF hydrates at the heating rate of 10 °C /min

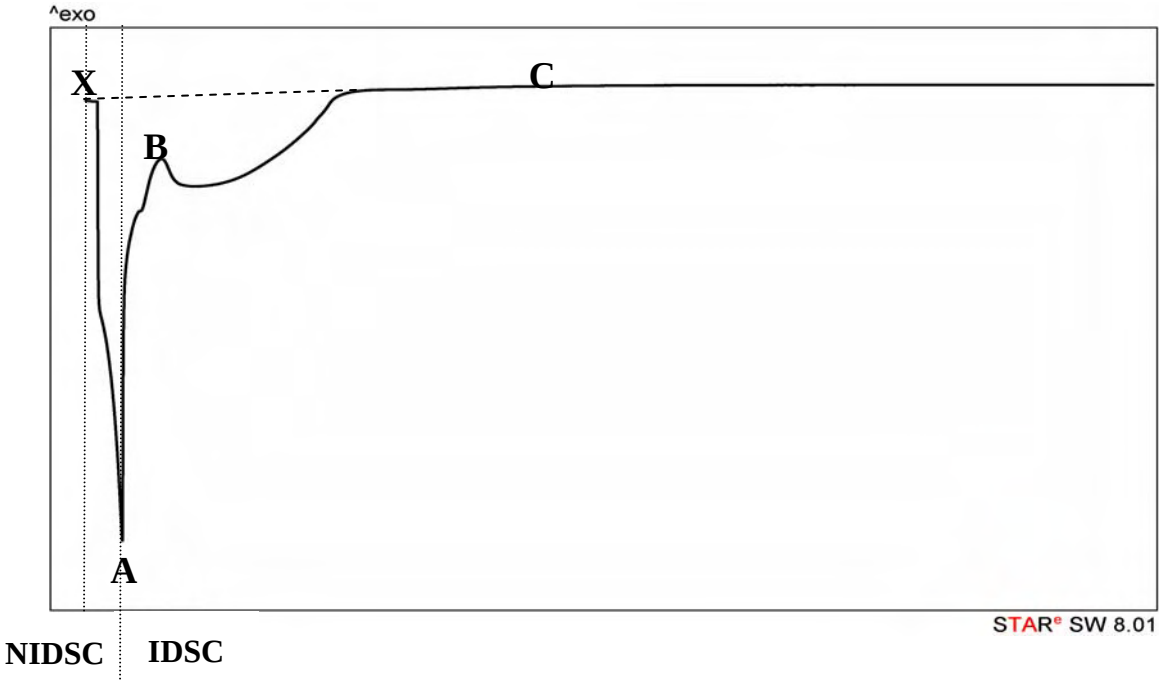

Figure 39 Model of NIDSC thermogram (X to A) before IDSC thermorgram (A to C) of NF hydrate during isothermal dehydration

The relationship between the stoichiometry of NF hydrates and total dehydration energy used from IDSC is presented in Figure 40. Hemipentahydrate NF showed the lowest dehydration energy that followed the theoretical basis of chemical dehydration. Dehydration energy should be lower for the lower stoichiomtry of the same hydrate compound. It is due to a less number of binding forces (particularly hydrogen bonds) between water molecules and the active moiety in the hydrated structure. However, dehydration energy of trihydrate NF was found not to be different than the pentahydrate NF. This result did not obey the general basis of dehydration as described above. This may be due to the lost of initial dehydration energy which was not accounted for by IDSC as discussed earlier. If the total energy, obtained by the regular NIDSC experiments were plotted against stoichiometry of NF hydrates, the relationship was found to be correlated to the energy and stoichiometry assumption of linearity more than when IDSC was used alone (Figure 40(open circle)). However, through this evaluation, the total dehydration energy of the pentahydrate NF was not critically higher than that of the trihydrate NF as was assumed if linearity was achieved. Another aspect to consider for dehydration of hydrates was regarding the types of hydrogen bonding in the hydrated structure. The shorter hydrogen bonds theoretically give stronger binding force and need more energy to break down (Jeffrey, 1997). This concept may explain the similarity of dehydration energy between lower stoichiometric trihydrate NF to the higher stoichiometric pentahydrate NF. However, this is only an assumption of this issue due to the crystallographic data of NF hydrates were not possible to be elucidated at this time.

Another factor which may govern the accurate calculation of the total dehydration energy is the positioning of water molecules within the crystal lattice. The model NF hydrates used in this study may have several sites for water molecules to reside. Thus, dehydration occurred in several steps and may lead to inaccurate calculation of energy for dehydration. A future good model proposed for the methods used in this experiment to prove the correlation of dehydration energy to the stoichiometry should have only one lattice site for water molecules to reside no matter what the stoichiometry should be.

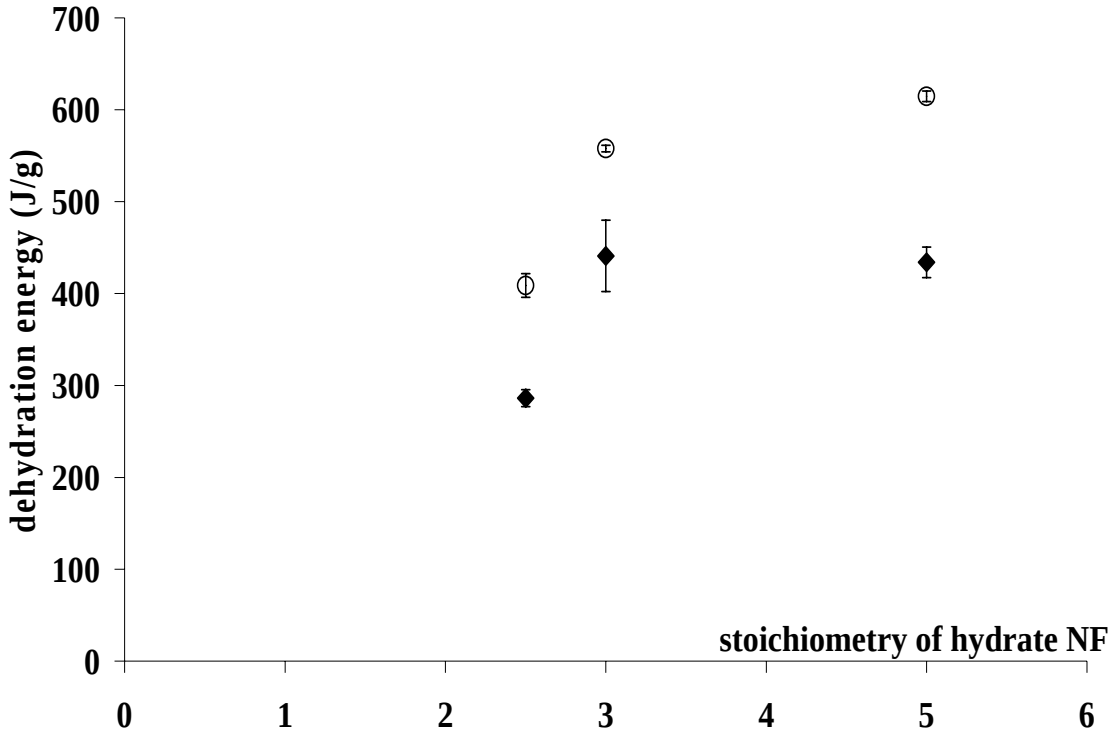

Figure 40 The relationship between stoichiometry and dehydration energy of NF hydrates obtained by different calculation methods (◆ IDSC method alone, ○ regular NIDSC)

Isothermal Dehydration of Dihydrate NF

Due to a difficulty in the reproducible production of dihydrate NF, the amount of dihydrate NF was very limited. Therefore, this study could not be performed with a typical IDSC as described in the experimental method section due to limited amount of sample. Thermo microscopy was alternatively chosen as preliminary investigation on the particle size reduction via thermal dehydration. Single particle of dihydrate NF was placed on glass slide over heating station of hot stage (HSM) without immersing oil under different T_{iso}. The t_{iso} was applied of up to 6 hours.

HSM results revealed that dihydrate NF lost an anisotropic property with respect to heating time at every T_{iso}. Disappearance of anisotropy was seen from the development of opaque region from outer part towards the inner core of the crystal (Figure 41). The unilluminated phase of dihydrate NF was found to be due to a dehydration process during molecular rearrangement in the crystal lattice (Byrn et al., 1999). Thus, the dehydration time was directly proportional to the time used to obtain total unilluminated phase. The results showed the time for total unilluminated phase at 80 $^{\circ}$C and 85 $^{\circ}$C were approximately 10 mins and at 90 $^{\circ}$C and 95 $^{\circ}$C were approximately 5 mins. The higher T_{iso} resulted in shorter dehydration time. The small particle of dehydrated dihydrate NF was not generated at every T_{iso} used. However, SEM of all heated dihydrate NF only showed cracks around external surface of the crystal (Figure 42). Thermal dehydration could not destroy dihydrate NF particle, the structural arrangement was stable even after all the water molecules were removed and could not damage the dihydrate NF to a small particle of anhydrous NF.

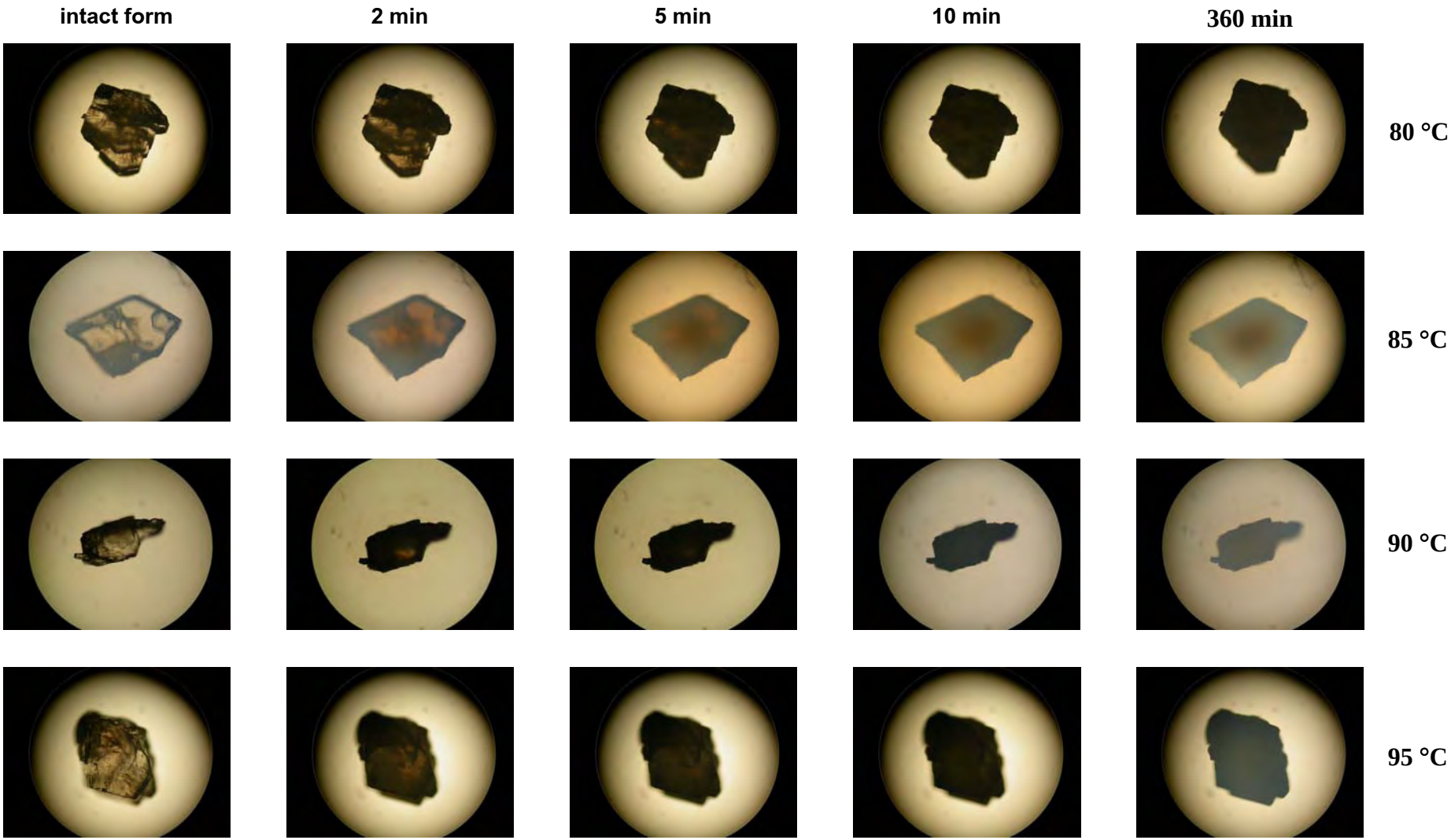

Figure 41 Photomicrographs of dihydrate NF during isothermal dehydration at various T_{iso} as a function of heating time

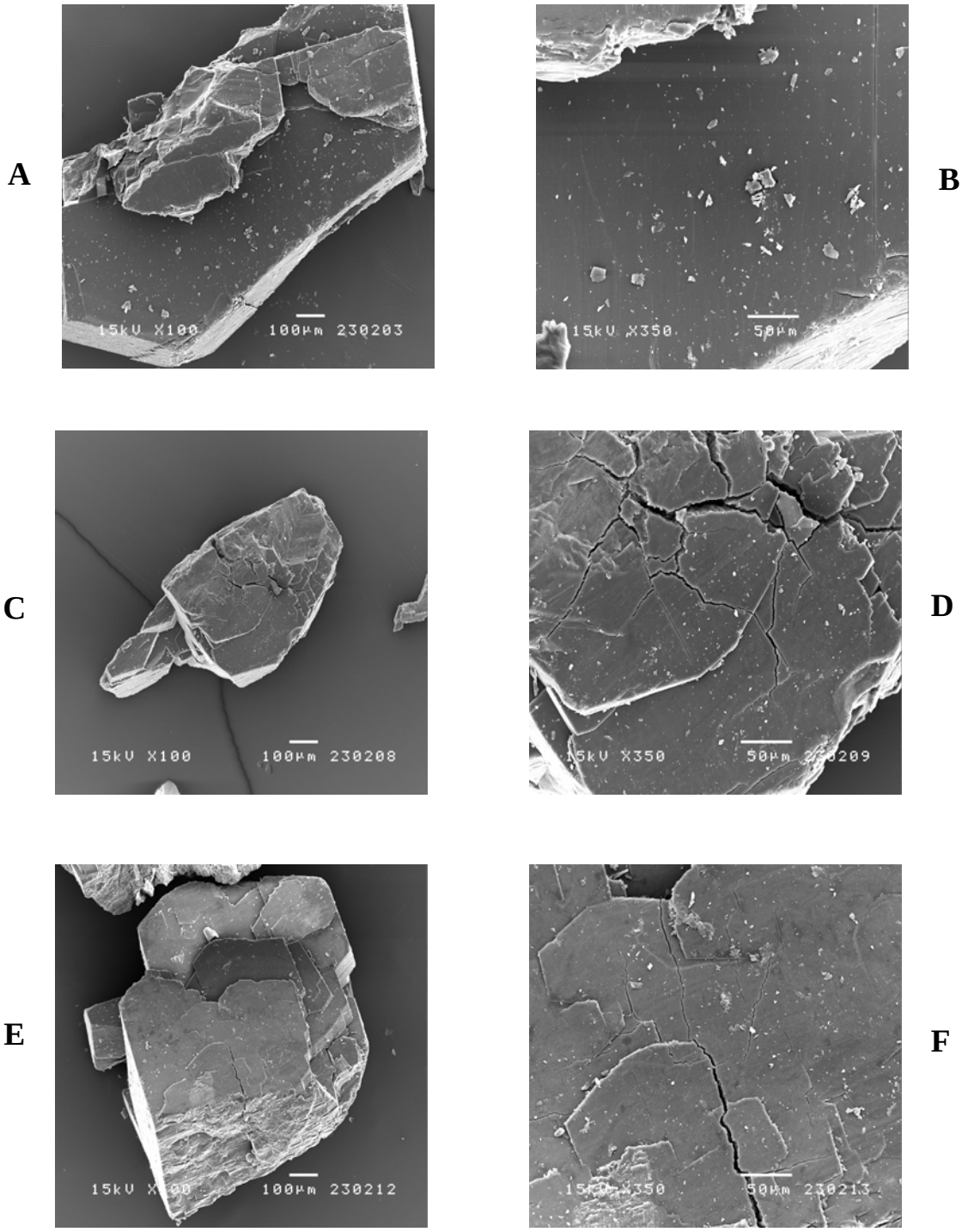

Figure 42 SEM photomicrographs of dihydrate NF after 360 mins of isothermal dehydration with respect to different T_{iso}. (A and B – intact dihydrate NF, C and D – 80 $^{\circ}$C of isothermal dehydration, E and F - 85°C of isothermal dehydration)

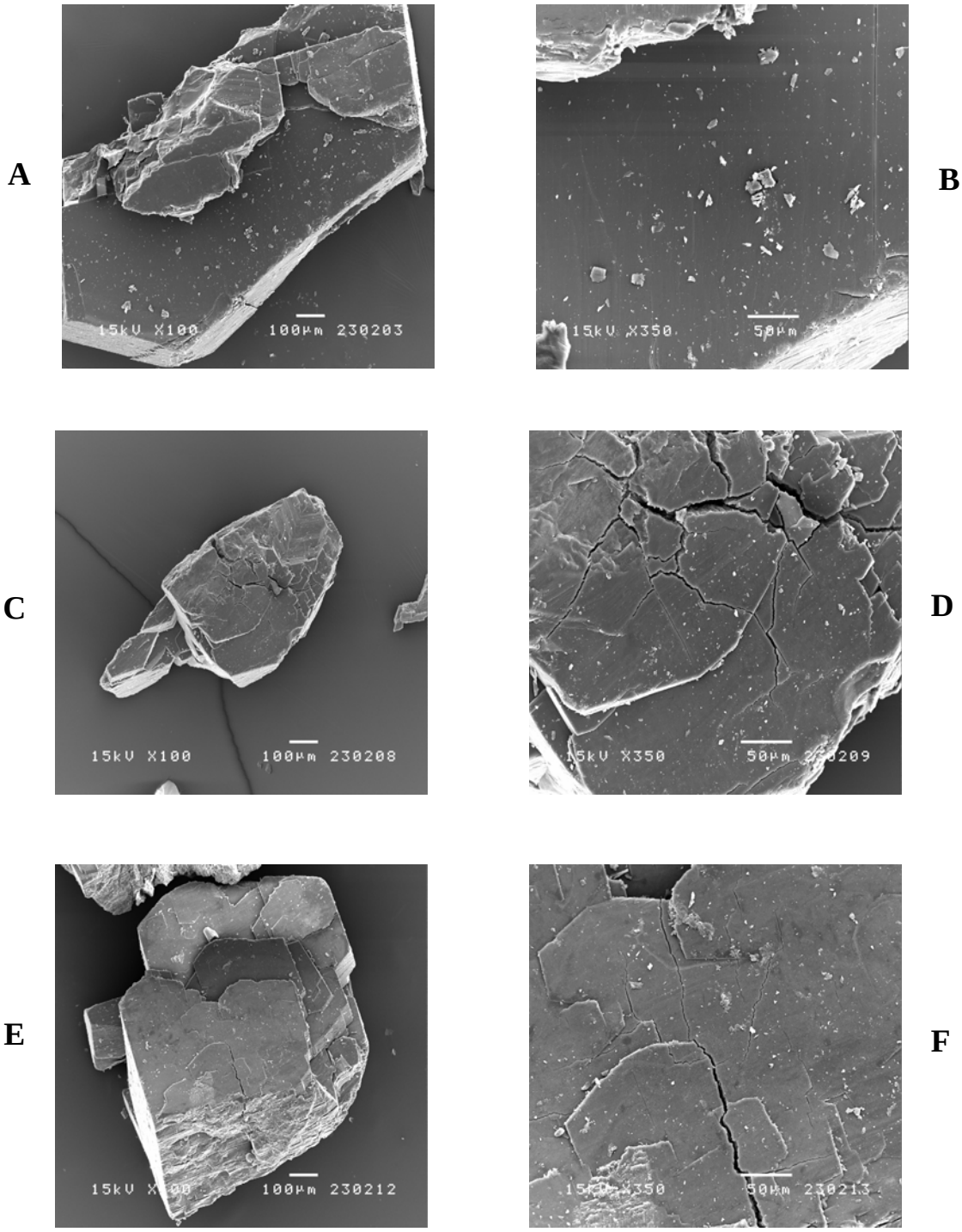

Figure 42 (cont.) SEM photomicrographs of dihydrate NF after 360 mins of isothermal dehydration with respect to different T_{iso}. (A and B – intact dihydrate NF, C and D – 90 °C of isothermal dehydration, E and F - 95°C of isothermal dehydration)

Explanation of unchanged particle size of dihydrate NF during thermal dehydration of two molecules of crystalline waters was of great interest. The single crystal structure of dihydrate NF has already been resolved (Florence et al. (2000)). Hydrogen bond acted as dominant bonding for NF amidst water in the crystal lattice. An atomic position of NF and waters in the dihydrate structure is shown in Figure 43. There were five hydrogen bonds in dihydrate NF that played a major role to stabilize the crystalline water in the dihydrate structure (Figure 44). The hydrogen bonds in dihydrate NF structure were moderate hydrogen bonding. Two hydrogen bonds were moderate to strong bonding while the other three bonds were moderate to weak bonding (Table 8). The primary water molecule (O1) connected to two NF moieties with two moderate to weak hydrogen bonds and also bound to the secondary water (O2) with a moderate to weak hydrogen bond. The secondary water molecule (O2) directly connected to two molecules of NF with moderate to strong hydrogen bonds and acted as a main barrier on dehydration. It showed that the second water of crystallization molecule was bound to NF moiety stronger than the primary water. In addition, DSC thermogram of dihydrate NF was shown to have two consecutive endotherms. It was assumed that the primary water molecule was theoretically removed from the dihydrate structure before the secondary water molecule. However, these two events for liberating the water molecules could not be distinctly separated. The water tunnel in dihydrate NF structure was also observed. It showed only one open-end tunnel along the *c* axis that allowed the easy removal of water molecule (Figure 45).

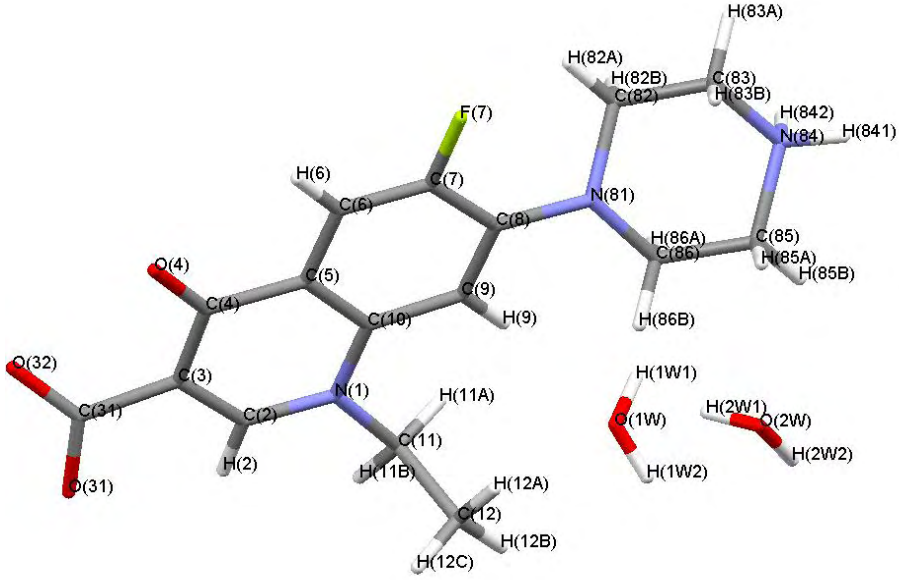

Figure 43 The atomic positions of NF moiety and water of crystallization molecules of dihydrate NF

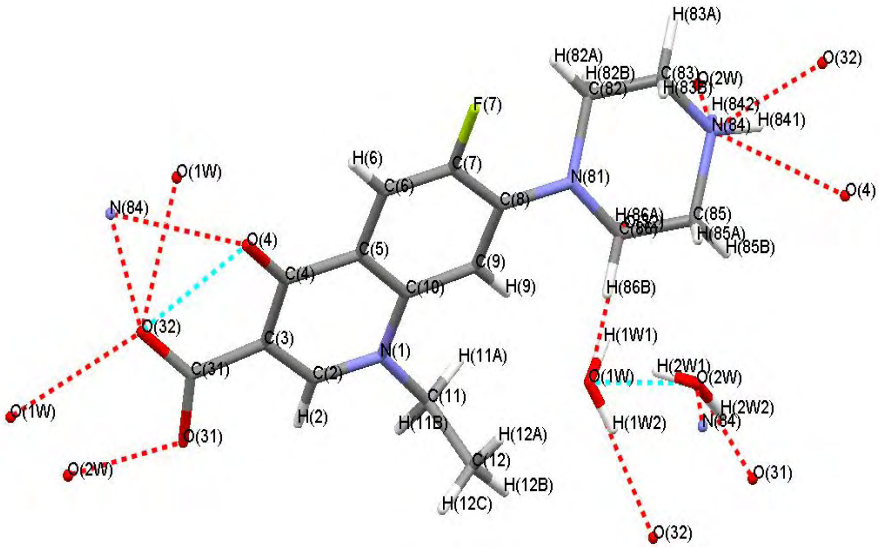

Figure 44 The hydrogen bonding in crystal lattice of dihydrate NF structure

Table 8 The hydrogen bond positions and molecular property in dihydrate NF crystal structure from crystallographic data

Bond definition	Hydrogen bond position	Bond length (Å)	Bond angle(°)	Type of hydrogen bond
	O(1W)-H(1W2)-O(32)			
A----B	O(1W)-O(32)	2.865	172.58	Moderate to
H-A	O(1W)-H(1W2)	0.896		weak
H----B	H(1W2)-O(32)	1.974		
	O(1W)-H(1W1)-O(32)			
A----B	O(1W)-O(32)	2.986	163.24	Moderate to
H-A	O(1W)-H(1W1)	0.950		Weak
H----B	H(1W1)-O(32)	2.064		
	O(1W)-H(2W1)-O(2W)			
A----B	O(1W)-O(2W)	2.783	153.81	Moderate to
H-A	O(1W)-H(2W1)	0.880		weak
H----B	H(2W1)-O(2W)	1.966		
	O(2W)-H(2W2)-O(31)			
A----B	O(2W)-O(31)	2.625	169.81	Moderate to
H-A	O(2W)-H(2W2)	0.967		strong
H----B	H(2W2)-O(31)	1.668		
	O(2W)-H(842)-N(84)			
A----B	O(2W)-O(2W)	2.712	169.26	Moderate to
H-A	O(2W)-H(842)	1.040		strong
H----B	H(842)-N(84)	1.684		

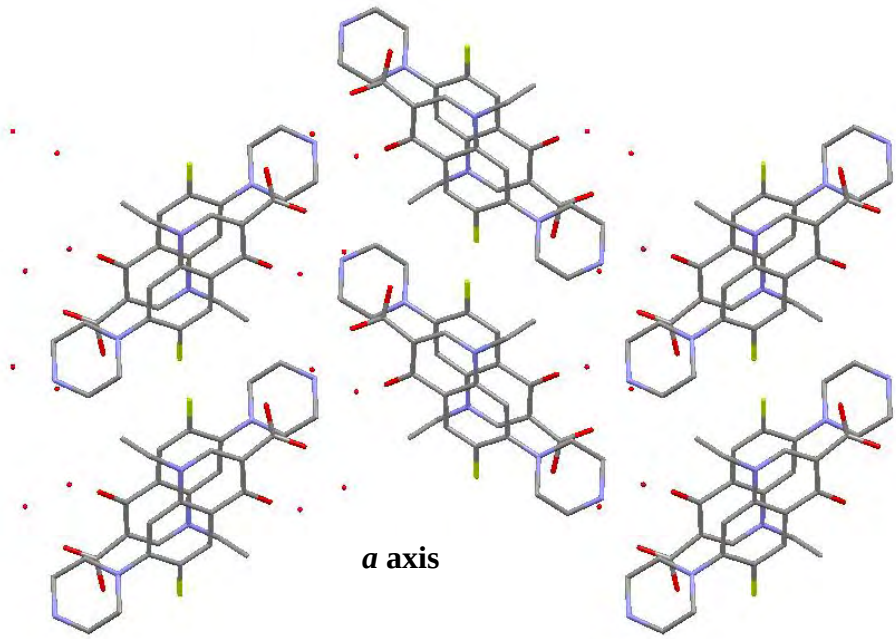

***a* axis**

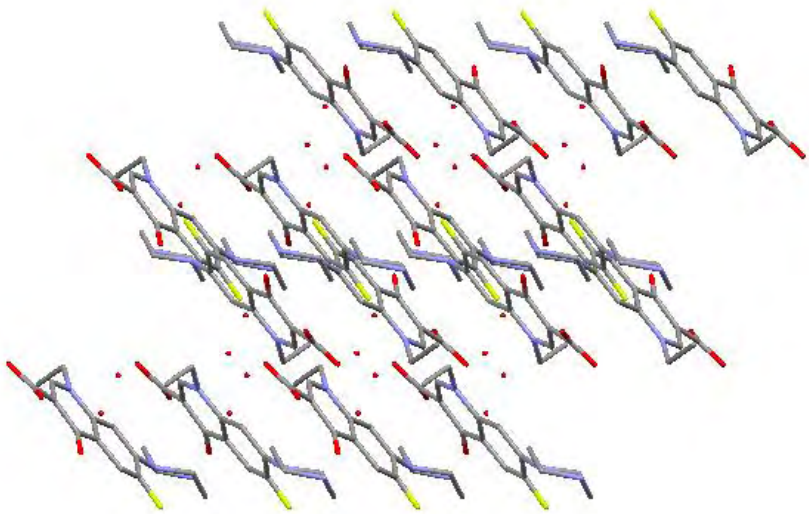

***b* axis**

Figure 45 The crystallographic arrangement of water channel in dihydrate NF structure along different unit cell axis (free red dots are crystalline water).

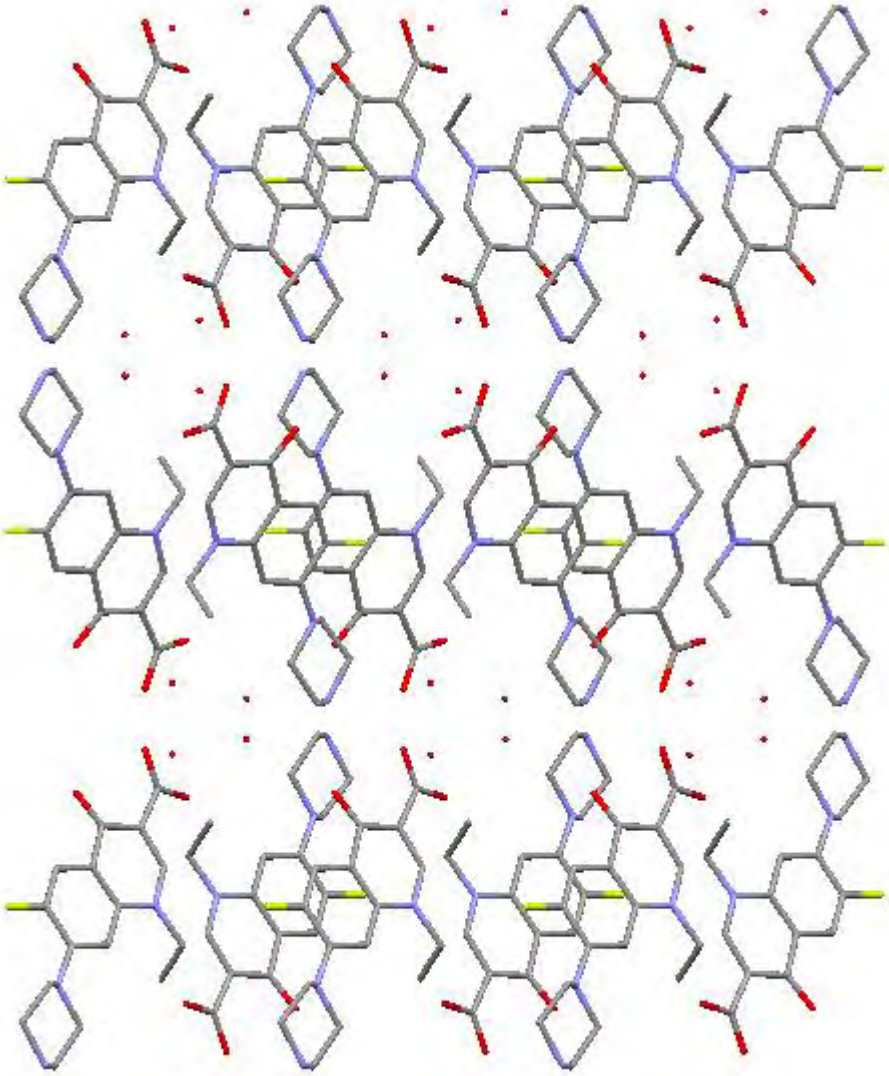

***c* axis**

Figure 45 (cont.) The crystallographic arrangement of water channel in dihydrate NF structure along different unit cell axis (free red dots are crystalline water)

In addition, the concept of the compactness of solvent packing or K_{chan} was also considered (Perlovich et al., 1996 and 1998). The more compact the crystal packing, the higher the K_{chan} value and resulted in the difficulty of dehydration. The crystallographic data of NF dihydrate were reported by Florence et al. (2000) and was generated from our experiment. Z value and unit cell volume of NF dihydrate structure are 4 and 1604.8 $Å^3$, respectively (Table 9). On the other hand, the essential data for the calculation of K_{chan} was a unit cell volume of the anhydrous NF Form A which was never reported elsewhere. There were two methods to obtain this data. The first method, a perfect crystal of anhydrous NF must be generated and resolved by single crystal X-ray diffractometry. Several attempts to

generate suitable crystal of anhydrous NF Form A were performed in this experiment but it was not successful. An alternative method was to employ the XRPD data. Software for crystal structure elucidation "PowderSolve®" under the license of Material Studio®, was used to elucidate the best possible anhydrous NF Form A crystal structure.

Table 9 Crystal data of dihydrate NF

Crystal data	Dihydrate NF
Empirical formula	$C_{16}H_{18}FN_3O_3.2H_2O$
Molecular weight	355.34
Space group	Monoclinic
	$P2_1/C$
a (Å)	8.2835
b (Å)	21.7276
c (Å)	9.5436
β	110.886
crystal cell volume (Å^3)	1604.8
Z	4

The first step of elucidation was the indexing of the unit cell with "Powder Indexing Program" by high quality XRPD pattern as an input data (Appendix D) and refined the simulated unit cell by "Powder Refinement Program". Finally, the PowderSolve® program was employed at the final stage of crystal structure elucidation. In this experiment, Powder Indexing and Powder Refinement programs generated different possible unit cells with different space group as seen in Table 10. However, these data could not be finalized by PowderSolve® program to generate only one accurate crystal structure of anhydrous NF Form A. Although the single correct crystal structure of anhydrous NF Form A was not obtained, the unit cell volume from Powder Indexing program could be used to roughly determine the K_{chan} of dihydrate NF. Powder Indexing program generated the several space groups with different unit cell volumes, the higher figure of merit (FOM) of the result from indexing generally indicated the more accurate unit cell data. From Table 10, the monoclinic space group with unit cell volume of 3682.59 Å^3 had a highest FOM. However, it was larger than the unit cell volume of dihydrate NF (1604.8 Å^3). In general, the unit cell volume of the anhydrous structure should be lower than the unit cell volume of the hydrated structure. Thus, the monoclinic space group with highest FOM was not used for the determination of

K_{chan}. The other results obtained by indexing, the four triclinic structures, showed high FOM with lower unit cell volume when compared to the unit cell volume of the dihydrate NF. These unit cell volume values were employed as representatives for possible anhydrous NF Form A unit cell volume.

The K_{chan} of dihydrate NF were calculated based on the unit cell volume of anhydrous NF Form A with the triclinic space group and are presented in Table 10. The estimated K_{chan} of dihydrate NF were in the range of 0.3368-0.6780. It was higher than those of risedronate sodium hemipentahydrate (equal to 0.1370) (Lester et al., 2006) and beclomethasone dipropionate monohydrate (equal to 0.1663). These results indicated that water of crystallization in dihydrate NF structure occupied the void space of around 33% to 68%. There was less free volume to allow for water mobility. Furthermore, a more close packing induced a strong hydrogen bonding between water and active species and led to higher bonding energy. Therefore, high value of K_{chan} in dihydrate NF supported the stability of crystal lattice during dehydration. In conclusion the main reason for dihydrate NF to retain the crystal size after dehydration largely depends on

1. The structure of dehydrated NF composed of moderate to strong hydrogen bonds
2. There was only one direction of water tunnel
3. The high compactness of solvent packing (K_{chan}).

Thus, the opportunity for the structure to collapse after dehydration and eventually led to significantly smaller particles of dihydrate NF was unlikely and the apparent particle size reduction energy was impossible to calculate.

Table 10 Crystallographic data of anhydrous NF Form A obtained from Powder Indexing program of MATERIAL STUDIO® software simulated with XRPD data

	Figure of Merit (FOM)	K_{chan} of dihydrate NF	Peak Used*	Unit cell							
				system	a (Å)	b (Å)	c (Å)	α (°)	β (°)	γ (°)	Volume (Å^3)
1	2.20	-	22 of 22	Monoclinic	21.13912	15.69688	13.03046	90	121.60200	90	3682.59
2	2.00	0.3368	22 of 22	Triclinic	18.75665	12.96237	7.23957	126.21100	92.06500	101.24500	1367.25
3	2.10	0.5878	23 of 23	Triclinic	20.72207	12.81180	7.80562	125.57900	114.38100	88.58800	1468.71
4	1.90	0.3834	22 of 22	Triclinic	20.08745	12.87875	7.25269	55.86900	107.98300	115.49700	1396.15
5	1.70	0.6780	23 of 23	Triclinic	18.42371	10.54013	8.02520	75.16900	93.56300	99.18300	1486.81
6	1.50	-	22 of 22	Monoclinic	31.18705	4.15313	29.05046	90	106.36700	90	3610.24

* The list of peaks used for indexing (Appendix D)

บทที่ 4

CONCLUSIONS

NF hydrates, was obtained from different methods. Different stoichiometry NF hydrates (dihydrate NF, hemipentahydrate NF, trihydrate NF and pentahdrate NF) were generated. Dehydration with desiccant of the pentahydrate NF resulted in the disordered NF, a new hydrated phase which has not been reported elsewhere. The levels of environmental moisture and temperature greatly affected the transformation of not only the anhydrous NF Form A but also the other stoichiometric hydrates. However, the reduction of moisture in an environment was less effective in removing crystalline water of NF hydrates.

The thermal dehydration behavior of hemipentahydrate NF, trihydrate NF and pentahydrate NF found to be complex and composed of at least two steps of dehydration. Unclear dehydration stages were found in the dehydration of hemipentahydrate NF whereas clear steps of dehydration were detected after thermal dehydration of trihydrate NF and pentahydrate NF. An incomplete dehydration of hemipentahydrate NF, trihydrate NF and pentahydrate NF generated the mixture of hydrated transitional phase and the anhydrous NF form A. However, the pure anhydrous NF Form A was found after the complete dehydration of the above three NF hydrates. Thermal dehydration induced only minor particle size reduction of hemipentahydrate NF, trihydrate NF and pentahydrate NF when statistically determined. However, when observed visually by SEM, thermal dehydration did not induce particle size reduction to the extent seen with BDM. Dehydration energy of different stoichiometry of NF hydrates obtained by regular NIDSC correlated well with the general conclusion that less energy of dehydration was required for the lower stoichiometric hydrates. However, the dehydration energy of trihydrate NF and pentahydrate NF were within the same range. It may be due to the location of water molecules and the strength of hydrogen bonding within the crystal lattice. The E_a of every NF hydrates obtained from solid state kinetic were positive and signified the temperature dependency of the rate of dehydration.

The total dehydration energy of NF hydrates were higher than the energy required for beclomethasone dipropionate monohydrate (Chinapak 2000). It was due to the higher bonding energy between crystalline water and NF molecules and the more compact structures with minimal void volume. Thus, the NF hydrates retained their structures after dehydration and resulted in an unchanged particle size. Conclusively, dehydration energy

and crystal structure void volume after dehydration are two of the factors which may be used and compared to the reference materials (risedronate sodium hemipentahydrate and beclomethasone dipropionate monohydrate) to preliminary determine the possibility of particle size reduction of hydrated structures.

The preliminary guideline for choosing organic hydrates for the particle size reduction via thermal dehydration was proposed. The most important factor was the compactness of crystal structure of hydrates. The hydrates with low K_{chan} should provide a high feasibility on structural collapse after dehydration due to more fragile anhydrous crystal structures. In addition, the directions of water channel or tunnel also played a key role on dehydration. The more directions of open-end water channel the higher dehydration rate. In term of binding forces between active moiety and crystalline water, hydrogen bonding is the fundamental attachment force in lattice structure of most hydrates. The number and strength of hydrogen bond indicates the dehydration possibility. After suitable hydrate model was selected, the recommended experiment for the particle size reduction via thermal dehydration should be performed. Isothermally dehydrated samples are evaluated for the particle size including solid state chemistry. Finally, one should be able to calculate the apparent particle size reduction energy and the total dehydration energy which are useful as reference values for future dehydration studies.

REFERENCES

Abdul-Fattah, A. M., Kalonia, D. S., and Piakl, M. J. 2007. The challenge of drying method selection for protein pharmaceuticals: Product quality implication. J. Pharm. Sci. published online: 24 Jan 2007.

Almarsson, Ö., and Zaworotko, M. J. 2004. Crystal engineering of the composition of pharmaceutical phases. Do pharmaceutical co-crystals represent a new path to improved medicines?. Chem. Commun (Camb) 17: 1889-1896.

Amolwan Chinapak. 2000. Particle size reduction by desolvation technique of a model drug: beclomethasone dipropionate. Master's Thesis. Department of Manufacturing Pharmacy, Faculty of Pharmaceutical Sciences, Chulalongkorn University.

Atkins, P., and Paula, J. 2002. Atkins' Physical Chemistry. 7th ed. New York, Oxford University Press.

Barbas, R., Marti, F., Prohens, R., and Puigjaner, C. 2006. Polymorphism of norfloxacin: evidence of the enantiotropic relationship between polymorphs A and B. Cryst. Growth Des. 6(6): 1463-1467.

Brodka-Pfeiffer, K., Häusler, H., Graß, P., and Langguth, P. 2003. Conditioning following powder micronization: influence on particle growth of sulbutamol sulfate. Drug Dev. Ind. Pharm. 29(10): 1077-1084.

Brown, M. E., Galwey, A. K., and Po, A. L. W. 1993. Reliability of kinetic measurements for the thermal dehydration of lithium sulphate monohydrate. :Part 2. Thermogravimetry and differenetial scanning calorimetry. Thermochim. Acta. 220: 131-150.

Byrn, S.R., and others. 1999. Solid State Chemistry of Drugs. 2nd ed. Indiana: SSCI.

Byrn, S. R., Xu, W., and Newman, A. W. 2001. Chemical reactivity in solid-state pharmaceuticals: formulation implications. Adv. Drug Deliv. Rev. 48: 115-136.

Buxton, P. C., Lynch, I. R., and Roe, J. M. 1988. Solid-state forms of paroxetine hydrochloride. Int. J. Pharm. 42(1-3): 135-143.

Caldwell, H. C. 1973. Labile triazinoindole hydrates. J. Pharm. Sci. 62(2): 334-336.

Chakravarty, S., Bhinge, A., and Varadarajan, R. 2002. A procedure for detection and quantitation of cavity volumes in proteins. J. Biol. Chem. 277(35): 31345-31353.

Chemburkar, S. R., et al. 2000. Dealing with the impact of ritonavir polymorphs on the later stages of bulk drug process development. Org. Process Res. Dev. 4(5): 413-417.

Childs, S. L., Chyall, L. J., Dunlap, J. T., Smolenskaya, V. N., Stahly, B. C., and Stahly, P.

G. 2004. Crystal engineering approach to forming cocrystals of amine hydrochlorides with organic acids. Molecular complexes of fluoxetine hydrochloride with benzoic, succinic, and fumaric acids. J. Am. Chem. Soc. 126(41): 13335-13342.

Chow, A. H. L., Tong, H. H. Y., Chattopadhay, P., and Shekunov, B. 2007. Particle engineering for pulmonary drug delivery. Pharm. Res. 24(3): 411-437.

Cordoba-Borrego, M., Cordoba-Diaz, M., and Cordoba-Diaz, D. 1999. Validation of a high-performance liquid chromatographic method for the determination of norfloxacin and its application to stability studies (photo-stability study of norfloxacin). J. Pharm. Biomed. Anal. 18(6): 919-926.

Crowley, K. J., and Zografi, G. 2002. Cryogenic grinding of indomethacin polymorphs ans solvates: Assessment of an amorphous phase formation and amorphous phase physical stability. J. Pharm. Sci. 91(2): 492-507.

Dong, Z., et al. 2002. Dehydration kinetics of neotame monohydrate. J. Pharm. Sci. 91(6): 1423-1431.

Duax, W. L., Cody, V., and Strong, P. D. 1981. Structure of the asthma drug beclomethasone dipropionate. Acta Cryst. B. 37: 383-387.

Florence, A. J., Kennedy, A. R., Shankland, N., Wright, E., and Al-Rubayi, A. 2000. Norfloxacin dihydrate. Acta Cryst. C. 56: 1372-1373.

Giron, D. 1995. Thermal analysis and calorimetric methods in the characterization of polymorphs and solvates. Thermochim. Acta. 248: 1-59.

Görbitz, C. H., and Hersleth, H. 2000. On the inclusion of solvent molecules in the crystal structures of organic compounds. Acta Cryst. B. 56: 526-534.

Haleblian, J., and McCrone, W. 1969. Pharmaceutical applications of polymorphism. J. Pharm. Sci. 58(8): 911-929.

Hakanen, A., and Laine, E. 1995. Characterization of two terfenadine polymorphs and a methanol solvate: kinetic study of the thermal rearrangement of terfenadine from the methanol solvate to the lower melting polymorph. Thermochim. Acta 248: 217-227.

Haleblian, J. K. 1975. Characterization of habits and crystalline modification of solids and their pharmaceutical applications. J. Pharm. Sci. 64(8): 1269-1287.

Himuro, I., Tsuda, Y., Sekiguchi, K., Horikoshi, I., and Kanke, M. 1971. Studies on the method of size reductionof medicinal compounds. IV. Solvate formation of chloramphenicol and its application to size reduction. Chem. Pharm. Bull. 19(5): 1034-1040.

Hirsch, C. A., Messengger, R. J., and Brannon, J. L. 1978. Fenoprofen: Drug form

selection and preformulation stability studies. J. Pharm. Sci. 67(2): 231-236.

Hogan, S. E., Buckton, G. 2001. Water sorption/desorption-near IR and calorimetric study of crystalline and amorphous raffinose. Int. J. Pharm. 227(1-2): 57-69.

Hu, T., Wang, S., Chen, T., and Lin, S. 2002. Hydration-induced proton transfer in the solid state of norfloxacin. J. Pharm. Sci. 91(5): 1351-1357.

Jeffrey, G. A. 1997. An introduction to hydrogen bonding. New York: Oxford University Press.

Katdare, A. V. 1984. Hydrate related dissolution characteristics of norfloxacin. Drug Dev. Ind. Pharm. 10(5): 789-807.

Katdare, A. V., and Bavitz, J. F. 1984. Study of the relationship between the initial rate of moisture sorption/desorption of norfloxacin tablets to the total moisture and temperature of surrounding environment. Drug Dev. Ind. Pharm. 10(7): 1041-1048.

Katdare, A. V., Ryan, J. A., Bavitz, J. F., Erb, D., and Guillory, J. K. 1986. Characterization of hydrates of norfloxacin. Mikrochim. Acta. 3: 1-12.

Khankari, R. K., and Grant, D. J. W. 1995. Pharmaceutical hydrates. Thermochim. Acta 248: 61-79.

Khawam, A., and Flanagan, D. R. 2005. Role of isoconversional methods in varying activation energies of solid-state kinetics I. isothermal kinetic studies. Thermochim. Acta. 95: 472-498.

Khawam, A., and Flanagan, D. R. 2006. Basics and applications of solid-state kinetics: A pharmaceutical perspective. J. Pharm. Sci. 95(3): 472-498.

Kishore, K. 1978. Study of solid state kinetics by differential scanning calorimetry. Anal. Chem. 50(8): 1079-1083.

Kitamura, S., Miyamae, A., Koda, S., and Morimoto, Y. 1989. Effect of grinding on the solid state stability of cefixime trihydrate. Int. J. Pharm. 56(2): 125-134.

Kitamura, S., Koda, S., Miyamae, A., Yasuda, T., and Morimoto, Y. 1990. Dehydration effect on the stability of cefixime trihydrate. Int. J. Pharm. 59(3): 217-224.

Kotny, M. J., and Conners, J. J. 2002. Water sorption of drugs and dosage forms. In J. Swarbrick,; and J. C. Boylan (ed) Encyclopedia of Pharmaceutical Technology, Vol 3, 2nd ed, pp. 2970-2987. New York: Marcel Dekker.

Laidler, K. J. 1984. The development of the Arrhenius equation. J. Chem. Edu. 61(6): 494-498.

Landgraf, K., Olbrich, A., Pauluhn, S., Emig, P., Kutscher, B., and Stange, H. 1998. Polymorphism and desolvation of flupirtine maleate. Eur. J. Pharm. Biopharm. 46(3):

329–337.

Lester, C., et al. 2006. Dehydration of risedronate hemi-pentahydrate: analytical and physical characterization. J. Pharm. Sci. 95(12): 2631-2644.

Lin, S., and Chien, J. 2003. In vitro simulation of solid-solid dehydration, rehydration, and solidification of trehalose dihydrate using thermal and vibrational spectroscopic techniques. Pharm. Res. 20(12): 1926-1931.

Mazuel, C. 1991. Norfloxacin. In K. Florey (ed.) Analytical Profile of Drug Substances. Vol 20, pp. 557-600. San Diego: Academic Press.

Millard, J. W., and Myrdal, P. B. 2002. Anhydrous beclomethasone dipropionate. Acta Cryst. E. 58: o712-o714.

Mosharraf, M., and Nyström, C. 2003. Apparent solubility of drugs in partially crystalline systems. Drug Dev. Ind. Pharm. 29(6): 603-622.

Narueporn Nachiengtung. 1997. Solid state characterization of beclomethasone dipropionate solvates and polymorphs. Doctoral dissertation. Department of Industrial and Physical Pharmacy, School of Pharmacy, Purdue University.

Nyquist, H. 1983. Saturated salt solutions for maintaining specified relative humidities. Int. J. Pharm. Tech. & Prod. Mfr. 4: 47-48.

O'Neil, M. J., et al. 2001. The Merck Index: An encyclopedia of Chemicals, Drugs and Biologicals. 13th eds, 1200-1201 pp. New Jersey.

Perlovich, G. L., Zielenkiewicz, W., Kaszkur, Z., Utzig, E., and Golubchikov, O. A. 1998. Thermophysical and structural properties of crystalline solvates of tetraphenylporphyrin and their zinc, copper and cadmium metallo-complexes. Thermochim. Acta. 311: 163-171.

Perlovich, G. L., Zielenkiewicz, W., Utzig, E., Kaszkur, Z., and Golubchikov, O. A. 1996. Thermophysical and structural investigations of crystalline solvates based on tetraphenylporphyrin and its copper complex. Thermochim. Acta. 279: 121-136.

Peterson, M. L., Hickey, M. B., Zaworotko, M. J., and Almarsson, Ö. 2006. Expanding the scope of crystal form evaluation in pharmaceutical science. J. Pharm. Pharmaceut. Sci. 9(3): 317-326.

Puechagut, H. G., Bianchotti, J., and Chiale, C. A. 1998. Preparation of norfloxacin spherical agglomerates using the ammonia diffusion system. J. Phram. Sci. 87(4): 520-523.

Redman-furey, N., et al. 2005. Structural and analytical characterization of three hydrates and an anhydrate form of risedronate. J. Pharm. Sci. 94(4): 893-911.

Sakata, Y., Shiraishi, S., and Otsuka, M. 2004. Charcterization of dehydration behavior of untreated and pulverized creatine monohydrate powders. Colloids Surf. B Biointerfaces. 35(3-4): 1851-191.

Sekiguchi, K., Horikoshi, I., and Himuro, I. 1968. Studies on the method of size reduction of medicinal compounds. III. Size reduction of griseofulvin by solvation and desolvation method using chloroform (3). Chem. Pharm. Bull. 16(12): 2495-2502.

Sekiguchi, K., Ito, K., Owada, E., and Ueno, K. 1964. Studies on the method of size reductionof medicinal compounds. II. Size reduction of griseofulvin by solvation and desolvation method using chloroform (2). Chem. Pharm. Bull. 12(10): 1192-1197.

Sekiguchi, K., Shirotani, K., Kanke, M., Furukawa, H., and Iwatsuru, M. 1976. Studies on the methods of particle size reduction of medicinal compounds. VI. Solvate formation of griseofulvin with benzene and dioxane. Chem. Pharm. Bull. 24(7): 1621-1630.

Sekiguchi, K., Tsuda, Y., and Kanke, M. 1974. Studies on the methods of size reduction of medicinal compounds. V. Size reduction of several sulfonamides by desorption of ammonia from their ammonia compounds. Chem. Pharm. Bull. 22(12): 2972-2978.

Sekiguchi, K., Tsuda, Y., Kanke, M., and Suzuki, E. 1978. Ammonia adducts of barbiturates and their application to particle size reduction. Chem. Pharm. Bull. 26(4): 1279-1290.

Steckel, H., Rasenack, N., and Müller, B. W. 2003. In-situ-micronization of disodium cromoglycate for pulmonary delivery. Eur. J. Pharm. Biopharm. 55(2): 173-180.

Stephenson, G. A., Groleau, E. G., Kleemann, R. L., Xu, W., and Rigsbee, D. R. 1998. Formation of isomorphic desolvates: creating a molecular vacuum. J. Pharm. Sci. 87(5): 536-542.

Šuštar, B., Bukovec, N., and Bukovec, P. 1993. Polymorphism and stability of norfloxacin,(1-ethyl-6-fluoro-1,4-dihydro-4-oxo-7-(1-piperazinil)-3-quinolino- carboxylic acid. J. Therm. Anal. 40: 475-481.

Suzuki, E., Shirotani, K., Tsuda, Y., and Sekiguchi, K. 1979. Studies on the method of size reduction of medicinal compounds. VIII. Size reduction by freeze-drying and the influence of pharmaceutical adjuvants on the micromeritic properties of freeze-dried powders. Chem. Pharm. Bull. 27(5): 1214-1222.

The Stationary Office. 2002. British Pharmacopoeia., Vol I. 1234pp. London.

Tsuda, Y., Kanke, M., Miyachi, I., Maeno, K., and Sekiguchi, K. 1980. Ammonia adducts of chloramphenicol and chloramphenicol palmitate and their application to particle size reduction. Chem. Pharm. Bull. 28(3): 947-955.

Turel, I. 2002. The interactions of metal ions with quinolone antibacterial agents. Coordination Chem. Rev. 232: 27-47.

United State Pharmacopeial Convention. 2004. The United State Pharmacopoeia (Asian edition). 27- The National Formulary. 1342 pp. Madison.

Venables, H. J., and Wells, J. I. 2001. Powder mixing. Drug Dev. Ind. Pharm. 27(7): 599-612.

Vitez, I.M., Newman, A. W., Davidovich, M., and Kiesnowski, C. 1998. The evolution of hot-stage microscopy to aid solid-state characterizations of pharmaceutical solids. Thermochim. Acta 324: 187-196.

Vyazovkin, S. 2000. Kinetic concepts of thermally stimulated reactions in solids: a view from a historical perspective. Int. Rev. Phy. Chem. 19(1): 45-60.

Vyazovkin, S., and Wight, C. A. 1997. Kinetics in solids. Annu Rev. Phys. Chem. 48: 125-149.

Willart, J. F., Gusseme, A., Hemon, S., Descamps, M., Leveiller, F., and Rameau, A. 2002. Vitrification and polymorphism of trehalose induced by dehydration of trehalose dihydrate. J. Phys. Chem. B 106(13): 3365-3370.

Yuasa, R., Imai, J., Morikawa, H., Kusajima, H., Uchida, H., and Irikura, T. 1982. Pharmaceutical studies on hydrates of AM-715 Physical characteristics and intestinal absorption. Yakugaku Zasshi 102: 469-476.

Zhou, D., et al. 2003. Model-free treatment of the dehydration kinetics of nedocromil sodium trihydrate. J. Pharm. Sci. 92(7): 1367-1376.

Zhu, H., Yuen, C., and Grant, D. J. W. 1996a. Influence of water activity in organic solvent + water mixtures on the nature of the crystallizing drug phase. 1. Theophylline. Int. J. Pharm. 135(1-2): 151-160.

Zhu, H., and Grant, D. J. W. 1996b. Influence of water activity in organic solvent + water mixtures on the nature of the crystallizing drug phase. 2. Ampicillin. Int. J. Pharm. 139(1-2): 33-43.

APPENDIX A

SI-HPLC

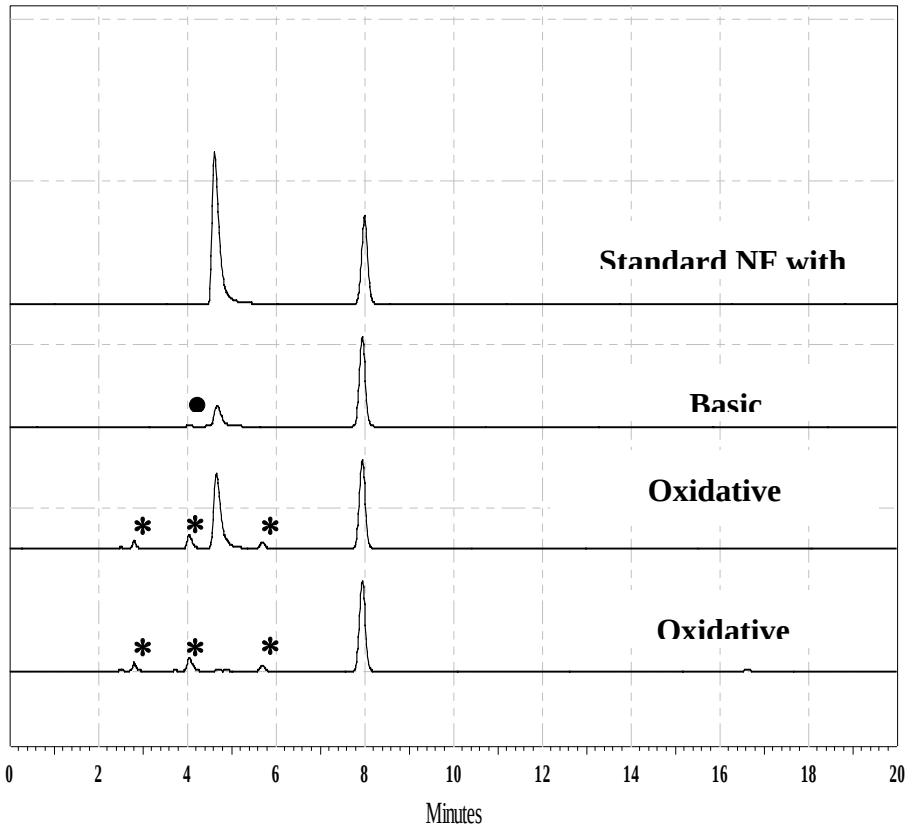

Comparative HPLC chromatograms of standard NF with methyl paraben (MP) as internal standard by SI-HPLC method. (* degradant from oxidative reaction and ● degradant from basic reaction)

APPENDIX B

THE RATE LAW

Classical chemical reaction of desolvation pharmaceutically follows the reaction schemes below:

$$A_{(S)} \longrightarrow B_{(S)} + C_{(g)}$$

So the rate of reaction usually declares as a function of the concentration of reactant or products. It should be derived as follows.

$$\text{Rate} = \frac{d[A]}{dt} = -\frac{d[B]}{dt} = -\frac{d[C]}{dt}$$

In general, rate of reaction, k, is commonly monitored with respect to the decrease of reactant or the increase of product in term of amount or concentration. Thus, it will be presents here.

$$\text{Rate} = -k[A]^n = k([A]_0 - [B])^n = k([A]_0 - [C])^n$$

Where A_0 is initial concentration of A and n is order of reaction.

In the case of desolvation, liberated gas is carried out from the system and made the [C] became to zero. If unimolecular reaction, n is 1, is considered. By following the reactant point of view, the rate would be illustrated as

$$\text{Rate} = \frac{d[A]}{dt} = -k[A]$$

By intergration

$$-\ln\frac{[A]}{[A_0]} = kt$$

Solid state kinetics will be observed the progress of reaction by describing the fraction of conversion (α) instead of the reaction concentration. The rate is hence transformed based on above relation and expressed as

$$\text{Rate} = \frac{d\alpha}{dt} = k(1-\alpha)$$

then be integrated as

$$-\ln(1-\alpha) = kt$$

In addition, unlike solution state, solid state kinetics should be varied depend on several factors. It can be commonly illustrated as

$$\frac{d\alpha}{dt} = kf(\alpha)$$

and

$$g(\alpha) = kt$$

where f(α) is the differential reaction model and g(α) is the integral reaction model.

The temperature dependence of the rate constant (k) is normally described by the Arrhenius relationship.

$$k = Ae^{-\frac{E_a}{RT}}$$

where A is the frequency factor, E_a is activation energy, R is the gas constant and T is absolute temperature. Combining above equations yield the relationship below.

$$\frac{d\alpha}{dt} = Ae^{-\frac{E_a}{RT}} f(\alpha)$$

and

$$g(\alpha) = Ae^{-\frac{E_a}{RT}} t$$

APPENDIX C

SOLID STATE KINETIC EQUATION

(Byrn et al., 1999; Dong et al., 2002)

Model	Mechanism
$[-\ln(1-\alpha)]^{\frac{1}{2}} = kt$	One-dimensional growth of nuclei (Avrami-Erofe'ev equation, *n*=2)
$[-\ln(1-\alpha)]^{\frac{1}{3}} = kt$	Two-dimensional growth of nuclei (Avrami-Erofe'ev equation, *n*=3)
$[-\ln(1-\alpha)]^{\frac{1}{4}} = kt$	Three-dimensional growth of nuclei (Avrami-Erofe'ev equation, *n*=4)
$\alpha^2 = kt$	One-dimensional diffusion
$(1-\alpha)\ln(1-\alpha) + \alpha = kt$	Two-dimensional diffusion
$(1-(1-\alpha)^{\frac{1}{3}})^2 = kt$	Three-dimensional diffusion (Jander equation)
$1-\frac{2}{3}\alpha-(1-\alpha)^{\frac{2}{3}} = kt$	Three-dimensional diffusion (Ginstling-Brounshtein equation)
$-\ln(1-\alpha) = kt$	First order reaction (Mampel)
$\frac{1}{(1-\alpha)}-1 = kt$	Second order reaction
$\frac{1}{2}\left(\frac{1}{(1-\alpha)^2}-1\right) = kt$	Third order reaction
$\frac{1}{3}\left(\frac{1}{(1-\alpha)^3}-1\right) = kt$	Fourth order reaction
$\ln\left(\frac{\alpha}{(1-\alpha)}\right) = kt$	Random nucleation (Prout-Tompkins equation)
$\alpha^{\frac{1}{2}} = kt$	Power law (*n*=1/2)
$\alpha^{\frac{1}{3}} = kt$	Power law (*n*=1/3)
$\alpha^{\frac{1}{4}} = kt$	Power law (*n*=1/4)
$\alpha = kt$	One-dimensional phase boundary reaction (zero-order mechanism)
$1-(1-\alpha)^{\frac{1}{2}} = kt$	Two-dimensional phase boundary reaction (contracting cylinder)
$1-(1-\alpha)^{\frac{1}{3}} = kt$	Three-dimensional phase boundary reaction (contracting sphere)

APPENDIX D

List of Peaks Used for Indexing

Group of 22 peaks	Group of 23 peaks
4.855	4.855
8.810	8.810
9.770	9.770
11.360	11.360
12.290	12.290
14.840	14.840
15.995	15.995
18.680	18.680
19.725	19.725
20.560	20.560
21.420	21.420
21.835	21.835
22.580	22.580
24.775	24.222
26.335	24.775
27.660	26.335
29.003	27.660
30.235	29.003
30.840	30.235
32.282	30.840
33.230	32.282
34.493	33.230
	34.493

High refined XRPD of anhydrous NF Form A

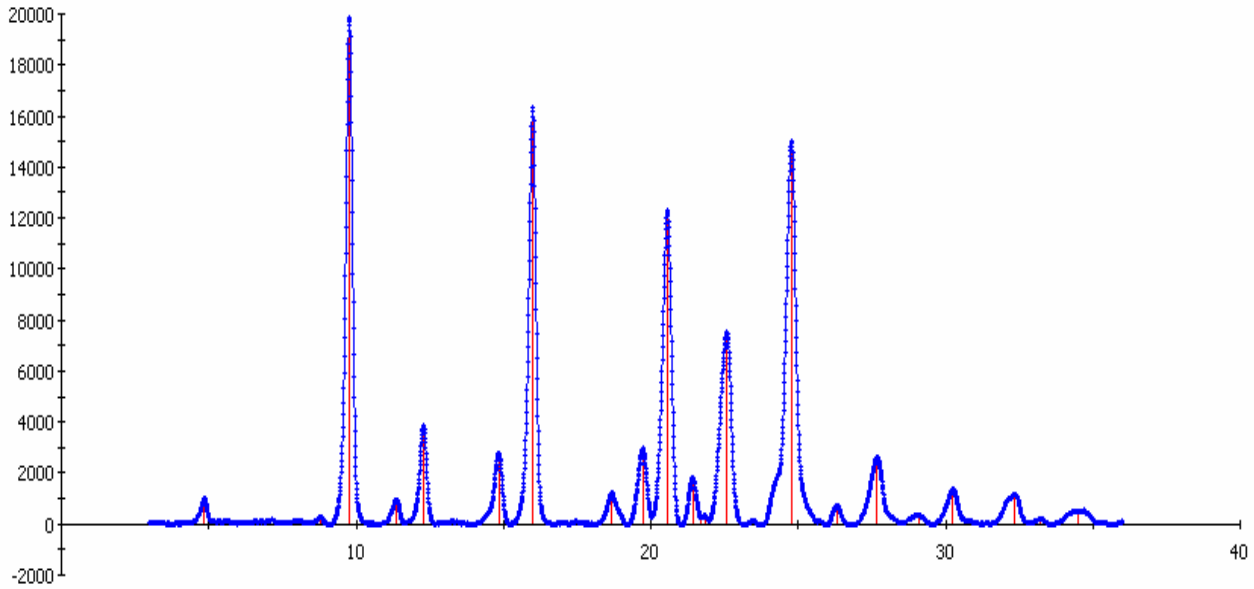

บทที่ 5

ข้อเสนอแนะสำหรับงานวิจัยในอนาคต

The most important factor for choosing organic hydrates for the particle size reduction via thermal dehydration was the compactness of crystal structure of hydrates. The hydrates with low K_{chan} should provide a high feasibility on structural collapse after dehydration due to more fragile anhydrous crystal structures. In addition, the directions of water channel or tunnel also played a key role on dehydration. The more directions of open-end water channel the higher dehydration rate. In term of binding forces between active moiety and crystalline water, hydrogen bonding is the fundamental attachment force in lattice structure of most hydrates. The number and strength of hydrogen bond indicates the dehydration possibility. After suitable hydrate model was selected, the recommended experiment for the particle size reduction via thermal dehydration should be performed. Isothermally dehydrated samples are evaluated for the particle size including solid state chemistry. Finally, one should be able to calculate the apparent particle size reduction energy and the total dehydration energy which are useful as reference values for future dehydration studies.

Output จากโครงการวิจัย

1.ผลงานตีพิมพ์ในวารสารวิชาการนานาชาติ

Wanchai Chongcharoen, Stephen R. Byrn, Narueporn Sutanthavibul. Solid State Characterization and Interconversion of Norfloxacin and its Hydrates. *J. Pharm. Sci.* 2008; 97(1):473-89.

2. ผลงานตีพิมพ์ในวารสารวิชาการในประเทศ

วันชัย จงเจริญ วีระเกียรติ บุญกนกวงศ์ และ นฤพร สุตัณฑวิบูลย์, การประยุกต์ใช้เคมิคัลโซลเวตในทางเภสัชกรรม. *Thai Pharm Health Sci J*. 2009; 4(3):377-386.

W. Chongchareon, Stephen R. Byrn and N. Sutanthavibul. Solid State Characterization and Interconversion of Norfloxacin Hydrates. The American Association of Pharmaceutical Scientists (AAPS) Annual Meeting and Exposition. October 29- November 2, 2006. San Antonio, Texas, USA.

3. การนำผลงานวิจัยไปใช้ประโยชน์

3.1 การได้รับเชิญเป็นวิทยากรบรรยาย

บริษัท เมดิก้าอินโนวา จำกัด
ธันวาคม 2551
หัวข้อ Application and Instrumentation of X-ray Diffractometry
หัวข้อ Application and Instrumentation of Thermal Analysis
วิทยากร อ. ดร. นฤพร สุตัณฑวิบูลย์

บริษัท มิลลิเมด จำกัด
วันที่ 28 พฤศจิกายน 2551
หัวข้อ ลักษณะผลึก Glucosamine Sulfate ที่มีผลต่อการดูดซึมยาเข้าสู่ร่างกาย
วิทยากร อ. ดร. นฤพร สุตัณฑวิบูลย์

สมาคมไทยอุตสาหกรรมผลิตยาแผนปัจจุบัน
กลุ่มอุตสาหกรรมยา สภาอุตสาหกรรมแห่งประเทศไทย
จัดการประชุมวิชาการ เรื่อง "มุ่งพัฒนาอุตสาหกรรมยา เพื่อคุณภาพชีวิต"
ณ ศูนย์การประชุมแห่งชาติสิริกิติ์
วันที่ 18-19 ธันวาคม 2550

หัวข้อ Preformulation of Pharmaceuticals
วิทยากร อ. ดร. นฤพร สุตัณฑวิบูลย์

บริษัท แม็กซ์เวย์ จำกัด
วันที่ 27 กรกฎาคม 2549
การประชุมเชิงปฏิบัติการเรื่องเทคนิคการผลิตอาหารเสริมรูปแบบเม็ดและแคปซูล
หัวข้อ คุณสมบัติทางเคมีและกายภาพของสารในสูตรตำรับ
วิทยากร อ. ดร. นฤพร สุตัณฑวิบูลย์

วิทยาลัยการสาธารณสุข
วันที่ 6 มิถุนายน 2549
วิชา เภสัชกรรมไทยประยุกต์ 5
หัวข้อ การพัฒนาตำรับ (Preformulation)
วิทยากร อ. ดร. นฤพร สุตัณฑวิบูลย์

สถาบันวิจัยจุฬาภรณ์ (Chulabhorn Research Institute)
วันที่ 10 กุมภาพันธ์ 2549
บรรยายเรื่อง Solid State Chemistry
วิทยากร อ. ดร. นฤพร สุตัณฑวิบูลย์

บรรยายเรื่อง Hydrates and its Applications
วิทยากร ภก. วันชัย จงเจริญ

หน่วยวิจัยและพัฒนาเภสัชภัณฑ์รูปของแข็ง
คณะเภสัชศาสตร์ จุฬาลงกรณ์มหาวิทยาลัย ร่วมกับ
บริษัท Mettler-Toledo (Thailand) จำกัด
วันที่ 9-10 สิงหาคม 2548
เรื่อง การประชุมเชิงปฏิบัติการเรื่องการประยุกต์การวิเคราะห์เชิงความร้อนใน
อุตสาหกรรมยา
หัวข้อ Solid state chemistry of pharmaceutical materials
หัวข้อ Basic principles behind thermal analysis
วิทยากร อ. ดร. นฤพร สุตัณฑวิบูลย์

3.2 การสร้างเครือข่ายความร่วมมือ

ภก. วันชัย จงเจริญ เดินทางไป Purdue University, W. Lafayette ประเทศสหรัฐอเมริกา เป็นระยะเวลา 8 เดือน เพื่อแลกเปลี่ยนเรียนรู้และดำเนินงานวิจัยส่วนที่เป็นการวิเคราะห์โครงสร้างทางของแข็งของ norfloxacin hydrate ต่างๆ โดยใช้ x-ray แบบผลึกเดี่ยว (single crystal x-ray diffractometry) และศึกษาการเปลี่ยนรูปในสถานะของแข็ง (solid state interconversion) ของ hydrate เหล่านั้น ร่วมกับ Professor Stephen R. Byrn และคณะ

3.3 การสร้างนักวิจัยรุ่นใหม่

สร้างบัณฑิต ระดับดุษฎีบัณฑิต 1 คนสู่อุตสาหกรรมยา (ภก. ดร. วันชัย จงเจริญ)

ภาคผนวก

Solid State Interconversion between Anhydrous Norfloxacin and its Hydrates

WANCHAI CHONGCHAROEN,[1] STEPHEN R. BYRN,[2] NARUEPORN SUTANTHAVIBUL[1]

[1]Faculty of Pharmaceutical Sciences, Chulalongkorn University, Bangkok, Thailand

[2]School of Pharmacy and Pharmaceutical Sciences, Purdue University, West Lafayette, Indiana

Received 9 March 2007; revised 22 June 2007; accepted 11 July 2007

Published online in Wiley InterScience (www.interscience.wiley.com). DOI 10.1002/jps.21165

ABSTRACT: This work is focused on characterizing and evaluating the solid state interconversion of norfloxacin (NF) hydrates. Four stoichiometric NF hydrates, dihydrate, hemipentahydrate, trihydrate, pentahydrate and a disordered NF state, were generated by various methods and characterized by X-ray powder diffractometry (XRPD), thermal analysis and Karl Fisher titrimetry. XRPD patterns of all NF hydrates exhibited crystalline structures. NF hydrate conversion was studied with respect to mild elevated temperature and various degrees of moisture levels. NF hydrates transformed to anhydrous NF Form A after gentle heating at 60°C for 48 h except dihydrate and trihydrate where mixture in XRPD patterns between anhydrous NF Form A and former structures existed. Desiccation of NF hydrates at 0% RH for 7 days resulted in only partial removal of water molecules from the hydrated structures. The hydrated transitional phase and the disordered NF state were obtained from the incomplete dehydration of NF hydrates after thermal treatment and pentahydrate NF after desiccation, respectively. Anhydrous NF Form A and NF hydrates transformed to pentahydrate NF when exposed to high moisture environment except dihydrate. In conclusion, surrounding moisture levels, temperatures and the duration of exposure strongly influenced the interconversion pathways and stoichiometry of anhydrous NF and its hydrates.

Keywords: norfloxacin; hydrate; hydration; solid state; dehydration; interconversion; X-ray powder diffractometry; thermal analysis

INTRODUCTION

Norfloxacin (NF) is a 4-fluoroquinolone antibacterial agent that has been widely used to treat various infectious diseases such as urinary tract infections, upper respiratory tract infections, bone and joint infections and sexually transmitted diseases. It has a powerful activity against aerobic gram-negative bacteria with less potential to kill gram-positive bacteria.[1] Several research publications have indicated that NF has a potential to form various solid state forms especially hydrates. Two forms of anhydrous state, Form A and B, were discovered and recently found to be enantiotropic.[2,3] Meanwhile, amorphous state was also generated and characterized.[2] Moreover, at least six hydrate forms of NF were reported but not characterized for its complete interconversion, that is, hemihydrate, sesquihydrate, dihydrate, trihydrate, hemipentahydrate, and pentahydrate.[4–9] Variable-temperature Fourier Transformed Infrared Spectroscopy (FT-IR) is used to monitor the transformation between anhydrous

Correspondence to: Narueporn Sutanthavibul (Telephone: +662-218-8276; Fax: +662-218-8279; E-mail: pooh@aut.co.th)

Journal of Pharmaceutical Sciences

and hydrate forms.[10] The IR spectra of anhydrous form show a shift of the carboxylate anion (unprotonated form) peak to the protonated carboxylic peak after heating. In addition, the NH_3^+ peak is also shifted to NH_2 peak position synchronously. This is due to the zwitterionic property of NF molecules at the carboxylic functional group and the piperazine ring. Thus, the hydrated forms may result in a more highly charged molecule and could be easily hydrated with water than the uncharged anhydrous NF form. This may in turn increase dissolution rate of solid dosage forms. Yuasa et al.[9] reported that hemipentahydrate NF had a dissolution rate similar to pentahydrate NF which was significantly higher than anhydrous NF. However, these three different solid forms did not show any significant difference in bioavailability.[9]

Various hydrate forms often have different physicochemical properties and enormously affect the pharmaceutical manufacturing processes including dosage form performances.[11–13] The different anhydrate and hydrate forms of magnesium stearate exhibit variation in lubrication efficiency due to dissimilarity of crystal lattice arrangement, particularly the spacing of lattice which is dependent on hydration state.[11] In addition, the path of conversion between anhydrate and hydrate of magnesium stearate was also reported and demonstrated that their transformation occurred in the condition encountered during pharmaceutical manufacturing.[14] Therefore, to define suitable processing parameters for magnesium stearate with maximum lubricating power, the data of solid state conversion pathway is required. On the dosage form performance point of view, the conversion between dihydrate and anhydrous forms of carbamazepine was extensively investigated. Kobayashi et al.[15] and Ono et al.[16] reported that anhydrous carbamazepine is converted to dihydrate upon hydration while dihydrate is transformed to anhydrous during heating. The dihydrate carbamazepine is shown to have lower intrinsic dissolution rate leading to lower bioavailability compared with anhydrous forms. Thus, the path of conversion of a solid drug substance must be fully understood in order to formulate a solid dosage form with stabilized desired solid structure and to ensure optimal therapeutic efficacy.

In the case of NF, previous studies have shown that anhydrous NF was converted to undefined NF hydrate due to exposure to moisture during tablet manufacturing and storage. This conversion had a significant impact on the dosage form performance of NF tablet.[17,18] The dissolution profile of moisture treated NF tablet is higher than that of original NF tablet. Due to the fact that NF is able to exist as more than one hydrate form, it is very important to investigate the complete paths of conversion among possible hydrates eventhough incomplete evidence about the paths of conversion of NF have been previously reported.[9] Hence, the aim of this study was to extensively explore and fully gather information on the interconversion phenomena of anhydrous NF and different NF hydrate produced.

EXPERIMENTAL SECTION

Materials

Norfloxacin (anhydrous) Form A was purchased from Sigma–Aldrich (St. Louis, MO). Isopropanol (IPA), acetone and dichloromethane were analytical grade reagents from Mallinkrodt Chemicals (Phillipsburg, NJ). Ammonium hydroxide (J.T. Baker, Phillipsburg, NJ), hydrogen peroxide, 30% w/v (PanReac, Barcelona, Spain), ortho-phosphoric acid (Univar, Seven Mills, Australia) was used. Salts for preparing saturated solution to provide different % relative humidities (% RH) were obtained from Unilab, Australia. Anhydrous calcium sulfate (Drierite, Xenia, OH®) was used as the desiccant. Double distilled water was employed throughout this study.

Preparation of NF Hydrates

Dihydrate NF

NF Form A was dissolved in a mixture of IPA and water (0.915 mol fraction of IPA) at 60°C in a light resistant container. The final NF concentration was equal to 1.5 mg/mL. The clear solution was allowed to cool down and left undisturbed at ambient condition to facilitate recrystallization. The resultant crystalline powder was harvested and kept in a tight and light-resistant container.

Trihydrate NF

Preparation of trihydrate NF was modified from the method reported by Puechagut et al.[7] Anhydrous NF Form A was dissolved in 20% w/v aqueous ammonia solution to give a final clear solution at a concentration of 17.5 mg/mL. Antisolvent was obtained by mixing 564 mL of acetone and 156 mL of dichloromethane. The

aqueous ammonia NF solution of 68.5 mL was gradually poured into antisolvent with continuous agitation. White and fluffy precipitates were developed and harvested. Dichloromethane was used to wash the resultant precipitates. The product was then placed in the drying oven at 50°C for approximately 1 h to remove residual solvents.

Hemipentahydrate and Pentahydrate NF

Hemipentahydrate and pentahydrate NF were prepared by hydration of anhydrous NF Form A at specified % RH level. Anhydrous NF Form A was placed under 75% RH and 100% RH at ambient temperature for 1 week to yield hemipentahydrate and pentahydrate, respectively.[5,9] Additionally, pentahydrate was also prepared by suspending anhydrous NF Form A in excess amount of double distilled water with continuous stirring. Dispersed solid was filtered and dried at ambient condition.

Solid State Characterization of NF hydrates

Thermal Analysis

The thermal properties of NF crystalline hydrates were evaluated usingDSC 822^e (Mettler Toledo, Zurich, Switzerland) with STAR^e software. Sample (5 mg) in an aluminum pan with one pinhole was evaluated from 30 to 230°C at a scanning rate of 10°C/min under nitrogen purge at 60 mL/min. TGA/SDTA 851^e (Mettler Toledo) was employed to investigate the liberation of volatile substance. The TGA operating conditions were the same as those used in the DSC study.

Hot Stage Microscopy (HSM)

Hot stage FP90 (Mettler Toledo) equipped with optical microscope Eclipse, E2000 (Nikon, Japan) was employed to visually evaluate solvates or hydrates.[19] Heating rate and temperature range were 10°C/min and 30–240°C, respectively. A small amount of sample was initially suspended in mineral oil and placed on a glass slide before being fixed on to the heating station. The liberation of gas bubbles at specified temperature was observed and recorded.

Karl Fischer Titrimetry (KF)

The water contents of NF hydrates were monitored using 720 KFS Titrino and 703 Ti Stand (Metrohm, Heraisu, Switzerland). Due to low solubility of NF hydrates in methanol, heating oven (KF 707; Metrohm) was selected as an additional attachment. Approximately 50 mg of the sample was inserted into the heating oven. The oven temperature of 160°C was gradually increased to initiate the evaporation of water molecules. Water vapor was carried by dried nitrogen gas to react with KF reagents in the titration vessel where water contents were finally quantified.

X-Ray Powder Diffraction (XRPD)

X-ray powder diffractometry was done using D500 diffractometer (Siemens, Karlsruhe, Germany) equipped with CuKα radiation at 40 kV and 20 mA. Samples were measured at a step size of 0.04°2θ with a scan speed 5°2θ/min from 5° to 35°2θ.

Fourier Transformed Infrared Spectroscopy (FT-IR)

ATR FT-IR model Spectrum One® (Perkin–Elmer, Shelton, CT) was employed to observe the changes in peak positions between anhydrous NF and NF hydrates. The samples were triturated and gently ground with dried potassium bromide in an agate mortar. The spectra were recorded as percent transmittance (%T) with respect to wavenumber in the range of 450 to 4000 cm^{-1}.

Stability Indicating High Performance Liquid Chromatography (SI-HPLC)

SI-HPLC method was modified from the method used by Cordoba-Borrego et al.[20] HPLC (LC 10-ADvP, Shimadzu, Japan) equipped with Hypersil BDS-C18 column in conjunction with C18-guard column was used. The mobile phase comprised of 0.1% v/v aqueous o-phosphoric acid:acetonitrile at volume ratio of 70:30. The flow rate was equal to 1 mL/min. UV detection was carried out at 278 nm. Degradation product of NF was prepared by dispersing NF in 30%w/v hydrogen peroxide in clear glass vial and was exposed to light and heat (80°C) in an oven up to 8 h. In addition, forced degradation in basic environment condition was evaluated according to the method used to prepare trihydrate NF. Small amount of anhydrous NF was added to 20% w/v aqueous ammonia solution and heated at 80°C to initiate degradation.

Scanning Electron Microscopy (SEM)

The morphology of sample was recorded with a JSM-5410LV (JEOL, Tokyo, Japan) at 15 kV. The sample was carefully attached on the metal stub.

It was then coated with gold by Sputter coater SCD040 (Balzers, Liechtenstein) for 3 min at 0.05 mbar, 15 mA with a working distance of 5 cm.

Solid State Interconversion of NF Hydrate

In an attempt to explore the interconversion pathways among NF hydrates and the anhydrous form, specific conditions were identified. Temperature and surrounding % RH were of main interest.

Effect of Relative Humidity on the Conversion of NF Anhydrous and NF Hydrates

The effect of % RH on the conversion of anhydrous NF Form A was evaluated. Preliminary study on sorption and desorption behaviors of anhydrous phase was investigated by dynamic vapor sorption (DVS) using symmetrical gravimetric analyzer (SGA-100, VTI Corporation, Hialeah, FL). Fifteen milligrams of anhydrous NF Form A was dried in a vacuum at 25°C for 6 h to minimize traces of surface associated water. Isothermic equilibrium condition of the cycle was 0.01% w/w within 15 min with a maximum step time of 75 min. The step change of % RH in both sorption and desorption phase were 5% RH/step. The change in sample weight against % RH was recorded.

Due to limited amounts of the samples obtained by DVS experiments, the sample at each equilibrium % RH was not sufficient to be collected in order to monitor for their solid state characteristics by XRPD. Thus, larger amounts of NF samples were exposed to specific moisture levels. The generation of various % RH in an air tight and light resistant container was made by using saturated solutions of lithium chloride (11.3% RH), magnesium chloride (32.8% RH), potassium carbonate (43% RH), sodium bromide (57.5% RH), sodium chloride (75% RH), potassium bromide (81% RH), potassium chloride (84% RH), dextrose monohydrate (87% RH), potassium nitrate (93.7% RH), and purified water (100% RH) at 25°C.[21,22] The drug was exposed to each relative humidity for 7 days before being characterized.

The preliminary results obtained by DVS and relative humidity exposures, indicated that phase transformation of anhydrous NF Form A to various stoichiometric hydrates occurred. Thus, every stoichiometric NF hydrate produced was subjected to an extremely high moisture level of 100% RH and very dry environment of 0% RH (Drierite®) and monitored for further transformation. The samples were stored for 7 days and then characterized by XRPD compared to the corresponding references. Additional storage time was needed in some cases where 7 days was insufficient to induce any transformation in the solid state.

Effect of Temperature on the Conversion of NF Hydrates

The temperature effect, particularly heating, was aimed to investigate dehydration of NF hydrates. A mild temperature of 60°C was selected in an attempt to avoid chemical degradation. NF hydrates were placed in the drying oven at 60°C for 48 h before being characterized by XRPD. However, additional exposure time of up to 1 month was needed for some NF hydrates to confirm the solid state transformation.

RESULTS AND DISCUSSION

Solid State Characterization of NF Hydrate

Anhydrous NF starting material was characterized by XRPD, DSC, and TGA. TGA revealed negligible mass loss of less than 1% w/w (Fig. 1A) which was in accordance with USP and BP specifications of anhydrous NF.[23,24] DSC experiment confirmed a single sharp endotherm at a temperature range of approximately 220 to 225°C for anhydrous NF (Fig. 1A). XRPD of anhydrous NF (Fig. 2A) showed characteristic peak positions identical to those reported for NF Form A.[3,5,9] It was hence concluded that the anhydrous NF in our experiment was polymorphic anhydrous NF Form A.

Slow recrystallization of NF solution in IPA: water mixture resulted in dihydrate NF. Thermal properties and water content of this hydrate are shown in Figure 1C. DSC and TGA thermograms showed endothermic peaks along with weight loss at the temperature range of 80–140°C. HSM also showed water vapor liberation by observing gas bubbles within the same temperature range (Fig. 3B). Water content obtained by KF titration agreed well with the weight change obtained by TGA (Tab. 1) which indicated a dihydrate stoichiometry. XRPD pattern of the dihydrate NF was not reported in any previous publications for reference. Thus, a single crystal X-ray diffraction data from crystal obtained by the above

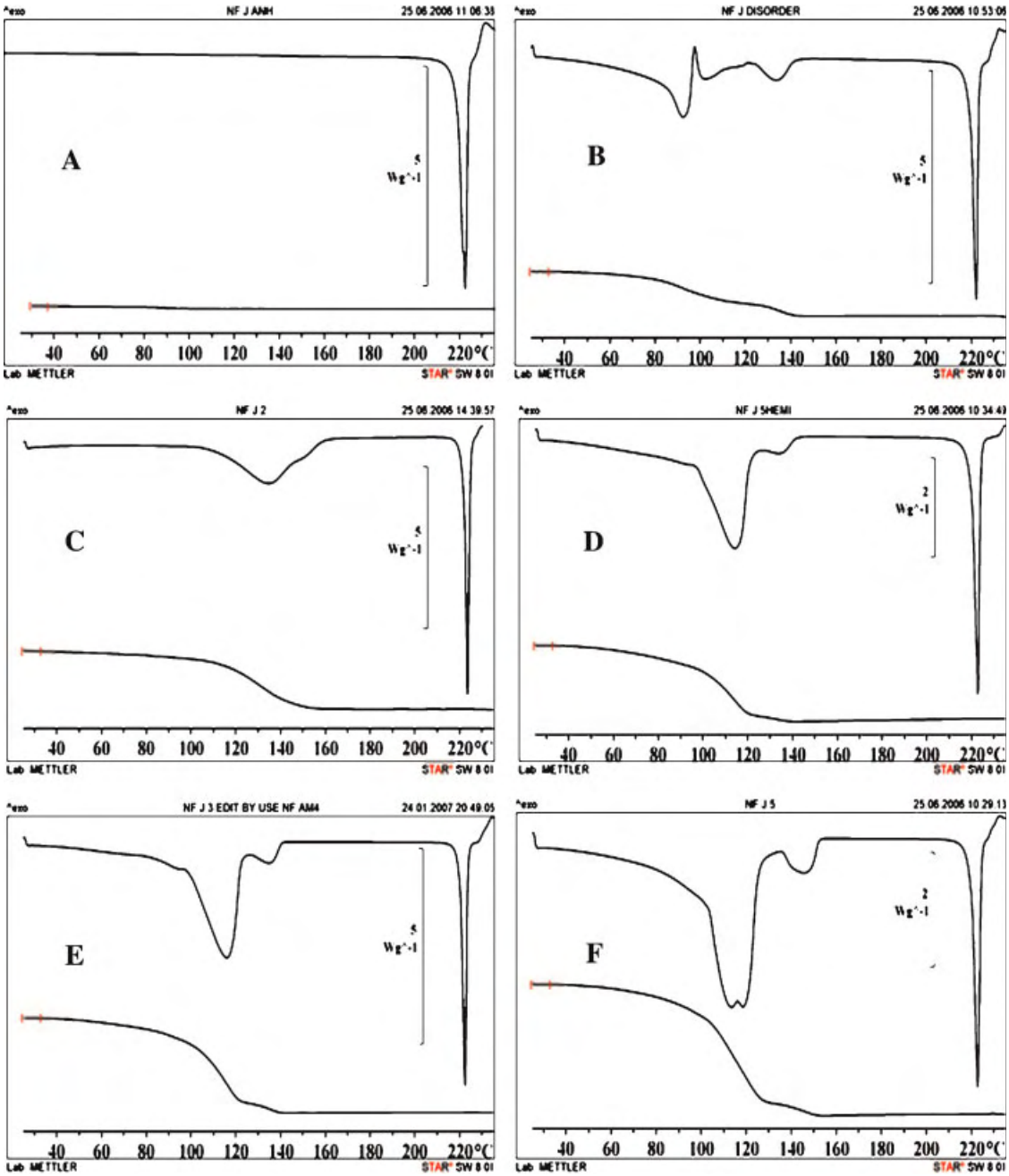

Figure 1. DSC and TGA thermograms of anhydrous NF Form A (A), disordered NF state (B), dihydrate NF (C), hemipentahydrate NF (D), trihydrate NF (E) and pentahydrate NF (F).

recrystallization method was compared to dihydrate NF single crystal X-ray diffraction data reported by Florence et al.[6] and were found to be identical. Therefore, the experimental XRPD pattern of dihydrate NF (Fig. 2C) was confirmed by the calculated powder diffraction pattern generated from single crystal X-ray diffraction data by MERCURY® software and served as reference XRPD pattern for dihydrate NF in future experiments. However, this recrystallization process was time-consuming and chemical degradation of NF is of great concern. The results obtained from SI-HPLC of the recrystallized dihydrate NF did not show sign of degradation. Thus, the quality of dihydrate NF produced was essentially free from degraded compounds and

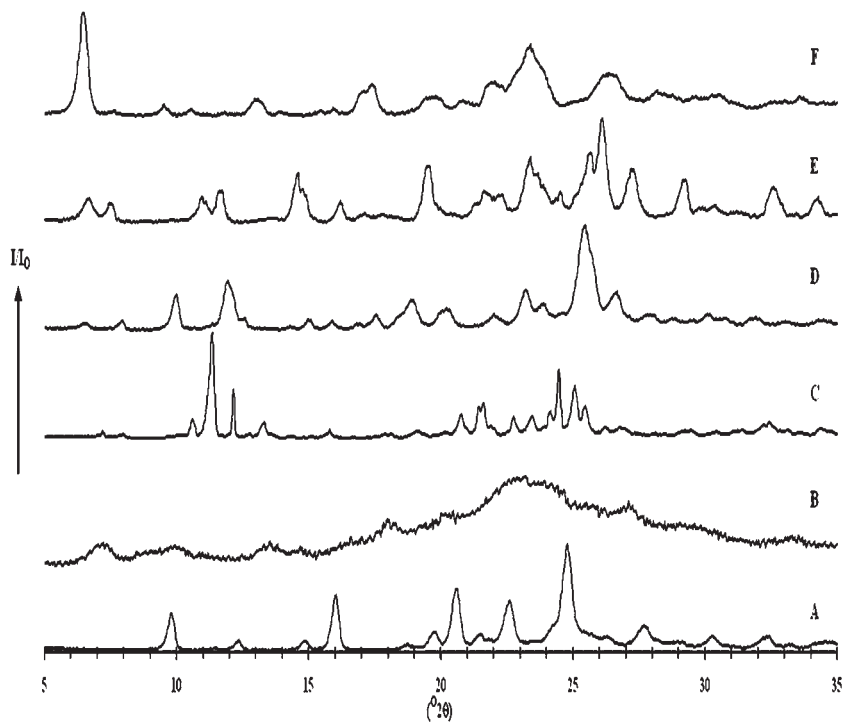

Figure 2. XRPD patterns of anhydrous NF Form A (A), disordered NF state (B), dihydrate NF (C), hemipentahydrate NF (D), trihydrate NF (E), and pentahydrate NF (F).

was acceptable to be used as the reference for future studies.

Trihydrate NF generated from antisolvent precipitation method was characterized. The results from HSM confirmed the existence of solvate or hydrate as seen from the evolution of vapor bubbles during heating. DSC showed a large endotherm immediately followed by another minor endotherm at the temperature range of 80–130°C (Fig. 1E). Total weight loss obtained by TGA was 14.81% w/w and occurred at the same temperature range as that of DSC endotherm (Fig. 1E). Meanwhile, KF titration confirmed the trihydrate stoichiometry of the crystalline precipitate (Tab. 1). XRPD pattern shown in Figure 2E was used as reference XRPD pattern of trihydrate NF due to the fact that no reference was available in any previous works. In addition, SI-HPLC did not detect any NF degradation after trihydrate NF was generated.

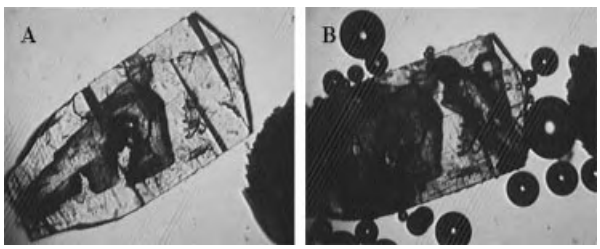

Figure 3. HSM photomicrographs of dihydrate NF immersed in mineral oil upon heating, at initial ambient temperature (A) and 100°C (B).

DSC analysis of the hemipentahydrate NF (Fig. 1D) and the pentahydrate NF (Fig. 1F) which were produced from direct exposure to moisture, showed large endotherm at 120°C followed by a smaller endotherm at approximately 140°C. TGA showed a two step weight loss at the same temperature as achieved by DSC. The total weight loss from TGA and the water content obtained from KF titration were in good agreement confirming the stoichiometry of the hemipentahydrate NF and the pentahydrate NF (Tab. 1). HSM showed continuous liberation of vapor bubbles during the temperature range corresponding to their DSC and TGA dehydration endotherms. XRPD of both hydrates are illustrated in Figure 2D and F and the XRPD patterns were essentially the same as XRPD of the hemipentahydrate NF and the pentahydrate NF reported by Yuasa et al.[9]

Table 1. Water Content (KF), Percent Weight Loss (TGA) and Stoichiometry between NF and Water Molecules

Method of Preparation	KF Water Content (%)	TGA % Weight Loss	Stoichiometry (NF:Water Molecule)
Recrystallization from IPA:water mixture	10.10 (0.08)	9.34 (0.136)	1:2.0
Exposure to 75% RH	11.55 (0.611)	12.12 (0.039)	1:2.5
Precipitate from aqueous ammonia solution	14.49 (0.342)	14.81 (0.046)	1:3.0
Exposure to 100% RH	20.55 (0.367)	20.87 (0.153)	1:5.0

SD shown in parentheses.

Pentahydrate NF, which was obtained from an alternative method of suspending anhydrous NF Form A in water, also provided the same thermal behavior and XRPD pattern (data not shown) as the one hydrated at 100% RH water vapor. However, the crystal habits of the two pentahydrate NF materials were different. Scanning electron micrographs of each solid were generated. Light yellow and coarse powder of anhydrous NF Form A (Fig. 4A) was converted to opaque white, needle-like fluffy pentahydrate NF after having directly came into contact with water (Fig. 4C). In contrast, exposure of anhydrous NF Form A to 100% RH did not change the appearance of the original powder even when the internal structure was found to be converted to the pentahydrate NF (Fig. 4B).

Another NF hydrate form found in this study, the disordered NF state, has not been previously reported elsewhere. Dehydration of pentahydrate NF via desiccation (0% RH) over time produced a so-called disordered NF state. DSC and TGA of the disordered NF state are shown in Figure 1B where a complex dehydration behavior was observed. Dehydration was detected during the first broad endotherm (100°C) and immediately followed by a sharp exotherm (115°C) and another broad endotherm. Mass loss of disordered NF state also took place over the same temperature range as found in the DSC study. The sharp exotherm was possibly due to the rearrangement of NF molecules after water molecules were partially removed. Disordered NF provided an XRPD pattern similar to the amorphous material (Fig. 2B). However, minor peak intensities in certain regions could still be observed.

In order to characterize the complex thermal behavior of the disordered NF, XRPD was utilized to monitor the molecular rearrangement of intact and heated disordered NF at predetermined times (Fig. 5). Disordered NF was heated from 25 to 120°C by DSC (D-I) and the XRPD pattern is displayed in Figure 5B. It showed increased crystallinity compared to the initial disordered NF. Initial disordered NF was also heated from 25 to 160°C (D-II) and its XRPD pattern is illustrated in Figure 5C. The solid obtained after D-II exhibited higher order than that of initial disordered NF and after D-I treatment and was

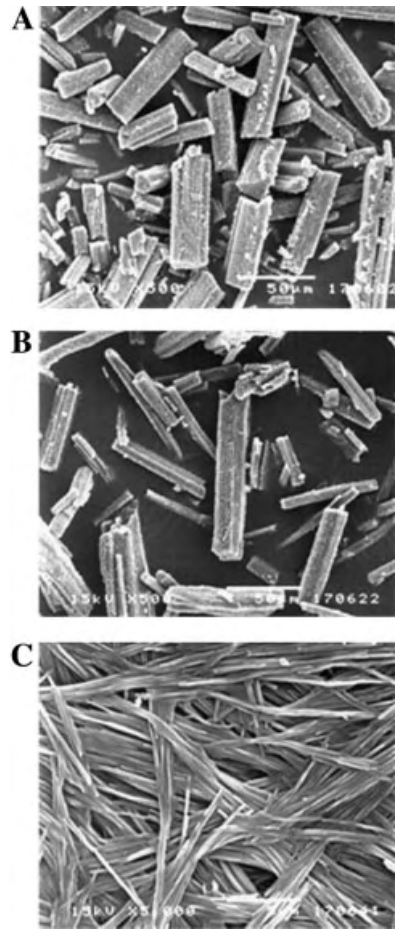

Figure 4. Scanning electron photomicrographs of anhydrous NF Form A (A), pentahydrate NF obtained from 100% RH vapor exposure (B) and pentahydrate NF from directly dispersed in water (C).

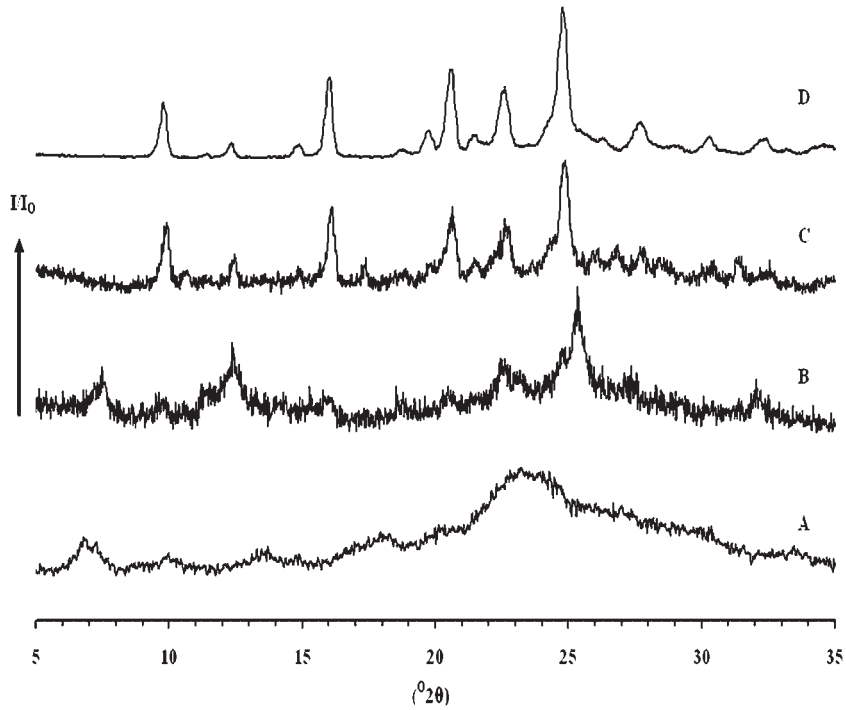

Figure 5. XRPD patterns of disordered NF state (A), after D-I (B), after D-II (C), and anhydrous NF Form A (D).

shown to be identical to that of the anhydrous NF Form A. TGA confirmed that the solid obtained after D-II treatment showed no weight loss. It could, hence, be concluded that the solid powder collected after D-II treatment is an anhydrous NF Form A. The total weight change from D-I to D-II was approximately 1.64% which was higher than the value allowed for anhydrous NF in the official monographs (less than 1%).[23,24] Thus, the solid powder resulted from D-I treatment was a hydrated transitional phase which, in turn, would convert to the anhydrous NF Form A upon further heating.

In general, materials of disordered molecular arrangement are more sensitive to moisture than the ordered crystalline phase. Consequently, the moisture sensitivity of the disordered NF was a critical issue. The disordered NF was thus exposed to various humidity levels for 7 days and the XRPD patterns were recorded (Fig. 6). The transformation of the disordered NF to the crystalline pentahydrate NF form was completed when at least 57% RH was used. At 32.8% RH, partial transformation to the pentahydrate NF was seen according to the presence of peaks at 6.40, 13.00, 17.28, 23.36, and 26.20°2θ. On the other hand, the disordered NF was stable under 11.3% RH for at least 2 months (data not shown) similar to the XRPD pattern after 7 days exposure to 11.3% RH. Thus, exposing the disordered NF to more than 32.8% RH would eventually generate the crystalline pentahydrate NF. However, at humidity of 11.3% RH or below, the disordered NF structure was retained.

Chemical interaction between water of crystallization and active moiety of every NF hydrate was investigated by spectroscopic FT-IR (Fig. 7). The signal at specific wavenumber can be interpreted in terms of the functional group of the material. The IR spectrum of anhydrous NF Form A exhibited main absorption peaks at 1732 and 1253 cm^{-1} indicating C=O and C–O bond stretching of carboxylic group, respectively. When water molecules are incorporated in to the crystal structure, the response of C=O and C–O are found to gradually decreased as a function of increased number of water of crystallization.[8] Meanwhile, the responses at 1584 and 1340 cm^{-1} of carboxylate anion are markedly increased. The above results suggested that structures of the carboxylic group in these hydrates are the carboxylate anion.[10] In addition, the responses in the regions of 3700–3250 cm^{-1} owing to OH stretching were clearly present in all NF hydrates,

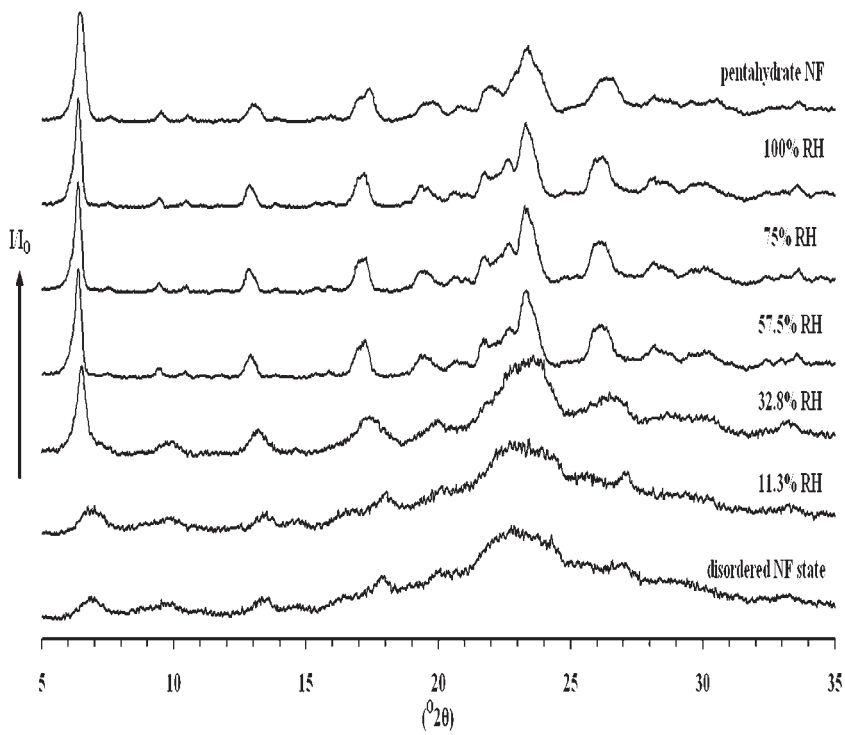

Figure 6. XRPD patterns of disordered NF state exposed to different relative humidities for 7 days.

signifying hydrogen bonding between carboxylic group and water molecules in the crystal structure.[12] The FT-IR spectrum of the disordered NF was also investigated. The presence of peaks at 1581 and 1334 cm^{-1} confirmed the occurrence of carboxylate anion identical to other hydrates and limited responses at 1732 and 1253 cm^{-1} indicated that C=O and C–O stretching of carboxylic group was disturbed by water molecule as well. It can be concluded that water molecules in disordered NF formed structural hydrogen bonds with NF molecules similar to those of other stoichiometric hydrates. Thus, it is believed that the disordered NF form was not a true amorphous state but a metastable phase with short range ordered structure.

Solid State Interconversion of NF Hydrate

XRPD patterns of NF hydrates (Fig. 2) were used as reference patterns to show specific characteristics of each form and were used to identify the solid state transformation. The following studies gathered evidences on the solid state transformation of NF hydrates under different environmental conditions, that is, relative humidities and temperatures. It should be noted that the observed trends are based on visual inspection of the diffraction patterns and are not intended to be quantitative.

Effect of Relative Humidities on Solid State Transformation of NF Hydrates

Moisture content in the environment usually plays the most pivotal part in hydrate formation of many organic compounds.[25,26] The anhydrous NF Form A placed under different relative humidities were found to form varying stoichiometric NF hydrates.[5,9] The moisture sorption study was used as a rough evaluation on the hydrate formation behavior due to moisture. Moisture vapor sorption data of the anhydrous NF Form A obtained by DVS showed that under 60% RH, the anhydrous stoichiometry was retained (Fig. 8). On the other hand, at moisture levels higher than 60% RH, anhydrous NF Form A showed a marked mass increase. The higher the relative humidity of the environment above 60% RH, the higher the weight gain. The final solid structure formed at the end of the sorption phase was later found to be pentahydrate NF by XRPD.

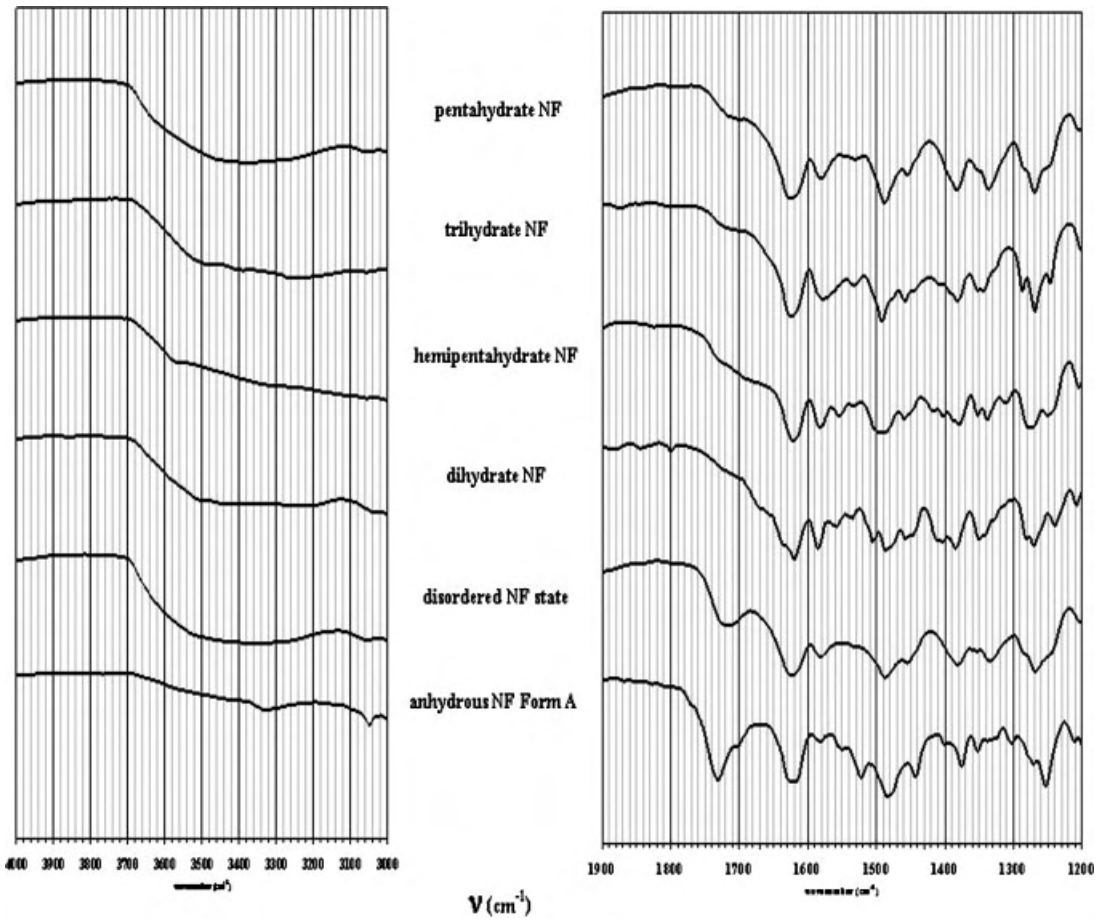

Figure 7. FT-IR spectra of anhydrous NF Form A, disordered NF state and other stoichiometric hydrates of NF.

Desorption phase of the induced pentahydrate NF showed that the pentahydrate NF was very stable even below 30% RH. However, when the humidity decreased below 20% RH, significant weight loss occurred. The result suggested that for dehydration of the pentahydrate NF to occur the environment must reach very low relative humidity. These data could be used to determine a suitable storage condition of NF raw material. The storage condition suggested for anhydrous NF Form A should be in an environment where moisture level is below 60% RH at room temperature. The pentahydrate NF form should not be stored in areas where relative humidity is below 20% RH to prevent dehydration.

The degree of hydration of anhydrous NF Form A with respect to relative humidity was investigated and characterized by XRPD (Fig. 9). The hemipentahydrate NF was achieved when anhydrous NF Form A was exposed to 75% RH as mentioned in the previous section. XRPD patterns of the anhydrous NF Form A which were stored between 81% RH to 87% RH, however, showed mixed characteristics at 6.48°2θ and 25.48°2θ of pentahydrate NF and hemipentahydrate NF, respectively. Increasing the moisture level was found to accentuate the intensity of the peak at 6.48°2θ. Meanwhile the intensity at 25.48°2θ was reduced. When anhydrous NF Form A was exposed to humidity higher than 93.7% RH, pure pentahydrate NF was found. In addition, exposure of the anhydrous NF Form A at very high humidity did not generate any degradation products as confirmed by SI-HPLC (data not shown) and the transformation was found to evolve through the presence of hemipentahydrate NF before eventually converting to the stable pentahydrate NF.

NF hydrates were placed under 100% RH for 7 days after which XRPD patterns were recorded. The XRPD results (data not shown) revealed that every sample converted to the pentahydrate NF, except the dihydrate NF. The dihydrate NF exposed to 100% RH showed mixed characteristics

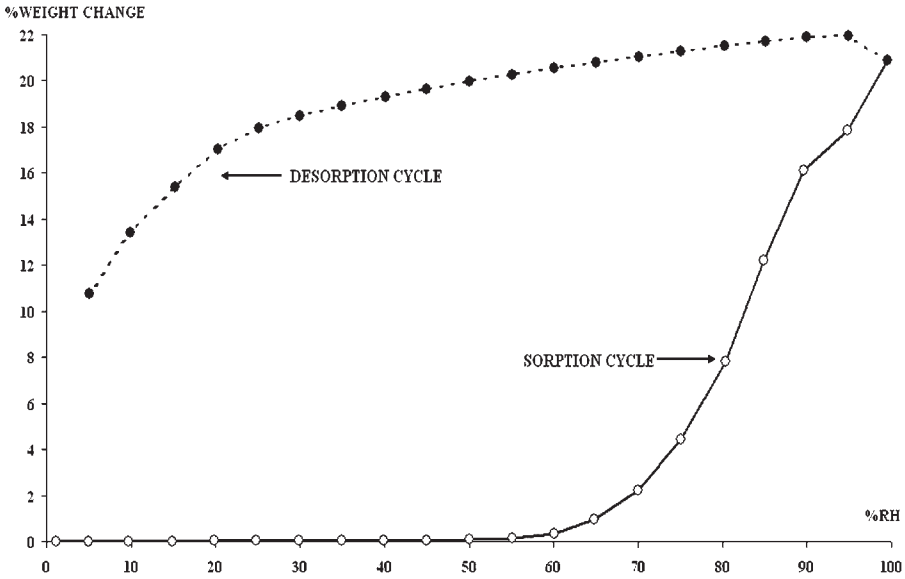

Figure 8. Dynamic water vapor sorption and desorption isotherms of anhydrous NF Form A at 25°C.

of both dihydrate NF and pentahydrate NF. It could be inferred that the pentahydrate NF was the most stable form in extremely high moisture environments.

On the other hand, NF hydrate exposures to 0% RH were also investigated. The pentahydrate NF was transformed to the disordered NF state as discussed earlier. The XRPD pattern of the hemipentahydrate NF at 0% RH is illustrated in Figure 10. The characteristic peak at 25.48°2θ was slightly shifted to lower angle of 24.84°2θ which corresponded to the anhydrous NF Form A. Meanwhile, the intensity at 26.68°2θ gradually decreased as a function of exposure time. The

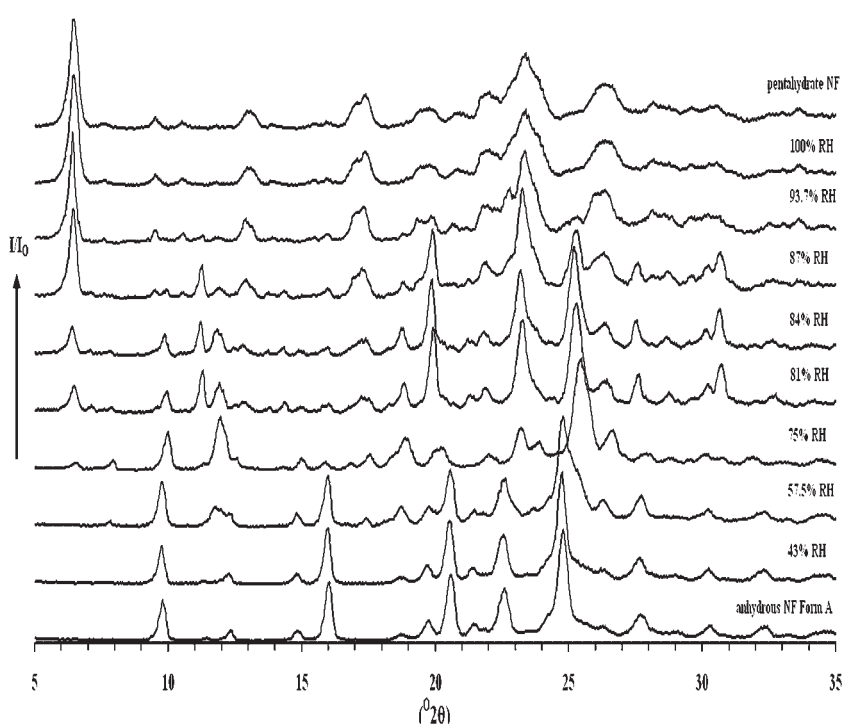

Figure 9. XRPD patterns of anhydrous NF Form A under different relative humidities for 7 days.

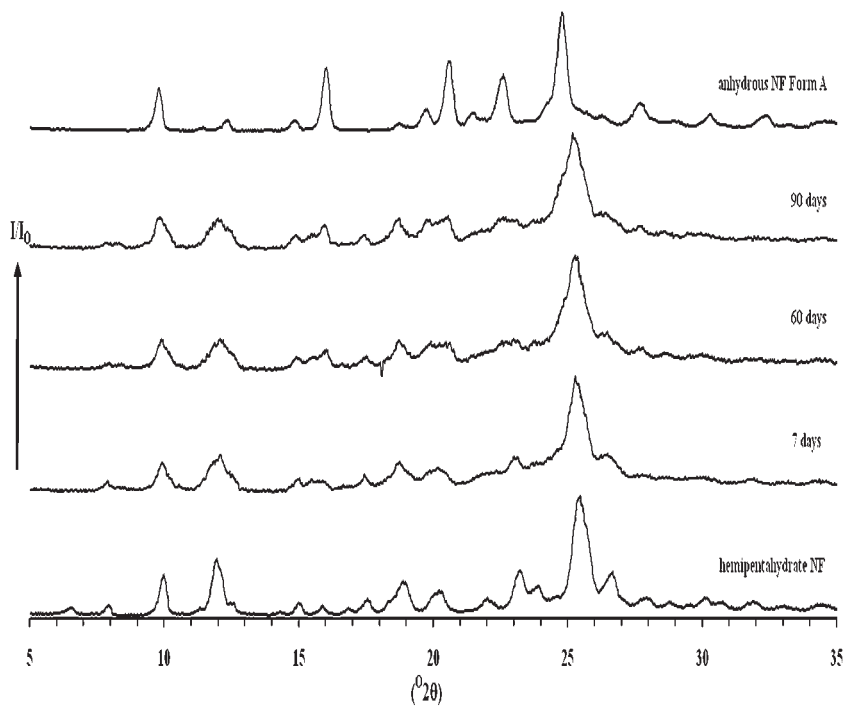

Figure 10. XRPD patterns of hemipentahydrate NF under desiccant (0% RH) as a function of exposure time.

longer contact time to dry environment led to the formation of a mixture of the two forms. The trihydrate NF showed the same phenomenon on the conversion to the anhydrous NF Form A during exposure to 0% RH condition. The XRPD patterns of the trihydrate NF during dehydration are shown in Figure 11. After 7 days of dehydration, peaks at 9.84, 20.52 and 24.84°2θ of the sample were found to be of the anhydrous NF Form A. Peak positions at 7.52 and 25.40°2θ were also apparent and related to the hydrated transitional phase similar to the heat treated (D-I) of the disordered NF state (Fig. 5B). Meanwhile, other strong and characteristic trihydrate peaks still existed. In summary, dehydration by reduction of environmental moisture was not an effective method to convert neither the hemipentahydrate NF nor the trihydrate NF to the pure anhydrous NF Form A even after 90 days exposure. Hence, the dihydrate NF was not further evaluated due to lack of dehydration efficiency by this approach.

Effect of Elevated Temperature on Solid State Transformation of NF Hydrates

Thermal dehydration is the most common way to prepare anhydrous materials in the pharmaceutical industry. There are many publications reported the polymorphic transformation or occurrence of desolvation upon thermal treatment.[27–30] In this study, a mild temperature of 60°C was selected to minimize potential chemical degradation associated with higher temperatures.

The disordered NF, hemipentahydrate NF and pentahydrate NF were heated at 60°C for 48 h. XRPD showed the transformation to the anhydrous NF Form A (Fig. 12). The residual water contents of the heated samples were investigated using KF titration. The water contents were 1.02, 0.60, and 0.46 for heated samples of the disordered NF, the hemipentahydrate NF and the pentahydrate NF, respectively. The results revealed that all heated samples were essentially anhydrous because the water content was approximately at or below the maximum limit (1%) for anhydrous NF specified in the monograph.[23,24] Note that the heated pentahydrate NF resulted in a similar XRPD pattern to that of the anhydrous NF Form A but with two additional peaks at 7.52 and 25.40°2θ (Fig. 12D). These two peaks were assumed to be the residual of the hydrated transitional phase (Fig. 5B) found during D-I treatment of the disordered NF state.

The results from the heated dihydrate NF and the heated trihydrate NF are shown in Figures 13 and 14, respectively. The XRPD of the dehydrated dihydrate NF revealed that a partial anhydrous

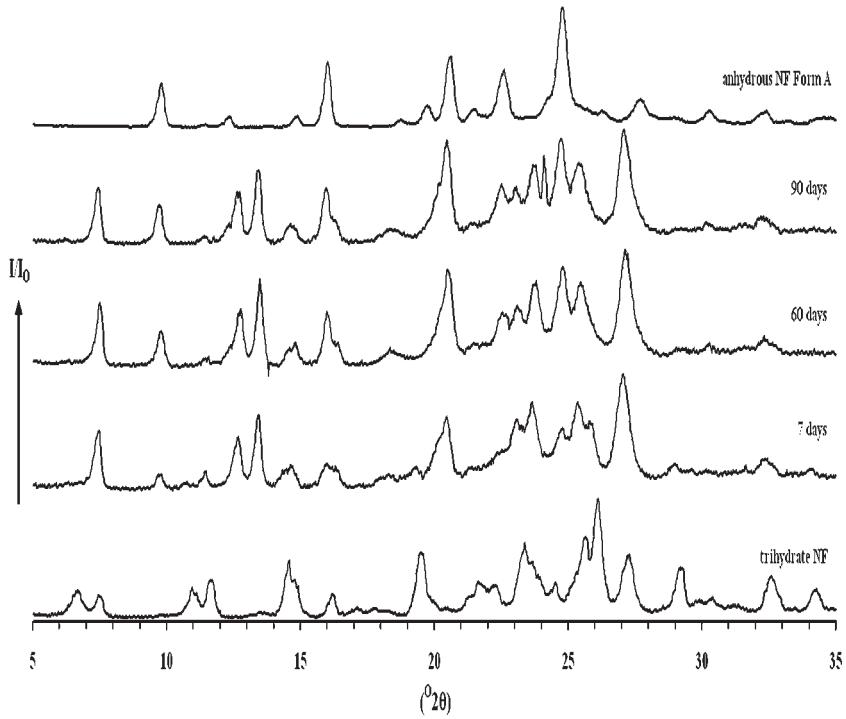

Figure 11. XRPD patterns of trihydrate NF under desiccant (0% RH) as a function of exposure time.

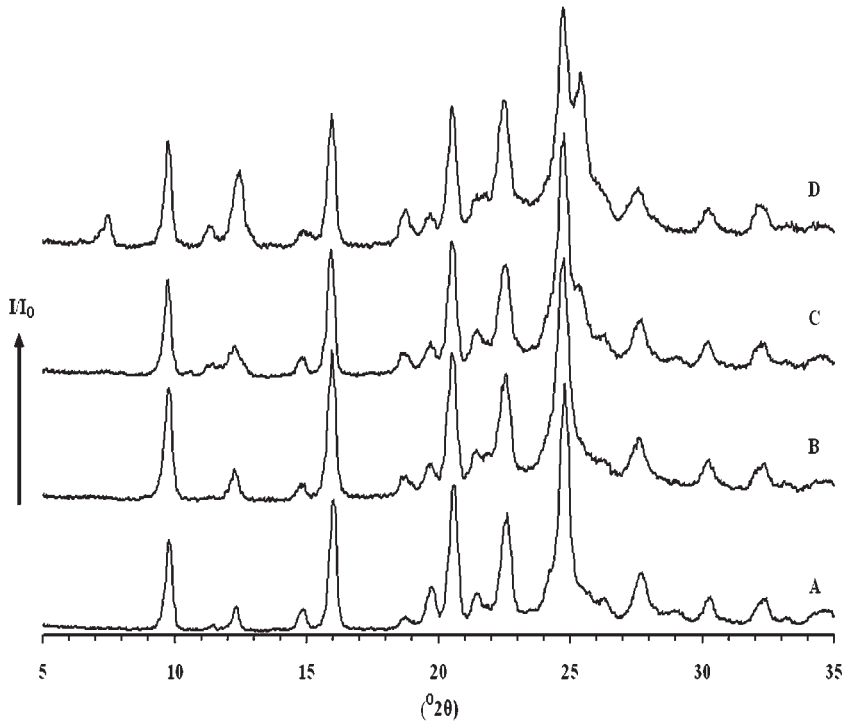

Figure 12. XRPD patterns of anhydrous NF Form A (A), disordered NF state (B), hemipentahydrate NF (C) and pentahydrate NF (D) after heated at 60°C for 48 h.

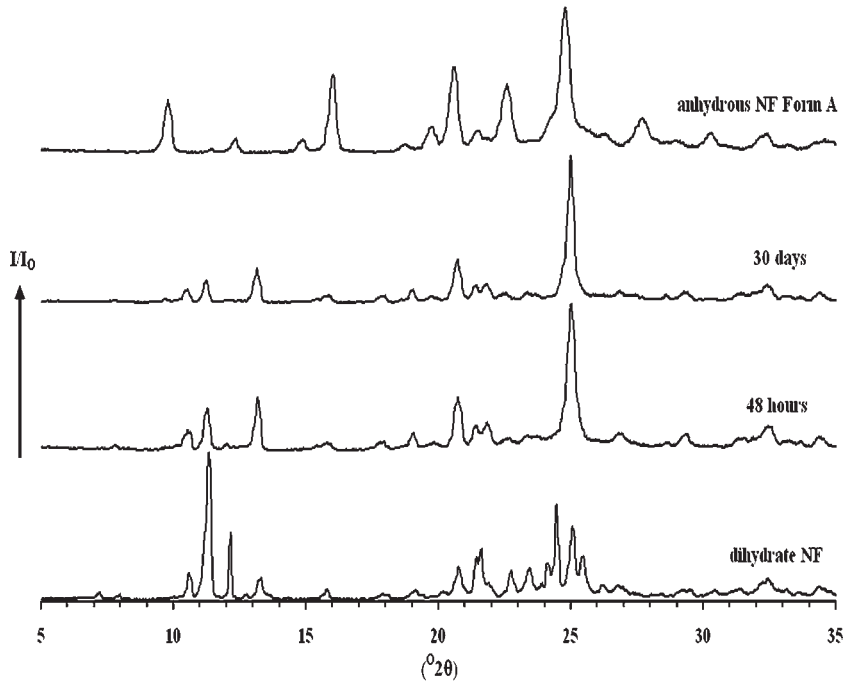

Figure 13. XRPD patterns of dihydrate NF after heated at 60°C for various time period.

phase was generated after thermal dehydration for 48 h. However, the peaks at 10.60, 11.32 and 13.16 and 25.00°2θ corresponding to the dihydrate NF were still present. Extended heating time of up to 1 month gave material with an identical pattern to that of the 48-h treated sample. Thus, the longer heating time did not fully convert the dihydrate NF to the anhydrous NF Form A. The

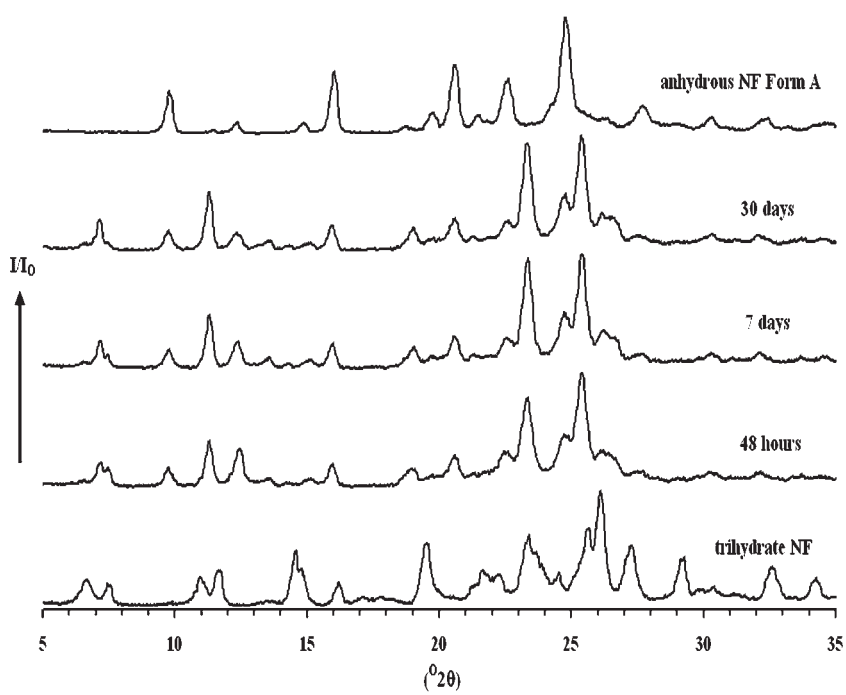

Figure 14. XRPD patterns of trihydrate NF after heated at 60°C for various time period.

trihydrate NF also did not show full conversion to the anhydrous NF Form A upon thermal dehydration. XRPD of the treated trihydrate NF indicated the anhydrous NF Form A peaks at 9.80, 16.04, 22.68, and 24.84°2θ. Additional peak positions at 7.52 and 25.40°2θ were also noticeable and related to the hydrated transitional phase (Fig. 5B) while the trihydrate NF peak at 23.36°2θ remained pronounce indicating mixture of the three forms. Extended thermal dehydration of the trihydrate NF at 60°C of up to 1 month did not generate the pure structure of anhydrous NF Form A.

The solid state interconversion of NF hydrates is summarized in Scheme 1. The conditions used in the proposed methodology of Scheme 1 were based on exposing anhydrous NF Form A and its hydrates to 100% RH (7 days), 0% RH (7 days) and 60°C (48 h). The anhydrous NF Form A and the other NF hydrate forms transformed to the pentahydrate NF when exposed to saturated water vapor. Meanwhile, the anhydrous NF Form A could be produced from thermal dehydration of the disordered NF state and hemipentahydrate NF. On the contrary, dihydrate NF, trihydrate NF, and pentahydrate NF were not fully converted to the anhydrous NF Form A upon heating. Dehydration of NF hydrates with the aid of desiccant did not provide pure anhydrous NF Form A. Instead, it generated the disordered NF state from the pentahydrate NF. The disordered NF state had specific rehydration behavior and instability against humidity such that it could easily be transformed to the pentahydrate NF starting at very low moisture of 32.8% RH compared to the anhydrous NF Form A where it needs 93.7% RH to convert to the pentahydrate NF.

An additional XRPD information on the relative rate of transformation was collected (Tab. 2). The rate of transformation mostly confirmed what was stated in Scheme 1, with minor exception. As previously reported, anhydrous NF Form A transformed to pentahydrate NF through hemipentahydrate NF as an intermediate at 100% RH but the relative rate of change to hemipentahydrate has not yet been stated up to this time. The characteristic peaks of hemipentahydrate NF were found to be clearly visible within less than 24 h before completely converted to pentahydrate NF in 7 days. In addition, triydrate NF was transformed to pentahydrate NF in 3 days at 100% RH which was less than the duration indicated in Scheme 1. Another difference is the transformation of pentahydrate NF to anhydrous NF Form A at 60°C where the residual peaks of hydrated transitional phase remained present with the anticipated anhydrous NF Form A longer than specified in Scheme 1 even after 7 days of exposure.

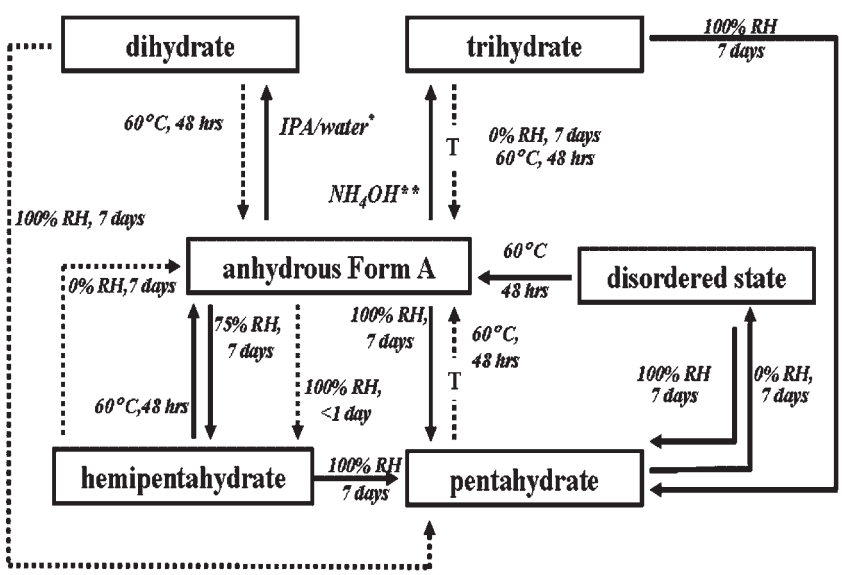

Scheme 1. Summary of the solid state interconversion of anhydrous NF Form A and its hydrates (—, complete transformation; ----, incomplete transformation; T, hydrated transitional phase; *, the dihydrate NF derived from recrystallization in the mixture of IPA and water; **, the trihydrate NF generated by antisolvent precipitation from aqueous ammonia NF solution).

Table 2. Relative Rates of Norfloxacin Solid State Transformation Which Induced Observed Solid Morphology at Specified Conditions

	100% RH		0% RH		60°C	
From	To	Time (Day)	To	Time (Day)	To	Time (Day)
Anhydrous	Hemipentahydrate[a]	<1	Anhydrous	Stable	Anhydrous	Stable
	Pentahydrate	7				
Dihydrate	Pentahydrate[a]	7	[b]		Anhydrous[a]	30
Hemipentahydrate	Pentahydrate	7	Anhydrous[a]	90	Anhydrous	2
Trihydrate	Pentahydrate	3	Anhydrous[a]	90	Anhydrous[a]	30
Pentahydrate	Pentahydrate	Stable	Disordered state	7	Anhydrous[a]	7
Disordered state	Pentahydrate	7	Disordered state	Stable	Anhydrous	2

[a]Indicates mixture of XRPD patterns between the original and the resultant solid morphology.
[b]Not observed.

CONCLUSIONS

NF hydrates could be generated by various approaches. The approaches used in this study include slow recrystallization from mixture of IPA and water, direct exposure of the anhydrous NF Form A under 75% RH, precipitation from basic ammoniated solution with antisolvent mixture to produce dihydrate NF, hemipentahydrate NF, and trihydrate NF, respectively. In addition, direct exposure of the anhydrous NF Form A to 100% RH and dispersing the anhydrous NF Form A in water could also produced the pentahydrate NF. The pentahydrate NF formed from different methods of preparation possessed different crystal habits while the internal lattice structures were identical. The hydrogen bonding between carboxylic groups could be detected using IR spectroscopy and the specific site of water of crystallization in dihydrate NF was defined using single crystal analysis. The levels of environmental moisture greatly affected the transformation of the anhydrous NF Form A and other stoichiometric hydrates. However, dehydration of the pentahydrate NF *via* reduction in moisture resulted in the disordered NF. Extremely dry environment, 0% RH, was ineffective in withdrawing the internal water molecules from NF hydrates. On the other hand, water of crystallization was removed by mild temperature elevation. However, the water of crystallization in the dihydrate NF and the trihydrate NF was partially removed by thermal energy and, thus, resulted in the mixture of the anhydrous NF Form A, their original hydrated structures and the hydrated transitional phase (for trihydrate). The information on the solid state interconversion of NF hydrates obtained in this study may be a crucial basic understanding for making sound judgment on the pharmaceutical product development strategies in the pharmaceutical industry.

ACKNOWLEDGMENTS

Sincere gratitude is directed toward The Thailand Research Fund (TRF), Chulalongkorn University Graduate Scholarship to Commemorate the 72nd Anniversary of His Majesty King Bhumipol Adulyadej and the Graduate School, Chulalongkorn University for financial support and to the Government Pharmaceutical Organization (GPO) for the assistance on KF studies. A special appreciation goes to Dr. Phillips E. Fanwick for single crystal X-ray structure elucidation of dihydrate NF.

REFERENCES

1. Turel I. 2002. The interactions of metal ions with quinolone antibacterial agents. Coordin Chem Rev 232:27–47.
2. Sustar B, Bukovec N, Bukovec P. 1993. Polymorphism and stability of norfloxacin, 1-ethyl-6-fluoro-1,4-dihydro-4-oxo-7-(1-piperazinil)-3-quinolinocarboxylic acid. J Therm Anal 40:475–481.
3. Barbas R, Marti F, Prohens R, Puigjaner C. 2006. Polymorphism of norfloxacin: Evidence of the enantiotropic relationship between polymorphs A and B. Cryst Growth Des 6:1463–1467.
4. Budavari S. 2001. The merck index. 13th edition. Merck and Co, Inc. White House, NJ.
5. Katdare AV, Ryan JA, Bavitz JF, Erb DM, Guillory JK. 1986. Characterization of hydrates of norfloxacin. Mikrochim Acta 3:1–12.

6. Florence AJ, Kennedy AR, Shankland N, Wright E, Al-Rubayi A. 2000. Norfloxacin dihydrate. Acta Crystallogr Sect C56:1372–1373.
7. Puechagut HG, Bianchotti J, Chiale CA. 1998. Preparation of norfloxacin spherical agglomerates using the ammonia diffusion system. J Pharm Sci 87:519–523.
8. Mazuel C. 1991. Norfloxacin. Analytical Profile of Drug Substances. pp. 557–600.
9. Yuasa R, Imai J, Morikawa H, Kusajima H, Uchida H, Irikura T. 1982. Pharmaceutical studies on hydrates of AM-715. Physical characteristics and intestinal absorption. Yakugaku Zasshi 102: 469–476.
10. Hu T-C, Wang S-L, Chen T-F, Lin S-Y. 2002. Hydration-induced proton transfer in the solid state of norfloxacin. J Pharm Sci 91:1351–1357.
11. Khankari RK, Grant DJW. 1995. Pharmaceutical hydrates. Thermochim Acta 248:61–79.
12. Byrn SR, Pfeiffer RR, Stowell JG. 1999. Solid state chemistry of drugs. 2nd edition. West Lafayette, IN: SSCI Inc.
13. Byrn SR, Xu W, Newman AW. 2001. Chemical reactivity in solid-state pharmaceuticals: Formulation implications. Adv Drug Deliv Rev 48:115–136.
14. Swaminathan V, Kildsig DO. 2001. An examination of the moisture sorption characteristics of commercial magnesium stearate. AAPS Pharm Sci Tech 2:28.
15. Kobayashi Y, Ito S, Itai S, Yamamoto K. 2000. Physicochemical properties and bioavailability of carbamazepine polymorphs and dihydrate. Int J Pharm 193:137–146.
16. Ono M, Tozuka Y, Oguchi T, Yamamura S, Yamamoto K. 2002. Effects of dehydration temperature on water vapor adsorption and dissolution behavior of carbamazepine. Int J Pharm 239: 1–12.
17. Katdare AV, Bavitz JF. 1984. Hydrate related dissolution characteristics of norfloxacin. Drug Dev Ind Pharm 10:789–807.
18. Katdare AV, Bavitz JF. 1984. Study of the relationship between the initial rate of moisture sorption/desorption on norfloxacin tablets to the total moisture and temperature of surrounding environment. Drug Dev Ind Pharm 10:1041–1048.
19. Vitez IM, Newman AW, Davidovich M, Kiesnowski C. 1998. The evolution of hot-stage microscopy to aid solid-state characterizations of pharmaceutical solids. Thermochim Acta 324:187–196.
20. Córdoba-Borrego M, Córdoba-Díaz M, Córdoba-Díaz D. 1999. Validation of a high-performance liquid chromatographic method for the determination of norfloxacin and its application to stability studies (photo-stability study of norfloxacin). J Pharm Biomed Anal 18:919–926.
21. Nyquist H. 1983. Saturated salt solutions for maintaining specified relative humidities. Int J Pharm Technol Prod Manuf 4:47–48.
22. Kotny MJ, Conners JJ. 2002. Water sorption of drugs and dosage forms. In: Swarbrick J, Boylan JC, editors. Encyclopedia of pharmaceutical technology. 2nd edition. New York: Marcel Dekker Inc. pp. 2970–2987.
23. The United State Pharmacopiea (Asian Edition). 2004. 27th edition. Rockville, MD: United States Pharmacopeial Convention, Inc.
24. British Pharmacopoeia. ed. 2002. The Stationary Office. London, UK.
25. Zhu H, Yuen C, Grant DJW. 1996. Influence of water activity in organic solvent + water mixtures on the nature of the crystallizing drug phase. 1 Theophylline. Int J Pharm 135:151–160.
26. Zhu H, Grant DJW. 1996. Influence of water activity in organic solvent + water mixtures on the nature of the crystallizing drug phase 2. Ampicillin. Int J Pharm 139:33–43.
27. Lin S-Y, Chien J-L. 2003. In vitro simulation of solid-solid dehydration, rehydration, and solidification of trehalose dihydrate using thermal and vibrational spectroscopic techniques. Pharm Res 20:1926–1931.
28. Willart JF, Gusseme AD, Hemon S, Descamps M, Leveiller F, Rameau A. 2002. Vitrification and polymorphism of trehalose induced by dehydration of trehalose dihydrate. J Phys Chem B 106:3365–3370.
29. Landgraf K-F, Olbrich A, Pauluhn S, Emig P, Kutscher B, Stange H. 1998. Polymorphism and desolvation of flupirtine maleate. Eur J Pharm Biopharm 46:329–337.
30. Hakanen A, Laine E. 1995. Characterization of two terfenadine polymorphs and a methanol solvate: Kinetic study of the thermal rearrangement of terfenadine from the methanol solvate to the lower melting polymorph. Thermochim Acta 248:217–227.

Review Article

การประยุกต์ใช้เคมิคัลโซลเวตในทางเภสัชกรรม

วันชัย จงเจริญ[1], วีระเกียรติ บุญกนกวงศ์[2]* และ นฤพร สุตัณฑวิบูลย์[2]

[1] บริษัท เมดิกา อินโนวา จำกัด

[2] ภาควิชาวิทยาการเภสัชกรรมและเภสัชอุตสาหกรรม
หน่วยพัฒนาเภสัชภัณฑ์และการถ่ายทอดเทคโนโลยี, ศูนย์นวัตกรรมทางยาและผลิตภัณฑ์สุขภาพ
คณะเภสัชศาสตร์ จุฬาลงกรณ์มหาวิทยาลัย

* Corresponding author: Veerakiet.B@chula.ac.th

บทคัดย่อ

สารประกอบทางเคมีประเภทที่เรียกว่า โซลเวต (solvate) หมายถึง สารเคมีที่มีโครงสร้างที่เกิดจากการรวมกันระหว่างสารเคมีหลักกับโมเลกุลของตัวทำละลาย (solvent) ซึ่งมีอัตราส่วนโดยจำนวนต่อกันที่แน่นอนตามปริมาณสัมพันธ์ (stoichiometry) ในกรณีที่โมเลกุลของตัวทำละลายนั้นเป็นน้ำซึ่งถูกจับอยู่ในโครงสร้างของสารจะเรียกสารประกอบนั้นว่า ไฮเดรต (hydrate) โดยทั่วไปโซลเวตหรือไฮเดรตจะมีสมบัติทางเคมีกายภาพแตกต่างไปจากสารนั้นในรูปไม่มีตัวทำละลาย คุณสมบัติดังกล่าว เช่น สภาพไหลได้ สมบัติในการยึดเกาะ ความสามารถตอกอัดได้ สภาพละลายได้ เสถียรภาพทางกายภาพและทางเคมี เป็นต้น ด้วยเหตุผลข้างต้นจึงมีการศึกษาวิจัยเพื่อนำเอาประโยชน์ที่เหนือกว่าของโซลเวตมาใช้ทางเภสัชกรรม โดยเฉพาะเพื่อปรับปรุงคุณสมบัติต่าง ๆ ของผลึกหรืออนุภาคของสารเคมี นอกจากนี้ ภาวะของสารเคมีที่เกิดเป็นโซลเวตชนิดที่ไม่เป็นไปตามปริมาณสัมพันธ์ (nonstoichiometric solvate) ก็มีประโยชน์ในการประยุกต์ใช้ทางเภสัชกรรมและทางเคมีเช่นกัน

คำสำคัญ: โซลเวต, ไฮเดรต, ภาวะพหุสัณฐานเทียม, การลดขนาดอนุภาค, สมบัติทางเคมีกายภาพ

Thai Pharm Health Sci J 2009;4(3):377-386[§]

บทนำ

สารประกอบทางเคมี (chemical compounds) สามารถจัดแบ่งประเภทตามสมบัติทางสถานะของแข็ง (solid state properties) โดยใช้ลักษณะรูปร่างภายนอก (habit) เช่น รูปทรงต่าง ๆ ของอนุภาคหรือผลึก และโดยใช้ลักษณะการจัดเรียงตัวของโครงสร้างภายใน (internal structure) หากพิจารณาลักษณะการจัดเรียงตัวของโครงสร้างภายในเป็นเกณฑ์ จะสามารถแบ่งประเภทของสารได้เป็นสองกลุ่ม โดยกลุ่มที่หนึ่ง คือ สารที่มีลักษณะการจัดเรียงตัวของหน่วยแลตทิซ (lattice unit) อย่างมีระเบียบแบบแผน หรือที่เรียกว่าสถานะผลึก (crystalline state) และกลุ่มที่สอง คือ สารที่มีลักษณะการจัดเรียงตัวที่อิสระหรือไม่มีแบบแผน หรือที่เรียกว่าสถานะอสัณฐาน (amorphous state) ซึ่งสารทั้งสองกลุ่มนี้มีคุณสมบัติทางเคมีกายภาพที่แตกต่างกันโดยสิ้นเชิง เช่น สารที่อยู่ในสถานะอสัณฐานจะมีความสามารถในการละลายน้ำได้ดีมากกว่าเมื่ออยู่ในสถานะผลึก

สารทางเภสัชกรรมที่ใช้ในการเตรียมเภสัชภัณฑ์ส่วนใหญ่จะอยู่ในรูปของแข็งผลึก (crystalline solid) มากกว่ารูปอสัณฐาน (amorphous form) อย่างไรก็ตาม สารในกลุ่มที่มีลักษณะเป็นของแข็งผลึกเองก็มีความแตกต่างและความหลากหลายอยู่มาก จึงทำให้สามารถจำแนกสารในกลุ่มนี้อย่างกว้าง ๆ ได้เป็น 2 กลุ่ม ได้แก่ กลุ่มแรกซึ่งเป็นสารที่มีโครงสร้างของสารเคมีหลักเพียงชนิดเดียวหรือเอนทิตีเดี่ยว (single entity) ซึ่งอาจมีความแตกต่างกันของการจัดเรียงตัวภายในโครงสร้างหรือที่เรียกว่าการเกิดภาวะพหุสัณฐาน (polymorphism)[1-4] และกลุ่มที่สองซึ่งเป็นสารที่มีโครงสร้างที่เกิดจากการรวมกันระหว่างสารเคมีหลักกับโมเลกุลของตัวทำละลายอินทรีย์ซึ่งอาจหมายรวมถึงน้ำด้วย อาจเรียกสารประกอบในกลุ่มนี้ว่า โซลเวต (solvate) หรือ

[§] 14th year of Srinakharinwirot Journal of Pharmaceutical Science

molecular adduct ซึ่งเป็นกลุ่มสารที่ได้รับความสนใจน้อย แต่พบว่ามีข้อดีหลายประการที่สามารถนำไปประยุกต์ใช้ในทางเภสัชกรรมได้อย่างมีประสิทธิภาพ การเกิด molecular adduct หรือ solvate จะขึ้นอยู่กับคุณสมบัติทางเคมีและขนาดที่เหมาะสมของโมเลกุลตัวทำละลายที่จะสามารถอยู่ในโครงสร้างของสารเคมีหลักได้ไม่ว่าจะด้วยแรงทางพันธะหรือความจำเพาะของขนาดต่อช่องว่างในโมเลกุลของสารหลักก็ตาม และจะต้องสามารถอยู่ได้อย่างเสถียรในสภาวะปกติอีกด้วย การเกิดสารประกอบประเภทนี้อาจถูกเรียกได้ว่าภาวะพหุสัณฐานเทียม (pseudopolymorphism)[2,5-9] อย่างไรก็ตาม แม้ว่าคุณสมบัติที่แสดงออกของพหุสัณฐานเทียม (pseudopolymorphs) จะมีลักษณะที่คล้ายกับพหุสัณฐาน (polymorphs) แต่ในความเป็นจริงแล้ว ลักษณะและคุณสมบัติของพหุสัณฐานเทียมเหล่านี้เกิดจากโมเลกุลของตัวทำละลายที่บรรจุหรือสอดแทรกอยู่ในโครงสร้างของสารหลักโดยที่แลตทิซผลึก (crystal lattice) ของสารหลักนั้นไม่ได้เปลี่ยนแปลงไปจากเดิมเลย จึงไม่อาจเรียกปรากฏการณ์การเกิดภาวะพหุสัณฐานเทียมว่าเป็นภาวะพหุสัณฐานได้

Molecular adduct ที่มีโมเลกุลของน้ำถูกจับไว้ในโครงสร้างหลัก นิยมเรียกว่า ไฮเดรต (hydrate)[10-11] ในทางเภสัชกรรมจะพบว่าวัตถุดิบทางยาจำนวนมากมีสภาพที่เป็นไฮเดรต เช่น ampicillin trihydrate และ amoxicillin trihydrate เป็นต้น ซึ่งมีข้อดีเหนือกว่ารูปแบบที่ปราศจากน้ำ (anhydrous form) อยู่หลายประการ นอกจากนี้ ในบรรดาโซลเวตเองยังสามารถแบ่งออกตามเกณฑ์การเกิดอัตราส่วนของโมเลกุลของสารหลักต่อโมเลกุลของตัวทำละลายอินทรีย์ในการก่อรวมตัวอย่างเสถียร ถ้าอัตราส่วนนี้เป็นไปเป็นตามปริมาณสัมพันธ์ (stoichiometry) จะเรียกโซลเวตชนิดนี้ว่า stoichiometric solvate หรือเรียกสั้น ๆ ว่า solvate แต่ถ้าอัตราส่วนนี้ไม่เป็นไปตามปริมาณสัมพันธ์ จะเรียกโซลเวตเหล่านี้ว่า nonstoichiometric solvate ซึ่งสารในกลุ่ม nonstoichiometric solvates นี้ยังสามารถแบ่งออกตามลักษณะการจัดเรียงตัวของตัวทำละลายอินทรีย์ในโครงสร้างหลักได้อีก โดยมีชื่อเรียกเฉพาะ เช่น cage, channel หรือ clathrate ในทางเภสัชกรรมสามารถพบรูปแบบ clathrate ได้ในวัตถุดิบบางชนิด เช่น warfarin USP 24[12]

การรวมตัวหรือการจัดเรียงตัวของโมเลกุลตัวทำละลายอินทรีย์ในโครงสร้างหลักที่แตกต่างกันย่อมส่งผลให้โซลเวตมีสมบัติทางเคมีกายภาพที่แตกต่างไปจากเอนทิตีเดี่ยวของสารชนิดเดียวกัน[11] โดยความแตกต่างนี้อาจเป็นข้อได้เปรียบหรือข้อจำกัดของการนำเอาโซลเวตมาใช้ในทางเภสัชกรรมก็ได้ ดังนั้น บทความนี้จึงได้รวบรวมประโยชน์และการประยุกต์ใช้โซลเวตในทางเภสัชกรรมเพื่อเป็นแนวทางในการพัฒนาการผลิตเภสัชภัณฑ์ต่อไป

การลดขนาดอนุภาคด้วยเทคนิค solvation และ desolvation

จากความรู้พื้นฐานที่เกี่ยวข้องกับโครงสร้างทางเคมีและความสามารถในการก่อรวมตัวระหว่างโครงสร้างหลักของสารเคมีกับโมเลกุลของตัวทำละลายอินทรีย์ที่มีความเหมาะสมกันทั้งในด้านขนาดและด้านสมบัติทางโครงสร้าง (เช่น ประจุและการเรียงตัว เป็นต้น) ทำให้โมเลกุลของสารทั้งสองสามารถอยู่ร่วมกันได้อย่างเสถียรด้วยแรงทางพันธะต่าง ๆ เช่น พันธะไฮโดรเจน (hydrogen bond) แรงทางไฟฟ้าสถิต (electrostatic force) หรือแรงแวนเดอร์วาลส์ (van der Waals force) รวมถึงความจำเพาะของการจัดเรียงตัวของโมเลกุลตัวทำละลายอินทรีย์ในช่องว่างของโครงสร้างสารเคมีหลักอีกด้วย เมื่อโซลเวตได้รับแรงกระตุ้น (เช่น จากการให้พลังงานในรูปความร้อนหรือแรงทางเชิงกล) จะสามารถเร่งหรือทำลายพันธะระหว่างโมเลกุลของตัวทำละลายอินทรีย์กับโครงสร้างหลัก ทำให้โมเลกุลของตัวทำละลายหลุดออกจากโครงสร้างหลัก และส่งผลให้เกิดความไม่สมบูรณ์ในโครงสร้างของโมเลกุลของสารเคมีหลักและ/หรืออาจเกิดการเปลี่ยนแปลงการจัดเรียงตัวของโครงสร้างภายในโมเลกุลหลักที่เรียกว่าการเกิดภาวะพหุสัณฐาน

กรณีที่เกิดความไม่สมบูรณ์ในโครงสร้างของสารเคมีหลัก โดยยังคงมีการจัดเรียงตัวของโครงสร้างภายในที่ไม่เปลี่ยนแปลงจะสามารถนำมาประยุกต์ใช้เพื่อการลดขนาดอนุภาคและอาจส่งผลไปสู่การเพิ่มพื้นที่ผิวของอนุภาคที่มีขนาดเล็กลง ซึ่งจะนำไปสู่การเพิ่มความสามารถในการละลายของยาที่ละลายน้ำได้น้อยโดยใช้การก่อเกิด molecular adduct ของสารเคมีกับโมเลกุลตัวทำละลายที่เหมาะสม แล้วไล่โมเลกุลของตัวทำละลายออกจากโครงสร้างด้วยวิธีการเพิ่มอุณหภูมิร่วมกับการลดความดัน การทำแห้งเยือกแข็ง (freeze drying) หรือการใช้แรงทางเชิงกล (mechanical stress) หลังจากเกิดโครงสร้างที่ไม่สมบูรณ์หรือเปราะบางแล้วอาจจะให้พลังงานเพียงเล็กน้อย เช่น การบดอนุภาคด้วยแรงเพียงเล็กน้อยก็จะสามารถทำให้ผลึกของสารนั้นแตกออกเป็นชิ้นเล็ก ๆ ได้ ทำให้มีพื้นที่ผิวโดยรวมมากขึ้นต่อน้ำหนักของสารที่เท่ากัน เมื่อเทียบกับอนุภาคก่อนทำการลด

ขนาด แต่ในบางครั้งพลังงานเชิงกลที่ให้เข้าไปหลังจากเกิดโครงสร้างที่ไม่สมบูรณ์แล้วอาจจะไม่มีความจำเป็นต่อการลดขนาดอนุภาคก็ได้ เนื่องจากหลังจากโมเลกุลของตัวทำละลายอินทรีย์ออกจากโครงสร้างหลักของสารเคมีจะเกิดการล้มหรือแตกออกเป็นชิ้นเล็ก ๆ ได้เอง ตัวอย่างการศึกษาวิธีการลดขนาดอนุภาคยาด้วย solvation-desolvation method ได้แสดงในตารางที่ 1

ปัจจัยที่มีผลต่อการลดขนาดอนุภาคด้วยเทคนิค solvation-desolvation นี้ ปัจจัยแรก คือ ***ชนิดของตัวทำละลายอินทรีย์***ที่ใช้ในการทำให้เกิด molecular adduct โดยพบว่าสารเคมีหลักชนิดใดชนิดหนึ่งสามารถเกิดการรวมตัวกับโมเลกุลของตัวทำละลายอินทรีย์ได้มากกว่าหนึ่งชนิด แต่ไม่จำเป็นที่โซลเวตทุก ๆ ชนิดจะสามารถเกิด desolvation แล้วจะทำให้ขนาดอนุภาคเล็กลงได้ นอกจากนี้ ***วิธีการทำ desolvation*** ยังมีความสำคัญต่อการลดขนาดอนุภาคด้วยเช่นกัน โดยพบว่าโซลเวตชนิดเดียวกันเมื่อใช้วิธีการทำ desolvation ที่แตกต่างกันอาจสามารถไล่ตัวทำละลายอินทรีย์ออกจากโซเวตได้แตกต่างกัน ซึ่งจะส่งผลถึงความสามารถในการลดขนาดอนุภาคของสาร

ปัจจัยต่อมาที่มีผลต่อการลดขนาดอนุภาค คือ ***อุณหภูมิ***ที่ใช้เพื่อไล่โมเลกุลของตัวทำละลายอินทรีย์ออกจากโครงสร้าง ซึ่งจะส่งผลโดยตรงต่อความสามารถในการลดขนาดอนุภาค จากการศึกษาของ Chinapak[20] พบว่าเมื่อใช้อุณหภูมิที่ต่ำเกินไปในการกำจัดน้ำออกจาก beclomethasone dipropinate monohydrate จะไม่สามารถลดขนาดอนุภาคของสารนี้ได้ ในขณะที่เมื่อใช้อุณหภูมิที่สูงขึ้นจะมีประสิทธิภาพในการลดขนาดอนุภาคได้ด้วยวิธีการเดียวกัน เนื่องจากการใช้อุณหภูมิที่ต่ำเกินไปจะไม่สามารถเหนี่ยวนำให้เกิดความไม่สมบูรณ์ของโครงสร้างที่มากพอ ดังนั้นการใช้วิธีลดความดันร่วมกับการเพิ่มอุณหภูมิในการไล่ตัวทำละลายอินทรีย์จึงเป็นทางเลือกที่เหมาะสมต่อการลดขนาดอนุภาคด้วยเทคนิคนี้ และยังเหมาะกับตัวยาที่ไวต่อความร้อนอีกด้วย เช่น sulfathiazole ammonia adduct ซึ่งอุณหภูมิที่สูงประมาณ 80 องศาเซลเซียสจะไม่เพียงพอต่อการ deammoniation จึงต้องใช้การลดความดันร่วมด้วยจึงจะสามารถไล่ ammonia ออกจากโครงสร้างของ sulfathiazole ได้ นอกจากนี้ปัจจัยที่เกี่ยวข้องกับ***จำนวนรอบ (cycle)*** ของการทำ solvation และ desolvation ยังส่งผลอย่างชัดเจนต่อขนาดอนุภาคที่ได้หลังจากผ่านกระบวนการนี้ เช่น griseofulvin chloroform adduct เมื่อผ่านการทำ solvation และ desolvation จำนวน 2 รอบทำให้ขนาดอนุภาคเล็กลงกว่าเริ่มต้น ในขณะที่เมื่อผ่านกระบวนการนี้เป็นจำนวนรอบมากขึ้นกลับไม่มีผลต่อการลดขนาดอนุภาค[21] และ chloramphenicol palmitate ammonia adduct ก็ให้ผลในทิศทางเดียวกัน[15]

อย่างไรก็ตาม การลดขนาดอนุภาคด้วยวิธีการนี้ สิ่งที่สำคัญและจำเป็นต่อการประเมิลผลขนาดอนุภาคที่เล็กลงคือพหุสัณฐานที่อาจเกิดขึ้นได้หลังจากการก่อ molecular adduct รวมถึงตัวทำละลายอินทรีย์ที่อาจตกค้างอยู่ในอนุภาคนั้นว่ามีปริมาณมากน้อยอยู่ในเกณฑ์ที่ยอมรับได้หรือไม่ และอาจจะเกิดอันตรายกับผู้ใช้ได้หรือไม่

ตารางที่ 1 การลดขนาดอนุภาคของสารบางชนิดด้วยเทคนิค solvation-desolvation

Chemical	Solvent	Desolvation method	Reference
Barbiturates	Ammonia	การเพิ่มอุณหภูมิร่วมกับการลดความดัน	13
Sulfonamides	Ammonia	การเพิ่มอุณหภูมิร่วมกับการลดความดัน	14
Chloramphenicol palmitate	Ammonia	การเพิ่มอุณหภูมิร่วมกับการลดความดัน	15
Chloramphenicol	Ammonia	การเพิ่มอุณหภูมิร่วมกับการลดความดัน	15
	Pyridine	การเพิ่มอุณหภูมิร่วมกับการลดความดัน	16
Griseofulvin	Benzene	การทำแห้งเยือกแข็ง (freeze drying)	17
	Chloroform	การเพิ่มอุณหภูมิร่วมกับการลดความดัน	18
	Dioxane	การเพิ่มอุณหภูมิร่วมกับการลดความดัน	19
Beclomethasone dipropionate	Water	Isothermal dehydration	20

การปรับปรุงสมบัติทางกายภาพของอนุภาคโดยเทคนิค solvation

การจัดเรียงตัวของโครงสร้างภายในผลึกอาจสะท้อนถึงสมบัติทางกายภาพของสารเคมีได้ เมื่อเกิดการเปลี่ยนแปลงของการจัดเรียงตัวภายในผลึก (โดยไม่มีการเปลี่ยนแปลงของพหุสัณฐานของสาร) จะส่งผลต่อสมบัติต่าง ๆ ของสารได้ ดังนั้นภาวะของการเกิดเป็น molecular adduct ก็ย่อมส่งผลกระทบต่อสมบัติดังกล่าวด้วยเช่นกัน เนื่องจากว่า ถึงแม้การจัดเรียงตัวของหน่วยแลตทิซในสารจะไม่เปลี่ยนแปลง แต่การมีโมเลกุลชนิดอื่น (ซึ่งคือ โมเลกุลของตัวทำละลายอินทรีย์) สอดแทรกหรือเกิดพันธะกับสารเคมีหลักย่อมทำให้สมบัติของสารที่แสดงออกเปลี่ยนแปลงตามไปด้วย ด้วยเหตุนี้ การเปลี่ยนแปลงสมบัติทางกายภาพของสารเมื่อเกิด solvation จึงมีประโยชน์และถูกนำมาประยุกต์ใช้ต่อการพัฒนารูปผลึกหรืออนุภาคในทางเภสัชกรรม จากการศึกษาพบว่า lactose และ dextrose monohydrate เมื่อถูกทำให้สูญเสียน้ำออกจากโมเลกุลไปบางส่วน จะทำให้อนุภาคที่ได้มีสภาพไหลได้ (flowability) และสมบัติในการยึดเกาะ (binding property) ที่ดีขึ้น เมื่อเทียบกับรูปแบบ hydrate ที่ยังมีโมเลกุลของน้ำอยู่ครบสมบูรณ์[22-24] ดังนั้น anhydrous lactose และ anhydrous dextrose จึงเป็นตัวเลือกที่ดีในการใช้เป็นสารเพิ่มปริมาณในกระบวนการผลิตยาเม็ดด้วยวิธีการตอกอัดโดยตรง (direct compression)

การเปลี่ยนแปลงรูปร่างผลึกของสารบางประเภทสามารถทำได้โดยเทคนิค solvation ตัวอย่างเช่น paracetamol ซึ่งผงยามีลักษณะผลึกรูปเข็ม ซึ่งเป็นลักษณะด้อยที่ไม่เอื้อต่อกระบวนการผลิตยาเม็ดด้วยวิธีการตอกอัดโดยตรง เนื่องจากผลึกรูปเข็มมีลักษณะการไหลที่ไม่ดีและยังปราศจากความสามารถในการยึดเกาะอีกด้วย จึงได้มีความพยายามในการพัฒนาวิธีการผลิตโดยการเติมสารปรุงแต่งยา (excipient) ชนิดต่าง ๆ รวมถึงการเปลี่ยนแปลงกระบวนการผลิตยาเม็ด paracetamol ด้วยวิธีที่หลากหลาย[25] แต่เป็นที่น่าสนใจว่าเมื่อ paracetamol เกิด solvation กับ dioxane แล้วกำจัด dioxane ออกจากผลึกที่ได้ จะทำให้รูปร่างผลึกเปลี่ยนแปลงไปจากเริ่มต้นโดยมีความกลมมากขึ้น ทำให้การไหลของผงยาดีขึ้นและบริเวณพื้นผิวของผลึกยังมีลักษณะ sintered-like อีกด้วย จากลักษณะเด่นทั้งสองประการนี้ทำให้ paracetamol-dioxane solvate ที่ทำการ desolvate แล้วสามารถตอกอัดโดยตรงได้ ซึ่งช่วยให้กระบวนการผลิตยาเม็ด paracetamol สะดวกรวดเร็วและลดต้นทุนการผลิตได้[26]

การเกิดโซเวตในระหว่างกระบวนการผลิตสามารถนำมาใช้เพื่อเปลี่ยนแปลงสมบัติของรูปผลึกของสารบางชนิดได้ Wong และ Mitchell[27] ศึกษา hydrate form ของ chlorpromazine (CPZ) ที่เกิดขึ้นในระหว่างการทำแกรนูลเปียกโดยใช้สารผสมระหว่าง ethanol และน้ำเป็น binding liquid หลังจากอบแห้งไล่น้ำออกบางส่วน พบว่าแกรนูลที่เกิดขึ้นมีความสามารถในการถูกตอกอัดได้ดีกว่าอนุภาคของวัตถุดิบ CPZ ซึ่งมีความสามารถในการถูกตอกอัดที่ต่ำมากและยังอาจส่งผลให้เกิด picking, laminating รวมถึง capping ได้ เมื่อทำการตรวจสอบพบว่า CPZ ในแกรนูลนั้นเปลี่ยนแปลงเป็นรูป monohydrate ดังนั้นสังเกตได้ว่า water of hydration ส่งผลต่อการเสียสภาพของอนุภาครวมทั้งการเกิด interparticulate bonding นอกจากนี้ ยังพบว่า carbamazepine dihydrate form มีคุณสมบัติในการตอกอัดที่เหนือกว่า α และ β form โดยเฉพาะ β form นั้นแทบจะไม่สามารถตอกอัดเป็นเม็ดได้เลย หรืออาจกล่าวได้ว่ามีความสามารถในการยึดเกาะที่ต่ำมาก อย่างไรก็ตาม แม้ว่า CBZ dihydrate จะมีสมบัติในการตอกอัดที่ดี แต่ภายใต้แรงตอกอัดที่เหมาะสมสามารถเหนี่ยวนำให้เกิดการเปลี่ยนแปลงเป็น β form ได้เช่นกัน ดังนั้นจึงต้องเฝ้าระวังการเปลี่ยนแปลงนี้[28]

Solvation state ของสารบางชนิดยังช่วยให้การสังเคราะห์สารเคมีในรูปแบบ ansolvate มีความเหมาะสมและคุ้มทุนต่อการผลิตหรือสังเคราะห์ โดยมีผลลดต้นทุนและแรงงานในการผลิต เนื่องจากได้ปริมาณผลผลิตที่มากขึ้น ตัวอย่างของการใช้โซลเวตช่วยในการสังเคราะห์ ได้แก่ gabapentin ในรูป monohydrate[29] เมื่อใช้ hydrate form ในการสังเคราะห์จะสามารถเพิ่มผลผลิตของการสังเคราะห์ได้มากกว่าเดิมถึงร้อยละ 12 และยังให้อนุภาคที่มีสมบัติทางกายภาพที่เหนือกว่าการสังเคราะห์แบบเดิมที่ไม่ใช้ hydrate form อีกด้วย

Amoxicillin N-methyl-2-pyrrolidone solvate เป็นสารเคมีที่ดูดความชื้น (hygroscopic) น้อยกว่า amoxicillin sodium ทำให้สามารถใช้ solvate form ซึ่งเป็นรูปแบบที่เสถียรมาเตรียมเป็นยาผงสำหรับฉีดได้โดยมีเสถียรภาพทางกายภาพและทางเคมีเป็นที่น่าพอใจ[30] นอกจากนี้ N-acetyl-muramyl-L-α-aminobutyryl-D-isoglutamine (ABU-MDP) ในรูปผลึก hydrate ก็มีความสามารถในการดูดความชื้นน้อยกว่า ABU-MDP ในรูป anhydrous ซึ่งมีความสามารถในการดูดน้ำและสามารถเกิดปฏิกิริยาเคมีที่รวดเร็วเมื่อเพิ่มอุณหภูมิ ในขณะเดียวกัน hydrate ของ ABU-MDP นั้น ยังให้ฤทธิ์เป็นตัวเสริม (adjuvant) ที่เหนือกว่า anhydrous form อีกด้วย[31]

กล่าวโดยสรุป solvate form ของสารบางประเภททำให้สมบัติทางเคมีกายภาพของผลึกเปลี่ยนแปลงไปจาก ansolvate form ซึ่งอาจมีทั้งข้อดีและข้อเสีย ดังนั้นเราจึงสามารถนำประโยชน์ที่เกิดขึ้นมาประยุกต์ใช้ในทางเภสัชกรรมได้ แต่การจะทำนายว่ายาหรือสารเคมีชนิดใดบ้างที่เมื่อเกิด solvation แล้วจะทำให้สมบัติทางกายภาพเป็นผลดีตามต้องการเป็นเรื่องที่ยาก และยังไม่มีการศึกษาเกี่ยวกับหลักการนี้มากนัก

Solvation state กับการประยุกต์ใช้ในตำรับยาเตรียม

Hydrate form ของสารต่าง ๆ มีความสามารถในการละลายในน้ำได้น้อยกว่า anhydrous form ของตัวมันเอง[32] เนื่องจากกฎของสมดุล เมื่อพิจารณาไฮเดรตที่อยู่ในสภาวะที่มีน้ำในระบบการละลายของไฮเดรตจะเป็นดังสมการ

$A.H_2O \leftrightarrow A_{(aq)} + H_2O$ ($A.H_2O$ คือ hydrate form ของสาร A)

เมื่อนำ $A.H_2O$ เติมลงในน้ำจะเกิดการแยกตัวของโมเลกุลน้ำออกจาก hydrate form จึงทำให้ในระบบมีปริมาณน้ำมากขึ้น และจากกฎของสมดุลจะทำให้เกิดการผันกลับไปทางด้านสารตั้งต้น ซึ่งทำให้มี $A.H_2O$ มากขึ้นหรือหมายถึง $A.H_2O$ มีค่าการละลายน้อยลงหรือมีการแตกตัวในน้ำน้อยลง

Hydration state ที่เสถียรสามารถใช้ในการตั้งตำรับยาน้ำแขวนตะกอนได้ ส่วนการใช้ anhydrous form เพื่อการเตรียมยาน้ำแขวนตะกอน เมื่อกระจายผงยาในกระสายยาที่เป็นน้ำจะทำให้มียาบางส่วนละลายสู่วัฏภาคน้ำอย่างรวดเร็วจนถึงสภาวะอิ่มตัวยิ่งยวด และเหลือยาบางส่วนตกผลึกกลับออกมาเป็นของแข็ง ต่อมาของแข็งบางส่วนจะละลายกลับเข้าสู่วัฏภาคน้ำอีกครั้งวนเวียนเช่นนี้ตลอดไป เรียกว่าเกิด Ostwald ripening แต่การตกผลึกกลับมาจะทำให้ผลึกที่เกิดขึ้นมีขนาดใหญ่ขึ้น (crystal growth) และมีการละลายที่เปลี่ยนแปลงไป รวมถึงอาจเกิดการอัดตัวแน่น (caking) ที่ก้นภาชนะ เนื่องจากเกิดการทับถมของตะกอนที่มีขนาดแตกต่างกัน หรืออาจกล่าวได้ว่าเกิดความไม่มีเสถียรภาพของผลึก ดังนั้นการใช้ hydrate form ซึ่งมีค่าการละลายต่ำกว่า anhydrous form จึงเหมาะกับการเป็นวัตถุดิบในการเตรียมยาน้ำแขวนตะกอน เนื่องจากลดโอกาสการตกผลึกที่มีขนาดเปลี่ยนแปลงไปจากเริ่มต้น Hoelgaard และ Møller[33] พบว่า metronidazole benzoate dihydrate มีความเหมาะสมในการเป็นวัตถุดิบในการเตรียมยาน้ำแขวนตะกอนมากกว่า anhydrate form I และ II

ถึงแม้ว่า hydrate form จะเหมาะสมในการใช้เป็นวัตถุดิบสำหรับการเตรียมยาน้ำแขวนตะกอน แต่ความเหมาะสมของขนาดผลึกเริ่มต้นและองค์ประกอบในตำรับก็สำคัญไม่ยิ่งหย่อนไปกว่ากัน ดังนั้นการลดขนาดของ hydrate form จึงยังคงจำเป็นก่อนนำไปเตรียมเป็นเภสัชภัณฑ์ แต่การลดขนาด hydrate form อาจส่งผลต่อการสูญเสียน้ำออกจากโครงสร้างผลึกได้ ซึ่งจะทำให้สารเริ่มต้นกลายเป็น anhydrous form แทน จึงต้องศึกษาให้ละเอียดเสียก่อนว่าเมื่อมีการลดขนาด hydrate form แล้วอนุภาคหรือผลึกที่ได้ยังคงเป็น hydrate form อยู่หรือไม่ และมีแต่ขนาดของอนุภาคเท่านั้นที่เปลี่ยนไป เช่น triazinoindole hydrate ที่ผ่านการลดขนาดด้วย air mill ยังคงให้รูป hydrate ที่มีขนาดเล็กลงและสามารถเพิ่มเสถียรภาพทางกายภาพได้เมื่อเตรียมเป็นเภสัชภัณฑ์รูปแบบยาน้ำแขวนตะกอน[34]

อย่างไรก็ตาม มีข้อมูลบางส่วนที่ขัดแย้งกับสมมติฐานข้างต้น เนื่องจากพบว่า hydrate form ของสารบางชนิดสามารถละลายน้ำได้ดีกว่า anhydrous form เช่น tranilast[35], acyclovir[36], และ carbamazepine[37] เหตุผลในเรื่องนี้คงต้องพิจารณาถึงรูปแบบของพหุสัณฐาน (polymorphic form) ของ hydrate form ที่อาจจะสามารถละลายน้ำได้ดีกว่าเมื่อเปรียบเทียบกับพหุสัณฐานของ anhydrous form จึงมีโอกาสสูงที่จะทำให้ hydrate form ละลายน้ำได้ดีกว่า anhydrous form

หากพิจารณาการละลายในน้ำของโซลเวตที่เกิดจากตัวทำละลายอินทรีย์ การละลายของโซลเวตในน้ำจะตรงกันข้ามกับการละลายของไฮเดรตในน้ำ เนื่องจากเมื่อละลายโซลเวตในน้ำ ตัวทำละลายอินทรีย์ในโซลเวตจะหลุดออกจากโครงสร้างผลึก และน้ำในระบบจะถูกใช้ไปเพื่อการล้อมรอบสารเคมีหลัก จึงทำให้โมเลกุลของโซลเวตกลายเป็นโมเลกุลของสารเคมีหลักที่มีน้ำล้อมรอบ ($A_{(aq)}$) ทิศทางของปฏิกิริยาในสมดุลจะไปข้างหน้ามากขึ้น ดังนั้นโซลเวตจึงสามารถละลายน้ำได้ดีกว่าไฮเดรต ตัวอย่างของยาหรือสารเคมีบางชนิดที่รูปแบบโซลเวตมีสภาพละลายได้ (solubility) มีค่ามากกว่าในรูปแบบไฮเดรตแสดงข้อมูลอยู่ในตารางที่ 2

ตารางที่ 2 รูปแบบโซลเวต (solvate form) ของยาหรือสารเคมีที่มีการละลายในน้ำดีกว่ารูปแบบไฮเดรต (hydrate form)

Chemical	Solvating molecule	Relative water solubility	Reference
Succinyl sulfathiazole	Pentanol	Pentanol > Anhydrous > Hydrate	32
Fludocortisone acetate	Pentanol	Pentanol > Hydrate	32
Urapidil	Methanol	Methanol > Anhydrous form I > Anhydrous form II	38
Oxyphenbutazone	Benzene Cyclohexane	Benzene > Cyclohexane > Anhydrous > Hemihydrate > Monohydrate	39
Sulindac	Acetone Chloroform	Chloroform ~ Acetone > Anhydrous	40
Sulfamethoxydiazine	Chloroform Dioxane	Amorphous > Dioxane > Chloroform > Form I and II	41
Glibenclamide	Pentanol Toluene	Pentanol >> Toluene > Anhydrous form I and II	42

ดังนั้นจึงมีความเป็นไปได้ที่จะนำเอา solvate form ของสารบางชนิดที่มีค่าการละลายสูงกว่า anhydrous form หรือ hydrate form มาใช้ในการตั้งตำรับยาเตรียม เพื่อช่วยให้สามารถละลายน้ำได้มากขึ้น และยังอาจส่งผลต่อโอกาสการเอื้อประโยชน์ในร่างกายได้ อย่างไรก็ตาม การประยุกต์ใช้โซลเวตนี้ต้องพิจารณาถึง solvating molecule ด้วยว่ามีอันตรายหรือเกิดพิษรุนแรงมากน้อยเพียงใด ถึงแม้จะไม่เป็นอันตรายมากแต่ปริมาณที่เกิดขึ้นนั้นอาจมากพอที่จะเกิดพิษทั้งในระยะสั้นหรือระยะยาวได้

Hydrate form ที่มีการละลายในน้ำต่ำกว่า anhydrous form นั้น ย่อมส่งผลต่อการเอื้อประโยชน์ของยาในร่างกาย (bioavailability) เนื่องจากเป็นที่ทราบกันอย่างกว้างขวางแล้วว่าการละลายเป็นขั้นตอนสำคัญในการกำหนดปริมาณยาที่ถูกดูดซึมเข้าสู่ร่างกาย ตัวอย่างเช่น ampicillin anhydrous สามารถละลายในน้ำได้ดีกว่า trihydrate form จึงให้การเอื้อประโยชน์ที่สูงกว่าทั้งในคนและสุนัข[43] ภายหลังมีการศึกษาพบว่าค่าการละลายของ ampicillin ในน้ำ ไม่ได้เป็นปัจจัยหลักที่กำหนดการเอื้อประโยชน์ในร่างกาย แต่องค์ประกอบของตำรับส่งผลต่อการเอื้อประโยชน์มากกว่า อย่างไรก็ตาม มีงานวิจัยบางรายงานแสดงให้เห็นว่า hydrate form ให้การเอื้อประโยชน์ที่สูงมากกว่า anhydrous form ตัวอย่างเช่น Kahela และคณะ[37] ศึกษาพบว่า carbamazepine (CBZ) dihydrate ให้การเอื้อประโยชน์ที่สูงกว่า anhydrous CBZ ทั้งนี้เหตุผลส่วนหนึ่งเนื่องมาจาก CBZ dihydrate มีความสามารถในการเปียก (wettability) และละลายได้ดีกว่า anhydrous CBZ และเนื่องมาจาก anhydrous CBZ มีอัตราการเกิดการโตของผลึก (crystal growth) อย่างรวดเร็ว ส่วน CBZ dihydrate มีอัตราการโตของผลึกช้ามาก จึงทำให้โดยรวมแล้ว anhydrous CBZ มีค่าการละลายต่ำกว่า CBZ dihydrate และทำให้ CBZ dihydrate มีการเอื้อประโยชน์ที่สูงกว่า anhydrous CBZ

ในปี ค.ศ. 1975 Haleblian[44] พบว่าอัตราการดูดซึมนอกกายของ monoethanol solvate ของ t-butyl acetate ของ hydrocortisone มีค่าสูงกว่า hemiacetone solvate และมากกว่า anhydrous form ประมาณ 5 เท่า และอัตราการดูดซึมนอกกายของ monoethanol solvate ของ t-butyl acetate ของ prednisone มีค่าสูงกว่า hemichloroform solvate และมากกว่า anhydrous form ประมาณ 2 เท่า ซึ่งเป็นไปตามสมมติฐานหรือหลักฐานที่มีการศึกษามาข้างต้น นอกจากนี้ยังมียาชนิดอื่น ที่ให้ผลการศึกษาในทิศทางเดียวกัน เช่น fluprednisolone t-butylamine solvate[45]

Solvation กับการเพิ่มเสถียรภาพทางเคมี

จากข้างต้นที่ได้กล่าวแล้วว่า solvation state ของสารย่อมแสดงสมบัติทางเคมีกายภาพที่แตกต่างออกไปจาก ansolvate form การศึกษาของ Haleblian[44] พบว่า hydrate form ของ cyanocobalamine (vitamin B12) ซึ่งเป็นวิตามินที่สลายตัวได้ง่ายและไวต่อทั้งแสงและอุณหภูมิจะมีเสถียรภาพทางเคมี

มากกว่า conventional vitamin B12 และ cefazolin monohydrate เป็นอีกตัวอย่างหนึ่งของสารที่มีเสถียรภาพดีกว่า anhydrous form แต่ในทางตรงกันข้าม บางครั้งการมี hydration state มากเกินไปกลับทำให้เสถียรภาพลดลงเนื่องจากมีแนวโน้มที่จะสูญเสียโมเลกุลของน้ำออกจากโครงสร้างได้มากขึ้น[46] Engel และคณะ[47] ยังแสดงให้เห็นว่า cephalexin monohydrate จะเสถียรต่อการสัมผัสกับความชื้นมากกว่า anhydrous form นอกจากนี้ cefadroxyl hemihydrates ยังมีเสถียรภาพทางเคมีมากกว่า monohydrate form ซึ่งเป็นรูปแบบที่ใช้ในการเตรียมผลิตภัณฑ์ในปัจจุบัน[48] และ cefixime trihydrate มีเสถียรภาพทางเคมีในสภาวะที่มีความชื้นมากกว่า partially hydrate และ anhydrous form[49]

Nonstoichiometric solvate กับการประยุกต์ใช้ในทางเคมีและทางเภสัชกรรม

Nonstoichiometric solvate หรือ clathrate มักไม่ค่อยมีประโยชน์ในทางเภสัชกรรมมากนัก เนื่องจากพบว่ามีสารจำนวนน้อยชนิดที่เกิดสภาวะเช่นนี้ แต่ก็มียาสเตียรอยด์บางชนิดที่ใช้ประโยชน์จาก clathrate ในการเพิ่มเสถียรภาพทางเคมีกายภาพของรูปแบบยาเตรียมได้[50] จากการศึกษาพบว่าปัญหาที่เกิดขึ้นจากการใช้ beclomethasone dipropionate (BCP) anhydrous micronized form ในการเตรียมเภสัชภัณฑ์รูปแบบยาแขวนตะกอนในสารขับดันชนิด CFC propellant 11 เพื่อบรรจุในอุปกรณ์ยาสูดกำหนดขนาด (metered-dose inhaler; MDI) ของรูปแบบยาละอองลอย (aerosol) คือจะเกิดการโตของผลึก (crystal growth) และไปอุดตันที่ actuator ของ MDI ทำให้ประสิทธิภาพการนำส่งยาเข้าสู่ระบบทางเดินหายใจลดลงเนื่องจากขนาดอนุภาคที่ใหญ่ขึ้นกว่าขนาดเริ่มต้น แต่กลับพบว่าเมื่อเตรียม BCP ในรูป nonstoichiometric solvate ด้วยสารขับดันชนิด propellant 11 (BCP-propellant 11 clathrate) แล้วนำมาใช้เป็นวัตถุดิบเริ่มต้นในการเตรียมยาแขวนตะกอนในสารขับดัน propellant 11 กลับไม่พบปรากฏการณ์ดังกล่าวข้างต้น

ประโยชน์อื่น ๆ ของ clathrate ที่สามารถประยุกต์ใช้กับสารเคมีต่าง ๆ[44] ได้แก่ การใช้แยกสารเคมีออกจากกันโดยอาศัยสมบัติพื้นฐานของ clathrate ที่ให้สถานะทางกายภาพต่างจาก intact form อาทิ การแยก thiophene ออกจาก benzene การแยก rare gas (เช่น argon กับ neon) ออกจากกัน หรือการจัดเก็บสารเคมีบางชนิดที่อยู่ในสถานะไอให้กลายเป็นสถานะของแข็ง (เช่น hydroquinone กับ inert gas) รวมถึงการจัดการกับสารเคมีที่เป็นพิษและระเหยได้โดยผ่านทาง clathrate ที่มีเสถียรภาพและไม่ทำให้สารนั้นระเหยได้ เช่น dimethyl mercury (ซึ่งเป็นสารระเหยง่ายที่มีพิษ) กับ 4-p-hydroxyphenyl-2,2,4-trimethyl thiochroman เป็นต้น

บทสรุป

จากพื้นฐานความรู้ทางเคมีร่วมกับการค้นพบลักษณะและสมบัติทางกายภาพที่แตกต่างกันระหว่างรูปแบบโซลเวต (solvate form) กับรูปแบบที่ปราศจากโซลเวต (ansolvate form) ของสารชนิดเดียวกัน สามารถนำไปสู่การประยุกต์ใช้ในทางเภสัชกรรมและทางเคมีได้อย่างกว้างขวาง ไม่ว่าการปรับปรุงลักษณะอนุภาคให้มีสมบัติตามต้องการ การเพิ่มเสถียรภาพทางเคมีกายภาพของสาร รวมไปถึงการใช้เป็นเครื่องมือในการลดขนาดอนุภาคหรือใช้เป็นทางผ่านในการสังเคราะห์สารเคมีบางชนิดเพื่อให้ได้ปริมาณผลผลิตที่เพิ่มมากขึ้น อย่างไรก็ตาม ข้อจำกัดที่สำคัญของวิธีการเหล่านี้ คือ โมเลกุลของตัวทำละลายอินทรีย์ที่ใช้มักจะเป็นอันตรายและไม่ปลอดภัย ยกเว้นในกรณีที่สามารถพัฒนาใช้ไฮเดรตแทนโซลเวตได้เนื่องจากโมเลกุลของน้ำไม่เป็นพิษ นอกจากนี้ การศึกษาถึงหลักเกณฑ์หรือทฤษฎีการเกิดโซลเวตในปัจจุบันยังมีองค์ความรู้ทางด้านนี้น้อยมากและยังไม่สามารถสรุปเป็นกฎเกณฑ์ที่แน่นอนได้ จึงยังคงเป็นข้อจำกัดของการใช้วิธีการนี้

เอกสารอ้างอิง

1. Baraldi C, Gamberini MC, Tinti A, Palazzoli F, Ferioli V. Vibrational study of acetazolamide polymorphism. *J Mol Struc* 2009;918:88-96.
2. Suitchmezian V, Jeβ I, Näther C. Investigations on the polymorphism and pseudopolymorphism of triamcinolone diacetate. *Int J Pharm* 2006;323:101-109.
3. Othman A, Evans JSO, Evans IR, Harris RK, Hodgkinson P. Structural study of polymorphs and solvates of finasteride. *J Pharm Sci* 2006;96(5):1380-1397.
4. Brittain HG, Grant DJW. Effects of polymorphism and solid-state solvation on solubility and dissolution rate. In: Brittain HG (ed.). Polymorphism in pharmaceutical solid. New York. Marcel Dekker, 1999.

5. Kamada K, Yoshimura S, Murata M, et al. Characterization and monitoring of pseudo-polymorphs in manufacturing process by NIR. *Int J Pharm* 2009;368:103-108.
6. Byrn SR, Pfeiffer RR, Stowell JG. Solid state chemistry of drugs, 2nd ed. Indiana. SSCI Inc., 1999.
7. Guillory JK. Generation of polymorphs, hydrates, solvates, and amorphous solids. In: Brittain HG (ed.). Polymorphism in pharmaceutical solid. New York. Marcel Dekker, 1999.
8. Morris KR. Structural aspects of polymorphism. In: Brittain HG (ed.). Polymorphism in pharmaceutical solid. New York. Marcel Dekker, 1999.
9. Bechtloff B, Nordhoff S, Ulrich J. Pseudopolymorphs in industrial use. *Cryst Res Technol* 2001;36(12):1315-1328.
10. Morris KR, Rodrigues HN. Hydrates. In: Swarbrick J, Boylan JC (eds.). Encyclopedia of pharmaceutical technology (Vol. 7). New York. Marcel Dekker, 1993.
11. Khankari RK, Grant DJW. Pharmaceutical hydrates. *Thermochim Acta* 1995;248:61-79.
12. United State Pharmacopeial Convention Inc. The United States Pharmacopoeia, 24th ed. Maryland. Rand McNally, 2000: pp.1750.
13. Sekiguchi K, Tsuda Y, Kanke M, Suzuki E, Iwatsuru M. Ammonia adduct of barbiturates and their applications to particle size reduction. *Chem Pharm Bull* 1978;26(4):1279-1290.
14. Sekiguchi K, Tsuda Y, Kanke M. Studies on the method of size reduction of medicinal compounds V: Size reduction of several sulfonamides by desorption of ammonia from their ammonia compounds. *Chem Pharm Bull* 1974;22(12):2972-2978.
15. Tsuda Y, Kanke M, Miyachi I, Maeno K, Sekiguchi K. Ammonia adducts of chloramphenicol palmitate and their applications to particle size reduction. *Chem Pharm Bull* 1980;28(3):947-955.
16. Himuro I, Tsuda Y, Sekiguchi K, Horikoshi I, Kanke M. Studies on the method of size reduction of medicinal compounds IV: Solvate formation of chloramphenicol and its application to size reduction. *Chem Pharm Bull* 1971;19(5):1034-1040.
17. Suzuki E, Shirotani K, Tsuda Y, Sekiguchi K. Studies on the method of size reduction of medicinal compounds VIII: Size reduction by freeze-drying and the influence of pharmaceutical adjuvants on the micromeretic properties of freeze-dried powders. *Chem Pharm Bull* 1979;27(5):1214-1222.
18. Sekiguchi K, Ito K, Owada E, Ueno K. Studies on the method of size reduction of medicinal compounds II: Size reduction of griseofulvin by solvation and desolvation method using chloroform (2). *Chem Pharm Bull* 1964;12(10):1192-1197.
19. Sekiguchi K, Shirotani K, Kanke M, Furukawa H, Iwatsuru M. Studies on the method of size reduction of medicinal compounds VI: Solvate formation of griseofulvin with benzene and dioxane. *Chem Pharm Bull* 1976;24(7):1621-1630.
20. Chinapak A. Particle size reduction by desolvation technique of a model drug: Beclomethasone dipropionate. M.Sc. in Pharm. (Industrial Pharmacy) thesis. Bangkok. Chulalongkorn University, 2001.
21. Sekiguchi K, Horikoshi I, Himuro I. Studies on the method of size reduction of medicinal compounds III: Size reduction of griseofulvin by solvation and desolvation method using chloroform (3). *Chem Pharm Bull* 1968;16(12):2495-2502.
22. Lerk CF, Andreae AC, Bohr AH, et al. Increased binding capacity and flowability of α-lactose monohydrate after dehydration. *J Pharm Pharmacol* 1983;35:747-748.
23. Lerk CF, Zuurman K, Kussendrager K. Effect of dehydration on the binding capacity of particulate hydrates. *J Pharm Pharmacol* 1984;36:399.
24. Wong DYT, Waring MJ, Wright P, Aulton ME. Elucidation of the compressive deformation behavior of α-lactose single crystals by mechanical strength and acoustic emission analyses. *Int J Pharm* 1991;72:233-241.
25. Garakeni HA, Ford JL, Rubinstein MH, Rajabi-Siahboomi AR. Highly compressible paracetamol II: compression properties. *Int J Pharm* 2000;208:101-110.
26. Facheux JM, Guyot-Hermann AM, Guyot JC, Confat P, Drache M, Huvenne JP, Bouche P. Compression ability improvement by solvation/desolvation process: application to paracetamol for direct compression. *Int J Pharm* 1993;99:99-107.
27. Wong MWY, Mitchell AG. Physicochemical characterization of a phase change produced during wet granulation of

chlorpromazine hydrochloride and its effects on tableting. *Int J Pharm* 1992;88:261-273.

28. Lefebvre C, Guyot-Hermann AM, Draguet-Brrugmans M, Bouché R, Guyot AC. Polymorphic transitions of carbamazepine during grinding and compression. *Drug Dev Ind Pharm* 1986;12:1913-1927.
29. Butler DE, Greenman BJ, U.S. Patent 4, 894, 476 (1990).
30. Heitman H, van der Drift JK, Leenderts EJAM, Grootveld HH, U.S. Patent 4, 318, 852 (1982).
31. Chan TW, Becker AR, U.S. Patent 4, 629, 782 (1986).
32. Shefter E, Higuchi R. Dissolution behavior of crystalline solvated and nonsolvated forms of some pharmaceuticals. *J Pharm Sci* 1963;52:781-791.
33. Hoelgaard A, Møller N. Hydrate formation of metronidazole benzoate in aqueous suspensions. *Int J Pharm* 1983;15:213-221.
34. Caldwell HC. Labile triazinoindole hydrates. *J Pharm Sci* 1973;76(2):334-336.
35. Kawashima Y, Niwa T, Takeuchi H, Hino T, Itoh Y, Furuyama S. Characterization of polymorphs of tranilast anhydrate and tranilast monohydrate when crystallized by two solvent change spherical crystallization techniques. *J Pharm Sci* 1991;80(5):472-478.
36. Kirstl A, Srcic S, Vrecer F, Šuštar B, Vojnovic D. Polymorphism and pseudopolymorphism: influencing the dissolution properties of the guanine derivative acyclovir. *Int J Pharm* 1996;139:231-235.
37. Kahela P, Aaltonen R, Lewing E, Anttila M, Kristoffersson E. Pharmacokinetics and dissolution of two crystalline forms of carbamazepine. *Int J Pharm* 1983;14:103-112.
38. Botha SA, Caira MR, Guillory JK, Lötter AP. Physical characterization of the methanol solvate of urapidil. *J Pharm Sci* 1989;78(1):28-34.
39. Stoltz M, Lötter AP, van der Waat JG. Physical characterization of two oxyphenbutazone pseudopolymorphs. *J Pharm Sci* 1988;77(12):1047-1049.
40. Tros de llarduya MC, Martín C, Goñi MM, Martínez-Uhárriz MC. Dissolution rate of polymorphs and two new pseudopolymorphs of sulindac. *Drug Dev Ind Pharm* 1997;23(11):1095-1098.
41. Moustafa MA, Ebian AR, Khalil SA, Motawi MM. Sulphamethoxydiazine crystal forms. *J Pharm Pharmacol* 1971;23:868-874.
42. Suleiman MS, Najib NM. Isolation of physicochemical characterization of solid crystal forms of glibenclamide. *Int J Pharm* 1989;50:103-109.
43. Poole JW, Bahal CK. Dissolution behavior and solubility of anhydrous and trihydrate forms of ampicillin. *J Pharm Sci* 1968;57(11):1945-1948.
44. Haleblian JK. Characterization of habits and crystalline modification of solids and their pharmaceutical applications. *J Pharm Sci* 1975;64(8):1269-1288.
45. Haleblian JK, Koda RT, Biles JA. Isolation and characterization of some solid phases of fluprednisolone. *J Pharm Sci* 1971;60(10):1485-1491.
46. Cise MD, Osborne HE. U.S. Patent 4, 104, 470 (1978).
47. Engel GL, Indelicato JM, Rose HA, U.S. Patent 4, 600, 773 (1986).
48. Marsili L, U.S. Patent 4, 962, 195 (1990).
49. Kitamura S, Koda S, Miyame A, Yasuda T, Morimoto Y. Dehydration effect on the stability of cefixime trihydrate. *Int J Pharm* 1990;59:217-224.
50. Nachiengtung N. Solid state characterization of beclomethasone dipropionate solvates and polymorphs. Ph.D. thesis. Indiana. Purdue University, 1997.

Review Article

Pharmaceutical Applications of Chemical Solvates

Wanchai Chongcharoen[1], Veerakiet Boonkanokwong[2]* and Narueporn Sutanthavibul[2]

[1] Medica Innova Co., Ltd., Bangkok 10310, Thailand

[2] Department of Pharmaceutics and Industrial Pharmacy

Pharmaceutical Development and Technology Transfer (PDT[T]) Unit, Drug and Health Products Innovation Promotion Center (CU.D.HIP)

Faculty of Pharmaceutical Sciences, Chulalongkorn University, Bangkok 10330, Thailand

* Corresponding author: Veerakiet.B@chula.ac.th

ABSTRACT

Chemical solvate means a structure of molecular adduct between crystal lattices and guest molecules with respect to certain stoichiometric arrangement. Guest molecules are mostly solvents including water. If water molecules are entrapped in crystal lattices, this chemical compound is called hydrate. Solvates or hydrates generally have different physicochemical properties from their original nonsolvated crystals. The examples of such properties are flowability, binding property, compressibility, solubility, chemical and physical stability. Research in solvate formation of various organic solids proves that it is beneficial to improve or modify some characteristics of former crystals. Our literature review indicates solvation and desolvation processes can be used to achieve desirable specific characteristics of organic solids. Various applications of solvate formation or modification are summarized and presented in this article. Furthermore, some cases of nonstoichiometric molecular adduct or so-called clathrate are one of the most promising advantages for pharmaceutical application and chemical management. Conclusively, solvation with or without desolvation step can be applied in numerous pharmaceutical and chemical aspects.

Keywords: Solvate, hydrate, pseudopolymorphism, particle size reduction, physicochemical properties

Thai Pharm Health Sci J 2009;4(3):377-386